NANOPHYTOPLANKTON PHYSIOLOGY AND THE CARBON CYCLE

BY

Siân Fôch-Gatrell

FOR THE DEGREE OF

DOCTOR OF PHILOSOPHY

THESIS PRESENTED TO THE UNIVERSITY OF EAST ANGLIA,

SCHOOL OF ENVIRONMENTAL SCIENCES

July, 2015

The work in this thesis was made possible through the support of the National Environment Research Council (NERC) and the School of Environmental Sciences, University of East Anglia.

Abstract

Laboratory experiments on the physiological response of members of the nanophytoplankton to temperature and light limitation and nutrient saturation were conducted in order to investigate if nanophytoplankton conforms to Plankton Functional Types (PFTs) for modelling purposes. This thesis concluded that nanophytoplankton does not follow all of the assumed physiological traits.

The Q_{10} estimates for members of the nanophytoplankton are considerably lower than Eppley, and since nanophytoplankton does not follow the Eppley curve at warmer temperatures, the results suggest that the Eppley assumptions cannot be used to describe nanophytoplankton. μ_{max0} is used as a temperature physiological modelling parameter (as well as Q_{10}) which are components of the exponential and linear fits. However, nanophytoplankton best fits to an optimum function which uses μ_{opt}, T_{opt} and dT as model parameters. These results are in contrast to the Eppley assumptions.

Using a dynamic photosynthesis model five phytophysiological parameters were derived including the maximum photosynthesis rate (P_m^C,), respiration rate (resp), the initial slope of the line (αchl), light inhibition (β^{chl}) and the maximum chlorophyll to carbon ratio (θ_{max}). These parameters were estimated using an acclimated model which used the instantaneous rates of photosynthesis to estimate the other parameters. The acclimated model gave the best fit (AIC = -3.75 *vs*. = -0.95). These results are in contrast to those used for PFT modelling purposes. Parameters are comparable for P_m^C, resp and θ_{max} but showed significant differences for α^{chl} and β^{chl} the latter of which was underrepresented in the dynamic model, and the former of which is used as a model parameter for PFT parameterization. Chlorophytes had stronger light inhibition (mean β^{chl}= 0.72 g C m^2 (mol photons g Chl a)$^{-1}$) than haptophytes (mean β^{chl}= 0.34 g C m^2 (mol photons g Chl a)$^{-1}$). β^{chl} is significantly lower for haptophytes (P = 0.002). Members of the nanophytoplankton showed relatively high μ_{max} (0.81 d^{-1} from the acclimated model fit) and mean

photosynthesis rates 1.8 P_m^C (d^{-1}) mean cell volume 37 μm^3). Maximum growth rates increased with increasing cell volume for all of the species.

Members of the nanophytoplankton alter their elemental stoichiometry and assimilated nutrients in excess of their requirements but as a PFT, there were no statistically significant deviations from Redfield. Under nutrient replete conditions Chl *a*:C increased linearly with increasing temperature and increased linearly with decreasing light. Overall, these results suggest that further physiological data is required in order to parameterize models to estimate nanophytoplankton physiological responses to climate change.

Table of Contents

Table of Abbreviations and SI units (International System of Units)

% = percent

P^C = carbon specific instantaneous rate of photosynthesis

P_m^C = carbon specific maximum rate of photosynthesis

Q_0^{N} = mol N (mol C)$^{-1}$ (subsidence N:C ratio)

Q_0^{P} = mol P (mol C)$^{-1}$ (subsidence P:C ratio)

R_{M} = d^{-1} (maintenance respiration)

f_A = Fraction of Q_0 allocated for affinity

< = less than

> = greater than

± = plus or minus

°C = degrees in centigrade

A.D. = anno domini

A.S.E = asymptotic error

A_0 = m^3 (mol N d)$^{-1}$ (affinity parameter)

AC = alternating circuit

AF = airborne fraction

AIC = Akaike information criterion

AMT = Atlantic Meridional Transect

ANOVA = Analysis of Variance

ATP = adenosine triphosphate

C = carbon

C_8H_9NO = acetanilide

$CaCO_3$ = calcium carbonate

Chemostat = chemical environement is static

Chl *a* = chlorophyll *a*

CHN = carbon, hydrogen, nitrogen

$CO\frac{2}{3}$ = carbonate

CO_2 = carbon dioxide

CO_3^{2-}= carbonate

CV = cross validation

D = dilution rate

DAPI = 4’6-diamidino-2-phenylindole

DGOM = dynamic green ocean model

DIC = dissolved inorganic carbon

DMS = dimethyl sulphide

DNA = deoxyribonucleic acid

DOC = dissolved organic carbon

DOM – dissolved organic matter

E.G. = *exempli gratia* (that is)

ESAW = enriched seawater artifical medium

et al. = *et* (and) *alii* (others)

Exp = exponential

Fe = iron

fmol = femtomole (equal to 10^{-15} moles)

g = gram

GF/F = glass fibre filters

Gt = gigatonnes

H_2 = hydrogen

HCl = hydrochloric acid

HCO_{3^-} = bicarbonate

Hg = mercury

HNLC = high nutrient, low chlorophyll

I = irradiance

I.E. = *id est,*

I_{opt} = optimum irradiance

IPCC = International Panel on Climate Change

JGOFS = joint global ocean flux study

$K_2S_2O_8$ = potassium persulfate solution

kg = kilograms

LED = light emitting diode

Lin = linear

Ln = natural log

LNLC = low nutrient, low chlorophyll

m = metre

Max = maximum

mg = milligrams

Min = minimum

ml = millilitres

mm = millimetres

N = nitrogen

N = nitrogen

n = number

N_2 = nitrogen gas

N_20 = nitrous oxide

NCP = net community production

NH_3 = ammonium

NH_4 = ammonia

nm = nanometres

NO_2 = nitrite

NO_3 = nitrate

NP = new production

NPP = net primary production

NPZD = nutrient phytoplankton-zooplankton-detritus

O_2 = oxygen

OA = ocean acidification

OAGCMs = ocean-atmosphere general circulation models

Opt = optimum

Opt = optimum

P = phosphorus

P = statistical threshold

PAR = photosynthetically active radiation

pCO_2 = partial pressure of CO_2

PCO_2 = partial pressure of CO_2

PFT = plankton functional type

Pg = petagram ($1x10^{15}$ gram)

pg = picogram ($1x10^{-12}$ gram)

pH = potential hydrogen

PI curve = photosynthesis *vs.* irradiance curve

P_{max} = maximum potential photosynthetic rate

PO_4 = phosphate

POC = particulate organic carbon

POM = particulate organic matter

PON = particulate organic nitrogen

POP = particulate organic phosphorus

ppm = parts per million

ppmv = parts per million by volume

Q_{10} = temperature coefficient

RCC = Roscoff culture collection

RCPs = representative concentration pathways

resp = respiration

RNA = ribonucleic acid

RP = regenerated production

RPM – revolutions per minute

rRNA = ribosomal ribonucleic acid

RSS = residual sum of squares

s = second

SEM = standard error of the mean

Si = silicon

SST = sea surface temperature

St Dev = standard deviation

T = time

TEM = transmission electron microscopy

TEP = transparent exopolymer particles

TGB = temperature gradient bar

T_{max} = temperature maximum

T_{min} = temperature minimum

T_{opt} = temperature optimum

UK = United Kingdom

WCRP = world climate research programme

WOA = World Ocean Atlas

WOCE = world ocean circulation experiment

α = alpha (initial slope of the PI curve)

α = m^3 g C (μE g Chl *a*)$^{-1}$ (light absorption coefficient)

α^{chl} = chlorophyll specific initial slope of the photosynthesis *vs*. irradiance curve

β = beta (light inhibition of the PI curve)

β^{Chl} = chlorophyll specific light

ζ = mol C (mol N)$^{-1}$ (cost of biosynthesis coefficient)

θ = theta (Chl *a*:C)

Θ_{max} = maximum Chl *a*:C

μ = growth rate

μl = microlitre

μm = micrometres (1×10^{-6} of a metre)

μ_{max} = maximum growth rate

μ_{opt} = optimum growth rate

Table of Tables

Table of Figures

Table of Equations

Declaration

I declare that the work presented in the thesis entitled “Nanophytoplankton Physiology and the Carbon Cycle” is my own work generated by myself and in part by my research group. I declare, that the work is, to my knowledge, novel and original. The work submitted here in this thesis, is for the degree of Doctor of Philosophy for the Department of Environmental Science at the University of East Anglia, and has not been submitted wholly or in part for any other University or for any jointly written publications.

Dedication

To my boy:

"The most powerful weapon on earth is the human soul on fire."

- Ferdinand Fôch

"And see the great Achilles, whom we knew.

Tho' much is taken, much abides; and tho'

We are not now that strength which in old days

Moved earth and heaven; that which we are, we are;

One equal temper of heroic hearts,

Made weak by time and fate, but strong in will.

To strive, to seek, to find, and not to yield."

- Ulysses, Lord
Alfred Tennyson

Acknowledgments

First and foremost, I would like to thank my supervisors Dr Erik Buitenhuis and Dr Gill Malin for their guidance and patience throughout my time as a PhD student. Erik has been the most patient and kind supervisor anyone could ask for. I am grateful for his dedication, his understanding and his subject knowledge. I would like to thank him for his constant guidance and encouragement, especially when times were particularly bleak. Gill has always had an open door for me and has been extraordinarily helpful in terms of pastoral care and organising the external help that I have required throughout my PhD. Thank you for your last minute comments on my thesis and your ongoing and helpful suggestions and direction for my work.

For his constant support and on-going help I would like to extend my deepest gratitude to the Marine Trace Gas Biology Laboratory Technician Mr Robert Utting. Without whom I would never have completed my PhD. I will be forever indebted to you for your support, encouragement, pastoral guidance and general helpfulness. I feel honoured to now count you among my friends. Thank you.

I would also like to thank specific individuals from the research group that I was fortunate enough to be involved with. For your help, friendship and support, these people made my time at the University of East Anglia a pleasure – Dr Steve Jones, Dr Beate Stawiarski, Dr Moritz Heinle, Dr Raffaella Nobili and Dr Sophie Chollet, thank you all.

To other members of my research group, I would also like to acknowledge you for your input and encouragement – Professor Corinne Le Quèrè, Oliver Andrews and Clare Enright.

On a final professional note, I would like to thank Professor Steve Hubbard from the Universities of Dundee and St. Andrews. Thank you for always being there.

From a personal viewpoint, I would like to thank all of my family and friends. My mum in particular, who stepped in when I needed her most and who made it possible for me to finish my PhD. I can never repay you and I can never thank you enough. You gave me the strength and the wisdom to carry on. Thank you. To my new mother friend Katie Grant who looked after my son for me so I could come to work, and who became the most unlikely but best of friends a girl could ask for. There are no words that can express how grateful I am to you… even if you only read these lines of my thesis, I hope to one day repay the kindness you have shown me through a very difficult time in my life. To Dr Amy Kirkham for you friendship, kindness, support, generosity and reiki!

To my lovely partner, Vasco; thank you for your support, thank you for your encouragement, thank you for absolutely everything you have done for the boy and I. Thank you for being there for me, now I hope that I can be there for you as we start our new lives together. I love you.

And to my son Nathan, I love you boy.

1. Chapter 1: Introduction

1.1 Rationale

The underlying theme of this work is based on the importance of the ocean and its biota (specifically marine phytoplankton) in regulating the atmospheric concentrations of carbon dioxide (CO_2), which is the main contributor to anthropogenic climate change. Understanding how climate change will affect the planet is currently one of the biggest questions facing the scientific community. Knowledge of the speed and ultimate impact of climate change on ecosystems and biogeochemical research is imperative. Taking a bottom up perspective one must begin with the effects of climate change on phytoplankton. Phytoplankton is the basis of the food chain in the marine environment and accounts for half the production of Earth's organic matter (Arrigo, 2007; Wohlers *et al*., 2009). Because of this, phytoplankton also removes CO_2 from the atmosphere and produce half the oxygen we breathe (Walker, 1980).

While attempting to relate phytoplankton production data to the climate change problem, literature reviews have shown that there is not enough physiological data available to statistically determine what specific traits distinguish Plankton Functional Types (PFTs). In 2005, analysis of both spatial and temporal distributions of PFTs showed that distinguishing traits do exist (Le Quèrè *et al*., 2005). By studying phytoplankton physiological responses to its environment to determine growth rate and composition (e.g. carbon: nitrogen: phosphorus: chlorophyll ***a*** – C:N:P:Chl ***a***) it was hoped that we can better understand its response to and feedback on a changing environment.

1.1.1 The carbon cycle

The biogeochemical cycle by which carbon is exchanged among the different biospheres of Earth is one of the most important cycles in the functioning of this planet (Fasham, 2003). The oceans contain the largest active pool of carbon. Oceanic carbon exists in the forms of 35700 petagram (Pg) of dissolve

inorganic carbon (DIC, which is HCO_3^- + CO_3^{2-} + CO_2, Buitenhuis *et al*., 2013a; Solomon *et al*., 2007; Emerson *et al*., 2008) and 662 ± 32 Pg C as dissolved organic carbon (DOC, Hansell *et al*., 2013) and a few Pg of particulate organic carbon (POC) in living marine biota and non-living detritus (Yamamoto, 1995; Fasham, 2003; Gardner *et al*. , 2006; Buitenhuis *et al*., 2013b). The most important exchanges of carbon in the oceans come from the interaction between the surface waters and the atmosphere (Fasham, 2003; Sabine *et al*., 2004) and the formation and destruction of organic matter via the biological processes of photosynthesis and respiration as well as the precipitation and dissolution of calcium carbonate (Emerson *et al*., 2008). This exchange occurs via CO_2 gas exchange, the flow of DIC and the burial of mineral $CaCO_3$ (Emerson *et al*., 2008). About 40% of the CO_2 added to the atmosphere since the industrial age has remained there, the rest has been distributed over the land and ocean carbon reservoirs (Sabine *et al*., 2004; Emerson *et al*, 2008). It is important to understand how this distribution will continue because this process is important in forecasting the predicted fate of CO_2 with anthropogenic climate change (Emerson *et al*., 2008). The amount of carbon in those respective reservoirs allows for a qualitative prediction of how much one sphere is dependent on another (Emerson *et al*., 2008).

Inorganic carbon – that is compounds with no carbon-carbon or carbon-hydrogen bonds - is important as a reactant in water since it regulates pH in the ocean and can vary as either a source or a sink of carbon to the atmosphere (Beaugrand *et al*., 2013). Particularly important are areas of upwelling and down-welling where carbon is released into the atmosphere and drawn down into the deep oceans respectively (Fasham, 2003; Bianucci *et al*., 2012; Doney *et al*., 2012).

The exchange of carbon between the surface waters and the atmosphere is controlled by photosynthesis and respiration as well as by physico-chemical characteristics that influence the solubility of CO_2 and hence its partial pressure (pCO_2). Photosynthesis and respiration are associated with the marine plankton. Marine phytoplankton in general terms is responsible for approximately 50-60% of the global biological uptake of CO_2 from the

atmosphere (Beardall *et al*., 2009; Fuschino *et al*., 2011). They are especially important in the regulation of the import and export of carbon between the atmosphere and the upper surface waters and therefore are significant in the carbon cycle (Fasham, 2003; Sigman *et al*., 2003). The carbon cycle in the marine environment begins with the basis of the marine ecosystem's food chain which comprises the phytoplankton. These microscopic algae combine energy from sunlight with CO_2 to form organic carbon in a process known as photosynthesis. This process provides them with the energy they require for metabolism and reproduction and the organic carbon is then cycled throughout the planktonic ecosystem by organisms that eat the phytoplankton (zooplankton), which are in turn ingested by larger organisms and so on as they progress up the food chain (Eppley *et al*., 1972). Not all of the originally produced organic carbon is utilized: approximately 10% of energy is transferred up each trophic level of the marine food chain; most of the rest is lost through respiration or as particulate material or detritus which sinks down from the upper sunlit (euphotic) portion of the marine ecosystem (Buitenhuis *et al*. 2013) – ultimately driving the transfer of CO_2 from the atmosphere to the ocean in a process known as the biological pump (Eppley *et al*., 1972; Sigman *et al*., 1993; Gorsky *et al*., 1999; Henson *et al*., 2011; Kim *et al*., 2011; Hansell *et al*., 2012). This sequestration or 'biological pump' has been effective in removing CO_2 from the atmosphere for millions of years (Sigman *et al*., 2003; Hansell *et al*., 2012). Again, most of this flux is eventually respired in the deep sea, while a small part ends up sequestered at the bottom of the deep ocean for millions of years (Henson *et al*., 2011).

The operation of the biological pump depends on many factors including the size of the sinking particles, how fast they are recycled as they sink, and whether or not they are associated with the shells of some plankton functional types (coccolithophores, diatoms and some zooplankton) (Gorsky *et al*., 1999; Klaas *et al*., 2002; Sigman *et al*., 2003; Ridgwell *et al*., 2011; Henson *et al*., 2011; Riley *et al*., 2012; Doney *et al*., 2012;). The significance (or not) of coccolithophores is hotly debated among the scientific community, as are the other factors that affect the biological pump, such as aggregation, size class,

competition and community structure (Gorsky *et al*., 1999; Steinberg *et al*., 2008; Kwon *et al*., 2009; Henson *et al*., 2011; Laufkötter *et al*., 2013). The downward flux of particulate organic carbon (POC) decreases significantly beyond the upper sun lit layers due to plankton metabolism (particularly bacteria and zooplankton) (Steinberg *et al*., 2008). As increasing levels of CO_2 enter the atmosphere it is possible that the effect of the biological pump may become stronger and result in a negative feedback; where the output of the systems opposes changes to the input of a system resulting in attenuated changes (Sigman *et al*., 2003; Henson *et al*., 2011; Kim *et al*., 2011; Schoo *et al*., 2012; Moazami-Goudarzi *et al*., 2012).

The biological pump is essentially moderated by atmospheric forcing, upper ocean physics and ambient chemistry, all of which may alter as the climate changes (Wohlers *et al*., 2009; Kim *et al*., 2011; Barnosky *et al*., 2012). As the climate changes the biological pump may be subject to both positive and negative feedback cycles. How effective the biological pump is depends greatly on regional variance based on species composition; their biogeochemical role and distinct environmental and nutrient responses (Kim *et al*., 2011). In essence, those factors used to distinguish plankton functional types by.

All the processes involved in the biological pump are coupled with the cycles of elements present in seawater, including oxygen, nitrogen, silicon, phosphorus and iron (Fasham, 2003). All of these individual cycles can strongly influence the function and strength of the biological pump, since it is the quantity of these elements that produce the limiting growth factors for phytoplankton and heterotrophic biomasses (Falkowski *et al*., 1992; Behrenfeld *et al*., 2006). The other organic matter found in phytoplankton (other than carbon) such as nitrogen, phosphorus and trace elements, like iron, are found in a particular ratio known as the Redfield Ratio. The global average for the Redfield Ratio is 106C:16N:1P (Redfield 1934), other elements are present in trace quantities, but they are still important for growth and metabolism – as such they also can be limiting factors (Behrenfeld *et al*., 2006; Emerson *et al*., 2008). Because phytoplankton are known to alter their nutrient stoichiometry

under differing environmental conditions but nutrient-saturated conditions (Menden-Deuer *et al*., 2000), it is hypothesized that nanophytoplankton nutrient stoichiometry will deviate from the Redfield ratios. It is thought that there will be an increase in N:P ratios with an increase in SST, and therefore an increased demand for N resulting in N-limitation (Toseland *et al*., 2013). Therefore it is hypothesized than nanophytoplankton will have N:P ratios close to Redfield.

What is important is how climate change (in particular increases in stratification and sea surface warming) can lead to alterations in the effectiveness of the biological pump because these factors could lead to a decreasing supply of nutrients and therefore a reduction in NPP (Net Primary Production) (Emerson *et al*., 2008).

When considering SST with the effectiveness of the biological pump, temperature-dependent physiological parameters become important. The maximum growth rate is an important factor in biogeographic distribution (*Buitenhuis et al*., 2008) and therefore in biogeochemical cycling and identifying plankton functional types for biogeochemical modeling (Sarthou *et al*., 2005). The hypothesis for members of the nanophytoplankton is that due to their small cell size, higher growth rates would be expected. The temperature dependent maximum growth rates of both single nanophytoplankers and nanophytoplankton as a PFT are hypothesized to best fit to an exponential function (Eppley, 1972). Nanophytoplankton is hypothesized to show a relationship between temperature range and isolation latitude; the majority of the nanophytoplankton isolates are from subtropical to tropical geographical locations and algae tend to grow below T_{opt} allowing for interspecific competition (Eppley, 1972). Finally, members of the nanophytoplankon are hypothesized to show an inverse relationship between temperature dependent cell volume and growth rate (Brown *et al*., 2004).

The other climate change-related factor affecting the efficiency of the biological pump is with ocean acidification and in particular its effect on calcifying organisms (coccolithophores, pteropods etc.). If coccolithophores

are less able to calcify, then this will affect the strength of the hard-tissue pump, which in turn may have a knock-on effect on the soft-tissue pump because the calcium carbonate acts as a ballasting effect to sinking material (Emerson *et al*., 2008).

Those climate-change related factors that affect the physiology of PFTs are important in determining NPP. As the climate-driven conditions change, the result may induce a change in biological rates, a change in PFT elemental composition and therefore a change in the way that biogeochemical cycles are coupled. For example, simulations suggest that low Chl *a*:C ratios are caused by nitrate availability, and light is primarily responsible for the increase in phytoplankton Chl *a* :C ratios in the upper sunlit layers (Wang *et al*., 2009). So, by determining more physiological derived data on PFTs, climate modelling can better predict global climate change patterns. It is hypothesized that nanophytoplankton will show an decrease in Chl *a*:C with increasing light and increase linearly with increasing temperature (Geider, 2006).

The strength of the biological pump is controlled by the fraction of the total primary production that is exported to the deep ocean (Henson *et al*., 2011). New production (NP) is fuelled by nitrogen supplied from vertical mixing and regenerated production (RP) is fuelled by nitrogen that is derived from the recycling of organic matter in the upper sunlit layers of the ocean (Dugdale *et al*., 1967). This is described over long time periods as the *f*- ratio and it is expressed as NP/(NP+RP) which states that over time, export (i.e. the biological pump) is equivalent to new production (Dugdale *et al*., 1967). Global estimates of carbon export are generally calculated from the linear relationship between the *f*-ratio and sea surface temperature (SST) with satellite-derived data on primary production and SST (Dugdale *et al*., 1967; Laufkötter *et al*., 2013). However, these calculations yield a global carbon export of ~12 Pg C yr^{-1}. While this is greatly different from the global carbon export algorithms of ~20 Pg C yr^{-1} (Eppley *et al*., 1979; Uitz *et al*., 2010), it is comparable to the food-web model of 11 Pg C yr^{-1} (Henson *et al*., 2011) and slightly higher than the value of 9.6 Pg C yr^{-1} obtained from an inversion of *in situ* ocean observations (Schlitzer, 2004). Additionally, the understanding of

the role of nitrification in the biological pump leads to difficulties in predicting global carbon export. Laws *et al*. (2000) estimate the *f*- ratio by estimating NP from the part of NPP that is supported by nitrate and RP from the part of NPP that is supported by ammonium. They thus assumed that nitrification occurred only in the deep sea. More recently, it is thought that nitrification in the upper sun lit layers equals that of nitrification in the deep waters (Yool *et al*., 2007; Henson *et al*., 2011) which means that half of the NPP that is supported by nitrate is part of the RP in the upper ocean. This suggests that using nitrate *vs*. ammonium based estimates of the *f* -ratio would result in an over-estimation of carbon export (Dugdale *et al*., 1967). The estimates of the f-ratio are very variable from 10 – 20% in oligotrophic waters, to 50% under bloom conditions (Chavez *et al*., 1995). The global mean estimate from 1995 was 14% (Chavez *et al.*, 1995).

Such massive dissimilarity in the estimation of global carbon export is a key indicator to the requirement of further research on carbon export. One of the reasons that carbon export is difficult to predict is because part of the carbon cycle that remains unaltered by the effect of increasing CO_2 emissions is still sensitive to climate change (Matsumoto *et al*., 2010). Specifically, the physical forcing like the Atlantic meridional circulation will have the greatest impact on the part of the carbon cycle that remains unaltered by increasing emissions of CO_2 and will lead to a significant reduction in global carbon uptake in the ocean (Matsumoto *et al*., 2010). In terms of the biological effects, it is expected that a reduction in the organic carbon export will be caused by a reduction in the supply of nutrients; an increase in organic carbon production will be ameliorated by the increase in SST, and a reduction in $CaCO_3$ will occur due to ocean acidification (Matsumoto *et al*., 2010).

Larger phytoplankton like diatoms and dinoflagellates have previously been understood to contribute more to carbon export (Gorsky *et al*., 1999; Sigman *et al*., 2003; Henson *et al*., 2011; Ridgwell *et al*., 2011; Stukel *et al*., 2011; Riley *et al*., 2012; Doney *et al*., 2012) than small phytoplankton cells like those that comprise the pico and nano functional types (Tilstone *et al*., 1999; Richardson *et al*., 2006; Uitz *et al*., 2010). This is usually due to aggregation and

gravitational effects (Smayda, 1970) of carbon sequestration, but Richardson *et al*. (2007) show that the direct (aggregation) and indirect contributions (consumption by larger organisms) to carbon export from smaller size classes of phytoplankton (here, specifically picoplankton) is proportional to their contribution to NPP (Richardson *et al*., 2007). Previous models have assumed that the carbon export from small sized class plankton functional types has been cycled via the microbial loop rather than being directly exported out of the euphotic zone (Richardson *et al*., 2007). They state that not all cells need to be large in order to be exported; aggregations of small cells, particularly in nutrient deplete water, can also settle out (Richardson *et al*., 2007; Stukel *et al*., 2011). However since this work, Stukel *et al*., in 2011 have concluded that zooplankton is the major driver of carbon export – at least in the Spring California Current Ecosystem. Clearly, size –related contribution to carbon export is a much debated topic because biologically mediated processes vary among marine ecosystems.

1.1.2 Global climate change and predictions

Climate change is a natural and normal phenomenon that is characterized by a statistically significant and lasting change in the distribution of weather patterns causing an alteration in the average climate for that particular period (Baronsky *et al*., 2012). The change can last temporally for periods of decades to millennia; but spatially it is global (Baronsky *et al*., 2012). Historically, climate change has been known to be caused by ocean circulation; biotic processes; variations in the output of the sun; plate tectonics and volcanic eruptions (Hof *et al*., 2011; Barnosky *et al*., 2012).

Analysis of ice cores from Antarctica showed that pre-industrial CO_2 mixing ratios (the abundance of one component of a mixture relative to another; in this case – air) over the periods of 1006 to 1978 A.D. were between 275 and 284 parts per million (ppm) (Etheridge *et al*., 1996). Lower levels were recorded between 1550 and 1800 A.D. this is likely due to a global colder climate (Etheridge *et al*., 1996). Etheridge states that the natural variations make it difficult to refer to a single pre industrial unit to describe CO_2 levels (Etheridge

et al., 1996), but that it was probably at around 280 ppm right before the onset of the industrial revolution (Canadell *et al*., 2007). Nevertheless, they were able to distinguish the major growth in CO_2 levels over the industrial period (anthropogenic CO_2) with the exception of the period between 1935-1945 when the CO_2 mixing ratios stabilised or decreased slightly (Etheridge *et al*., 1996). This is attributed to natural variations of the carbon cycle on a decadal timescale (Etheridge *et al*., 1996). The analysis of Etheridge, 1996 calculated a 25% increase in CO_2 mixing ratios by 1996, since the onset of the industrial period (Etheridge *et al*., 1996). Natural variation was easily identified during periods of glaciations, the CO_2 levels lowered consistently by about 80 ppm (Etheridge *et al*., 1996). Smaller variations were possibly caused by the feedback of the climate on the carbon cycle (Etheridge *et al*., 1996).

Between 1750 and 2012, humans have released 590 ± 75 Pg C from fossil fuel combustion, land use change and cement manufacturing (GCP, 2013). This release of carbon has caused atmospheric pCO_2 to increase by 115 parts per million by volume (ppmv) (GCP, 2013). Even the CO_2 emissions growth rate has increased; for example, between 2000 and 2006 the emissions compared with the previous decade increased from 1.3% to 3.3% y^{-1} (Canadell *et al*., 2007).

As of 2013, the global average atmospheric CO_2 level is 395 ppmv (Paquay *et al*., 2013). This is a 40% increase from pre-industrial levels (Paquay *et al*., 2013). This is the highest level the Earth has experienced over the last 650,000 years and probably even over the last 20 million years (Canadell *et al*., 2007; Pearson *et al*., 2000). According to the International Panel for Climate Change (IPCC), carbon emissions may lead to atmospheric CO_2 levels of around 700 ppmv (Paquay *et al*., 2013), with a global mean temperature rise of between 3.3°C and 5.8°C (SRES8.5 scenario, IPCC, 2014) by 2100 relative to the middle of the 20th century.

Climate change predictions are made through modeling approaches (Koffi *et al*., 2011; Friedlingstein *et al*., 2003; Lin *et al*., 2011). The output from the first two simulated projections from the ocean-atmosphere general circulation

models (OAGCMs) (Cox *et al*., 2000; Dufresne *et al*., 2002; Friedlingstein *et al*., 2003) showed that the climate-carbon cycle interactions results in a positive feedback; meaning that it acts to increase the magnitude of this perturbation. What remains unknown is how extensive this increase may be (Friedlingstein *et al*., 2003). However, most of the uncertainty in the temperature projections arises from different CO_2 emission scenarios (so called representative concentration pathways (RCPs)), i.e. from future human decisions, and not from differences between different Earth system models (IPCC, 2013).

Future climate change forced by a 1% per year increase in atmospheric CO_2 has shown to have a positive feedback between the climate and the carbon cycle (Friedlingstein *et al*., 2001) by reducing ocean (and land) uptake of CO_2 by 35% at 4 x CO_2. The reduction in oceanic carbon uptake is due to a combination of increased SST reducing CO_2 solubility, the impact of reduced vertical mixing on the efficiency of the biological pump and changes in the biogeochemical cycling of CO_2 (Friedlingstein *et al*., 2001). When cumulated, the effect is a reduced oceanic uptake of CO_2, predominantly at higher latitudes (Friedlingstein *et al*., 2001). It has also been argued that the reduced efficiency of the ocean CO_2 sink can lead to a long-term increase (over 50 years) in the CO_2 airborne fraction (AF) (which is the ratio of annual increase in atmospheric CO_2 to the CO_2 emissions from anthropogenic sources). Canadell *et al*., 2007 shows that increases in AF amounts to 18% of the increase in the atmospheric CO_2 growth (Canadell *et al*., 2007). The AF is a function of physical and biological processes governing CO_2 exchanges as well as the trajectory for anthropogenic emissions (Canadell *et al*., 2007). From the period 2000 – 2006 half of the anthropogenic emissions remained in the atmosphere (0.45) and the rest was distributed between the land (0.30) and ocean sinks (0.24) (Canadell *et al*., 2007). The increase in AF implies that the anthropogenic emissions have increased faster than the CO_2 sinks (Canadell *et al*., 2007).

The World Ocean Circulation Experiment (WOCE) was part of the World Climate Research Programme (WCRP) encompassing almost 30 countries to

make *in situ* and satellite measurements of the Earth's oceans between 1990 and 1998 in order to better understand the physical processes that govern the oceans and the climate. The Joint Global Ocean Flux Study (JGOFS) was conceived in the late 1980s in an attempt to study the ocean's carbon cycle with specific emphasis on carbon exchange, cycling and export within the ocean and including across the air-sea boundary (Hanson *et al*., 2000). Both of these studies show that the uptake of CO_2 from anthropogenic emissions is actually not evenly distributed throughout the ocean (Sabine *et al*. 2004). Highest concentrations are found in the North Atlantic (Sabine *et al*., 2004). The North Atlantic actually holds an astounding 23% of the total absorbed anthropogenic emissions, despite only consisting of 15% of the total ocean volume (Sabine *et al*., 2004). Conversely, the Southern ocean has absorbed a mere 9% of the total. About 60% of the total oceanic CO_2 sink is in the Southern Hemisphere oceans which is proportional to the ocean volume in that hemisphere (Sabine *et al*., 2004). Because the emissions are absorbed via sea-air exchange, most of the highest concentrations of absorbed anthropogenic CO_2 are found in the upper layer above the thermocline (Sabine *et al*., 2004). Variations in penetration depth are determined by how rapidly the uptake is transported to the deep ocean, this is generally associated with convergence zones and along isopycnal gradients (Sabine *et al*., 2004). This accounts for the high concentrations in the Atlantic where there is a low Revelle number (measure of resistance by bicarbonate chemistry to atmospheric CO_2 being absorbed in the ocean surface) (Sabine *et al*., 2004), meaning that atmospheric CO_2 is strongly buffered by the ocean. Without oceanic uptake, atmospheric CO_2 would actually have been 471 ppm in 2012 rather than 393 ppm (GCP, 2013b).

1.1.3 Anthropogenic climate change

Anthropogenic climate change refers to the human activities that impact on the climate changing. These can include production of greenhouse gases emitted by the activity of humans, which has become a particular problem since the industrial revolution (onset from about 250 year ago) (Doney *et al*., 2012). The most prevalent of these is the emission of carbon dioxide from fossil fuel

combustion and the production of aerosols (atmospheric particles), CO_2 emitted from cement manufacture, land use changes (e.g. animal agriculture and deforestation) and ozone depletion. The IPPC Fourth report (2007) concludes that the post-industrial rise in atmospheric greenhouse gases do not come from natural mechanisms but from human activity. This increase in burning of fossil fuels is predicted to lead to significant changes in the climate (IPCC, 2007).

Currently, about half of the present emissions (Cox *et al*., 2000; Doney *et al*., 2000; Emerson *et al*., 2008; Eby *et al*., 2009) are being absorbed by the ocean and terrestrial ecosystems. The estimates for the oceanic sink for global anthropogenic CO_2 from 1800 – 1994 is ~48% of the total emissions (Sabine *et al*., 2004). In the period 2003 – 2012 this had gone down to 27% (GCP, 2013). The terrestrial ecosystem sink was also 27% (GCP, 2013).

With rising CO_2 and climate change, the ecosystems of the ocean will be affected by shifts in temperature, ocean circulation, stratification, nutrient input, oxygen content and ocean acidification (Doney *et al*., 2012). The sea surface temperature is expected to rise by 1.8°C – 4°C (Solomon *et al*., 2007; Doney *et al*., 2012). These physico-chemical factors impact on the biological ecosystems, insofar that phytoplankton community structure and diversity will be affected (Doney *et al*., 2012). Population-level regime shifts have already occurred as a result of plankton physiological intolerances to new environments, coupled with alterations in dispersal patterns, local extinctions and invasions and changes in species interactions at community level (Bopp *et al*., 2005; Doney *et al*., 2012). These climate-driven responses could result in novel ecosystems (Doney *et al*., 2012), most obviously, these impacts will likely be seen at the poles and the tropics. Polar ecosystems are more sensitive to sea-ice retreat and tropical species are more sensitive to the upper increases in SST (Doney *et al.*, 2012).

As we have already seen, the distribution of phytoplankton biomass geographically, and in turn the NPP is defined by the availability of light and nutrients in the marine ecosystem (Behrenfeld *et al*., 2006). In turn, these

growth-limiting factors are dependent on ocean physics forcing, the dynamic processes of mixing and stratification, upwelling, dust deposition (particularly important for iron) and the cyclical nature of the sun (Behrenfeld *et al*., 2006). Global NPP has been estimated from satellite colour of chlorophyll content, which provides a quantitative basis on which to link NPP to environmental factors (Behrenfeld *et al*., 2006). The impact of climate change is thought to result in a reduction in NPP with simulations suggesting that with 2x CO_2 (twice the pre-industrial concentration), increased stratification will lead to both a reduced supply in nutrients and an increase in light intensity, in the OPAICE model (coupled with Arpege via OASIS) the net result of this was a global reduction in marine productivity of 6% by 2100 (Bopp *et al*., 2001). The OPAICE model solves primitive equations on a curvelinear grid which has a meridional resolution higher at the equator to account for enhanced dynamics (average resolution = 2° longitude by 1.5° latitude). The grid has 30 levels vertically, 10 for the first 100 m of the ocean (reaches 5000 m). It also has vertical diffusion and viscosity coefficients to describe turbulent kinetic energy throughout the water column. Therefore OPAICE is able to predict turbulence in and below the mixed layer (therefore the mixed layer depth varies in time). The model also used isopycnal parameters of lateral diffusivity as well as includes a sea-ice model to take into account thermodynamics (Bopp *et al*., 2001).

1.1.4 Plankton Functional Types

PFTs are conceptual groupings of plankton species with a common ecosystem function (Le Quèrè *et al*., 2005). These groupings were outlined by a group of scientists from the Dynamic Green Ocean Project in 2003. The common functions relate to food webs, or biogeochemical cycling (Le Quèrè *et al*., 2005). The PFTs should have a distinct set of physiological requirements that govern their biogeochemical role and the PFT behaviour should have important effects on other PFTs while at the same time having a quantitative importance in at least some part of the global ocean (Le Quere *et al*., 2005). But because these groupings are not distinct and do not relate solely to the physiological

characteristics or size class, it may be difficult to determine their importance in carbon export (Anderson, 2005b).

With the changing climate, if the new environmental conditions are tolerable, one of two results will occur; either acclimation (individual physiological adjustment) or adaptation (increased abundance of tolerant genotypes over generations) (Doney *et al*., 2012). If the new environmental conditions prove to be intolerable, then one of two results may occur; migration (by individuals or populations), or death and perhaps local extinction (Doney *et al.,* 2012).

The changes in the marine environment may benefit some PFTs or may act to the detriment of others. This could be because of increased availability in nutrients, reduced energetic maintenance costs or a reduced competition or predation (Doney *et al*., 2012). However, experiencing changing environmental conditions outside of the normal range is usually stressful and thus causes suboptimal physiological responses (Doney *et al*., 2012). Where this happens, the result will be higher mortality rates, reduced growth rates, smaller sizes of multicellular organisms and reduced reproduction (Doney *et al*., 2012). In order to relate the physiological responses of PFTs in changing environment, laboratory data are incorporated into biogeochemical models in an effort to determine which PFTs will profit and which will not.

1.1.5 Nanophytoplanker

The geographic factors that define nanophytoplankton as a PFT are that it does not bloom in the open ocean but is most abundant in oligotrophic waters, contributing to about 45% of the total biomass (Uitz *et al*., 2006). Conversely, in eutrophic waters its total biomass totals only about 21% (Uitz *et al*., 2006). But interestingly, in terms of the absolute content (in mg Chl *a* m^{-2}) the increase in chlorophyll *a* actually triples for nanophytoplankers from oligotrophic water to euphotic waters (Uitz *et al*., 2006). Analysis of the vertical profile of nanophytoplankton has shown it to be predominant in all parts of the water column irrespective of stratification or well mixed waters (Uitz *et al*., 2006). Nanophytoplankton is also an important contributor to the

Southern Ocean in terms of number but not biovolume and are generally more abundant in areas of low chlorophyll *a* concentrations (Detmer *et al*., 1997). Across the Atlantic Meridional Transect (AMT) cruises, nanophytoplankton contribution to carbon fixation in the surface waters was 30 – 50% and higher than the total chlorophyll *a* contributions (10 – 20%); despite the dominant fraction coming from picophytoplankton (carbon fixation: 50 – 70% and chlorophyll *a* 80-90%) (Poulton *et al*., 2006).

Table 1.1 Nanophytoplankton comprise autotrophic eukaryotes with a size range between 2-20 µm. For this thesis, species of non-calcifying nanophytoplankton have been chosen and include the following species:

Roscoff Culture Collection (RCC) number	**Species**	**Class**	**Diameter µm**
1348	*Isochrysis galbana*	Haptophyte	5
1448	*Prymnesium calathiferum*	Haptophyte	4
1406	*Pleurochrysis gayraliae*	Haptophyte	3
905	*Imantonia rotunda*	Haptophyte	3
261	*Pseudoscourfieldia cf. marina*	Chlorophyte	4
661	*Chlorella stigmatophora*	Chlorophyte	3
916	*Prasinoderma coloniale*	Chlorophyte	3
647	*Micromonas pusilla*	Chlorophyte	2
21	*Ochromonas distigma*	Chrysophyte	5
91	*Scripsiella trochoidea*	Dinoflagellate	20

The nanophytoplankers used for this thesis comprise haptophytes, chlorophytes, a dinoflagellate and a chrysophyte (Table 1.1). Superfamilies are groups of phytoplankton that can be distinguished via groups of proteins with enough similar structural evidence to support a common evolutionary ancestry. Superfamilies include the Green superfamily (appropriated chlorophyll *b* as the ancestry pigment) and the Red superfamily (that appropriated chlorophyll *c*);

but for N:P there are only significant differences between phyla (among those tested from the Green superfamily are prasinophytes and chlorophytes; and from the red superfamily are dinoflagellates, haptophytes and chrysophytes) (Quigg *et al*., 2003). The non-calcifying haptophytes are a genera that show the presence of a haptonema at once point throughout their life history and they comprise approximately 11 genera with about 80 species (*Prymnesiophyceae*) (Thomsen *et al*., 1994). Species are distinguished from one another based on morphological differences and number of types of organic scales covering the cell body (via transmission electron microscopy – TEM). Although according to Pacific Ocean surveys the biomass and contribution of the haptophytes is relatively low (about 13 ± 9 %) its contribution to the nanophytoplankton functional group is relatively consistent worldwide and about 37 ± 20% (Thomsen *et al*., 1994).

The dinoflagellates comprise a large group of protists, all with flagella. Many are marine and many are photosynthetic. Of the free living species there are currently around 1,555-1,700 described marine dinoflagellates (Gómez, 2005; Taylor *et al*., 2008). They range greatly in size from about 5 μm to 2000 μm. They are identified by being unicellular and possessing two unequal flagella from the ventral cell side (Gaines *et al*., 1985). The transverse flagellum beats to the left of the cell, and the longitudinal flagella beats posteriorly (Gaines *et al*., 1985). Some have a cell covering known as a cortex which is composed of membranes, flattened vesicles called alveolae and other structures (Netzel *et al*., 1984) and are morphologically identified as being thecate or athecate species (sheathed, or unsheathed) (Menden-Deuer *et al*., 2000). Of the photosynthesizing dinoflagellates (those with chloroplasts), most possess a dinokaryon (nucleus) (Spector, 1984). Although dinoflagellates are classified as eukaryotes, they do not possess nuclei that are characteristic of a eukaryote. This is because the nuclei lack histones and nucleosomes and they also maintain continually condensed chromosomes during mitosis (Steidinger *et al*., 1996).

Chlorophytes are the green algae and can be multi or unicellular. They are structurally very diverse, although the ancestral type is thought to be a

unicellular flagellate with two identical flagella (Mattox *et al*., 1984). Chlorophytes have a nucleus and chloroplasts that are anterior and surrounded by two membranes, and the thylakoids are stacked into lamellae (Mattox *et al*., 1984). They are known as the green algae because they have both chlorophyll *a* and *b* in the same proportions as higher plants (Mattox *et al*., 1984).

Chrysophytes are the golden algae that comprise a large group of mostly unicellular photosynthetic flagellates. Nearly all are thought to become facultatively heterotrophic in the absence of plentiful light, or in the presence of plentiful DOC (dissolved organic carbon) (Waggoner, 1995). They are distinguished primarily by the structure of the flagella in motile cells. The cell contains two specialized flagella – the active flagellum is orientated towards the direction of movement and the smoother- in- appearance, second flagellum is orientated in the opposite direction (Waggoner, 1995).

1.1.6 Nanophytoplankton as a PFT

Prior to 2003 most global ocean biogeochemical modelling efforts used NPZD models (nutrient – phytoplankton – zooplankton – detritus). Because biogeochemical cycling is explicitly linked to plankton, it was decided that the best course of action would be to include PFTs in biogeochemical models (Le Quéré *et al*., 2005; Le Quéré *et al*., 2009). This led to the evolution of Dynamic Green Ocean Models (DGOM) based on the identification of PFTs in order to identify the ecosystem processes that are important to the biogeochemical cycles of the various elements and their interactions (Le Quéré *et al*., 2005).

Biogeochemical cycling in the marine environment is explicitly linked to the activity of PFTs. Modeling has proven to be complicated due to the complex nature of biology (Anderson, 2005). The current understanding of marine ecology, a lack of data and great species diversity has aggravated the situation (Anderson, 2005; Laufkötter *et al*., 2013).

The concentrations of phytoplankton PFTs are driven by two primary factors; growth and mortality by zooplankton (Buitenhuis *et al*., 2013). Both of these processes are important in determining the total carbon export – specifically for

each plankton functional type. JGOFS calls for the modeling of carbon export and hopes to describe the net community production (NCP) as the difference between autotrophic net photosynthesis and heterotrophic respiration (Hanson *et al*., 2000). Models need to be able to resolve spatial influences on primary production. By determining more physiological data on nanophytoplankton as a plankton functional type one can hope to achieve better model parameters (Williams, 2000). Biogeochemical models use a dynamic model to estimate light physiological responses in plankton; therefore it is hypothesized that nanophytoplankton photosynthetic parameter best fits to a dynamic model (Geider *et al*., 1996; 1998).

1.1.7 Nanophytoplankon and carbon export

The Southern Ocean is considered to be an important sink for atmospheric CO_2 and due to the sensitivity of the driving mechanisms to climate change it is an important area for research (Bathmann *et al*., 2000). Previous studies suggest that diatoms contribute much of the primary production in the Southern Ocean, but also that nanophytoplankton dominates in seasonal blooms (Uitz *et al*., 2010).

Carbon export in the North Atlantic is much more difficult to resolve; biomass in the surface layers is low and particulate matter has a high turnover (Doney *et al*., 2000). It is thought that only a fraction of the fixed carbon is exported by gravitational sinking and advection (Doney *et al*., 2000). Any export flux is supported by the action of vertical nutrient fluxes that act to sequester carbon in the deep ocean and in the thermocline for significant time periods, but which could change with the changing climate (Doney *et al*., 2000). Export accounts for 2/3s of the ocean CO_2 sink, while the effect of solubility in colder water accounts for the remainder (Doney *et al*., 2000).

A review of plankton functional types from satellite observations by Uitz *et al*. revealed that nanophytoplankton not only contributes to a ubiquitous 30-60% of the total primary production, but that this percentage equates to about 44% of the carbon export (approximately 20 Pg C yr^{-1}) (Eppley *et al*., 1979; Uitz *et al*., 2010). However, their size based classification did not exclude

coccolithophores and phaeocystis from the nanophytoplankton (Uitz *et al*., 2010), while the PlankTOM10 model does. Generally nanophytoplankton is thought to contribute 5 Pg C yr^{-1} NPP in the Atlantic; 9 Pg C yr^{-1} in the Pacific; 4 Pg C yr^{-1} in the Indian Ocean; 0.2 Pg C yr^{-1} in the Arctic; 1.7 Pg C yr^{-1} in the Southern Ocean; 0.2 Pg C yr^{-1} in the Mediterranean Sea; 9.2 Pg C yr^{-1} in the tropics and 4.6 Pg C yr^{-1} at the equator (Uitz *et al*., 2010).

Previous models made simple assumptions that resulted in minimal biological impact on carbon export because all of the DIC required to fuel the growth of phytoplankton came from upwelled nutrients resulting in no net gas exchange (Michaels *et al*., 2000; Doney *et al*., 2000; Emerson *et al*., 2008). Mostly this is because of model assumptions (e.g. constant Redfield ratios) but often the biological observations contradict these assumptions, generally because their influence is dynamic and reliant of the chemistry and the physics of the ocean.

As the climate changes, it is likely that the ocean will acquire an increase in the input of limiting nutrients from the atmosphere as dust patterns alter (Jickells et al., 2007). Therefore, it is possible that the rate of carbon export can change with feedback to the build-up of greenhouse gases (Denman *et al*., 2000). If climate change causes changes in the Redfield Ratio (106:16:1 – C:N:P) then the utilization of carbon relative to the other limiting nutrients could mean that either more or less carbon will be exported (Denman *et al*., 2000). Research from Toseland *et al*., state that in warmer oceans phytoplankton will produce higher N:P ratios which will in turn increase the demand for N. The consequence for this relating to carbon export is a shift towards N-limitation (Toseland *et al*., 2013). Changes in nutrient concentrations from industrial atmospheric sources, and also from agricultural runoff will also impact on the rate of carbon exchange. Physiological experimentation to see whether the nutrient uptake generally differs from the Redfield Ratio or if it remains the same with climate change parameters will allow insights into biological mechanisms and carbon export as well as the inferred degree of nutrient limitation of phytoplankton growth and cellular composition (Denman *et al*., 2000). Other studies have confirmed a departure from the Redfield Ratio where

the stoichiometry, in particular of C:N and C:P are usually higher than Redfield (Denman *et al*., 2000).

1.2 Aims and approaches

PFTs have been distinguished by their biogeochemical role; distinct environmental and nutrient requirements, their impact on other PFTs, and by their quantitative importance in at least some specific geographic location (Le Quèrè *et al*., 2005). Specifically, nanophytoplankton species were subject to three main physiological experiments that are relevant to climate change. Firstly, a temperature limitation experiment where the algae were grown in batch cultures in a temperature gradient bar; secondly a light limiting experiment where the algae were grown in batch cultures at limiting to saturating light intensities; and lastly, a nutrient experiment where the algae were grown nutrient replete media. The experiments were designed to determine growth rate, cellular composition (specifically C:N:P:Chl *a*), photosynthesis rates and parameters. These physiological aspects were determined for comparison with other PFTs and for parameterization of a global biogeochemical model (PlankTOM10). For temperature physiology, the model uses the parameters μ_{max0} d^{-1} and $Q_{10}^{0.1}$. For light physiology, the model uses α^{Chl} g C m^2(mol photons g Chl)$^{-1}$ and θ_{min} and θ_{max} g C g Chl^{-1}. PlankTOM10 Currently has 10 PFTs to enable the use of marine ecosystems as a means to better understand and predict the importance of living systems in the ocean to current aspects of climate change. The parameterization of such a model is especially important so that their predictive outputs can mirror that of remote satellite and field data as much as possible (Le Quèrè *et al*., 2005).

2 Chapter 2: Methodology

2.1.1 Description of species used

Table 2.1 Nanophytoplankers from the Roscoff Culture Collection (RCC) (roscoff-culture-collection.org).

Class	RCC number	Species	Isolation latitude	T_{opt} °C	Mean cell vol at T_{opt} μm^3/cell
Haptophyte	1348	*Isochrysis galbana*	54°08' N, 4°77'W	25	38 ± 0.88
Haptophyte	1448	*Prymnesium calathiferum*	14°64'N, 61°W	25	38 ± 0.32
Haptophyte	1406	*Pleurochrysis gayraliae*	55°45'N, 4°55'W	15	11 ± 0.72
Haptophyte	905	*Imantonia rotunda*	48°45'N, 3°57'W	20	12 ± 0.50
Chlorophyte	261	*Pseudoscourfieldia cf. marina*	14°30'S, 73°20'W	30	24 ± 6.32
Chlorophyte	661	*Chlorella stigmatophora*	59°21'N, 10°35'E	15	23 ± 3.26
Chlorophyte	916	*Prasinoderma coloniale*	8°20'S, 141° 15'W	25	15 ± 0.29
Chlorophyte	647	*Micromonas pusilla*	54°11'N, 7°54'E	25	2.3 ± 0.32
Chrysophyte	21	*Ochromonas distigma*	47°86'N, -0°25'W	25	84 ± 1.92
Dinoflagellate	91	*Scripsiella trochoidea*	49°19'N, 123°15'W	20	258 ± 3.70

Table 2.1 shows the species that were used. They were chosen to represent a wide range of geographical locations in an effort to define nanophytoplankton as a global functional type; they span coastal to open ocean and tropical to temperate waters (Figures 2.1 and 2.2), but no polar species were included. All of the cultures were unialgal but probably not axenic. The isolation latitude

data come from the Roscoff website and the temperature optimum (T_{opt}), mean cell volume and statistical data were empirically derived for the purpose of this thesis (Chapter 3).

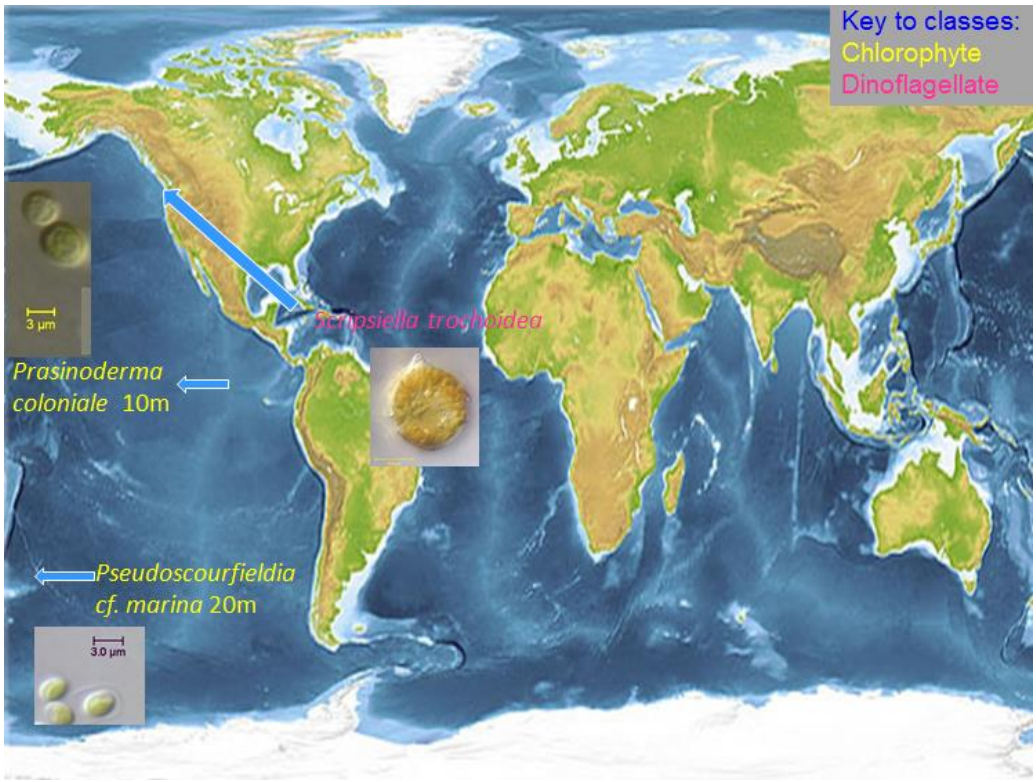

Figure 2.2 Isolation location of the species from the Roscoff Culture Collection (RCC). The images of the algae are also from the RCC website. The phytoplankton species name are colour coded, the class are shown in the legend. The arrows indicated approximate isolation location and the sampling depth is stated where known. (Planetary Visions, 2014).

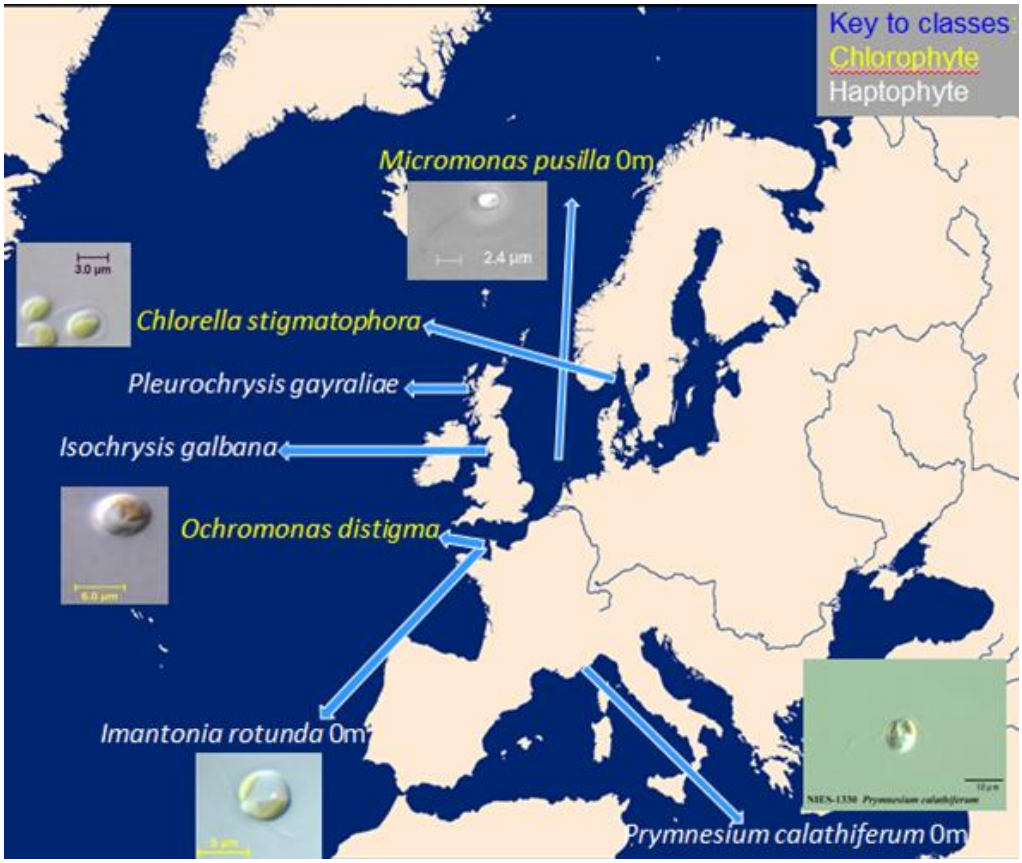

Figure 2.3 Isolation locations of the species from the Roscoff Culture Collection (RCC). The images of the algae are also from the RCC website. The phytoplankton species names are colour coded, their classes are shown in the legend. The arrows indicate approximate isolation locations and the sampling depth is stated where known. Wikimedia maps, 2014.

2.1.2 Stock cultures for experimental data

Stock cultures were grown in either f/2 or ESAW media (Enriched Seawater Artificial Medium (Harrison *et al.*, 1980; Berges *et al.*, 2000; available at: https://ncma.bigelow.org/ (Harrison *et al.*, 1980; and kept in MLR 251 Plant Growth Chamber Incubators (Panasonic Biomedical Sales Europe BV, Loughborough, UK).

Table 2. 1 Temperatures for stock culture maintenance. The numbers represent the RCC number codes.

Temperature °C	8	15	17	22
Culture (RCC)	661	647, 905	1348, 1406	21, 91, 261, 916, 1448

2.1.3 Change in fluorescence as a growth rate proxy

In vivo fluorescence was measured as a proxy for cell number using a Turner fluorometer model 10AU (Tunzi *et al*., 1974; Slovacek *et al*., 1977; Brand *et al*., 1981b; Karsten *et al.,* 1996; Gustavs *et al.,* 2009). Fluorescence is the emission of electromagnetic radiation by (in this example) chlorophyll *a*. The Turner fluorometer measures the light emitted (at 680 nm in the red range) from the chlorophyll molecules after excitation at a specific wave length of 440 nm, because chlorophyll *a* has an absorption maximum in blue wavelengths. However, the relationship between the chlorophyll *a* concentration and the measured fluorescence values can vary interspecifically and intraspecifically (Slovacek *et al*., 1977). In order to ensure that the growth rates calculated from the fluorometer were accurate, they were compared to growth rates calculated from cell numbers (via a Coulter Counter – see section 2.1.4). In addition, growth rates were measured on cultures only after they were acclimated to the culture conditions to obtain stable chlorophyll *a*/cell contents.

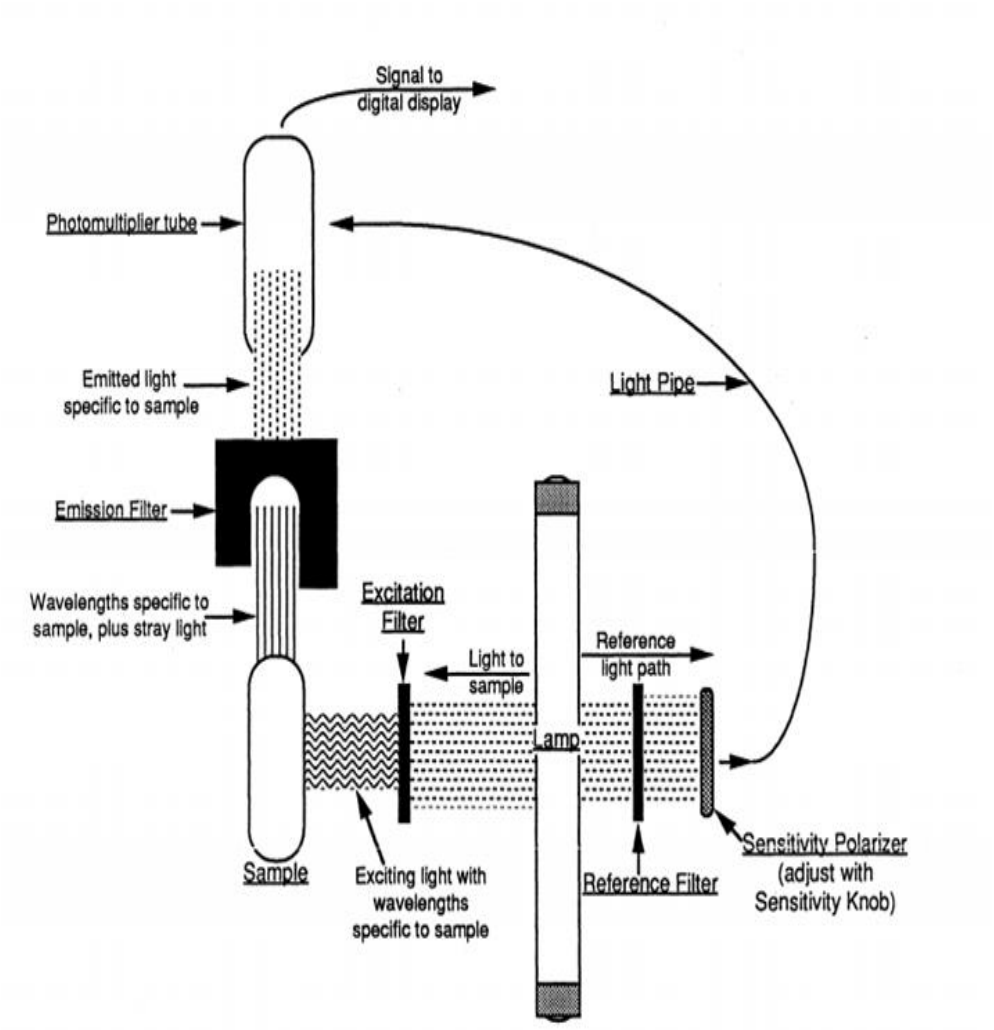

Figure 2.4 Schematic for the Turner AU-10 fluorometer when used for analysis of fluorescence in discrete batch phytoplankton cultures in glass tubes. Turner Designs, 1999.

The excitation of light is affected by numerous factors that include the health of the cells, dissolved organic matter (DOM), particulate organic matter (POM), turbidity (can cause scattering), cell morphologies (where shape and composition can interfere with the excitation signal), temperature (i.e. as temperature increases fluorescence decreases), nutrients and diurnal cycles. Therefore the Turner fluorometer is a semi-quantitative tool. An additional problem with the linearity of the fluorometer is if the concentration of cells becomes too high and the passage of the excitation light through the sample is impeded. This can be overcome with careful comparison to previous daily measurements because at very high cell concentrations, there would be a large decrease in fluorescence. Variation will also become apparent with the light

history of the culture; for example, phytoplankton adapted to high light conditions will produce a lower fluorescence response per unit chlorophyll than dark-adapted phytoplankton. To overcome some of these issues it is important to run a blank sample which would represent the constituents of the body of liquid that house the phytoplankton. It is also important to swirl the cultures before running a sample and use untainted vials to reduce the effects of turbidity. Measurements were made around the same time of the day to reduce the impact of diurnal cycles or the changes in algal pigments due to light availability.

2.1.4 Growth rate calculations

The *in vivo* fluorescence of each culture was measured daily with a Turner Fluorometer 10AU (see section 2.1.3). Each culture was measured within 1.5 hours of the onset of the light cycle (to minimize diel effects), care was taken to ensure that the borosilicate vials were untainted on the outside (to reduce turbidity or refraction effects) and each sample was swirled gently before measuring. A blank value for medium alone was subtracted from the final fluorescence reading. The growth rates were calculated in SYSTAT using the slope of a linear regression of Ln (fluorescence) against time (T) over the logarithmic growth phase, which usually started on day three after subculturing. The growth rate of each species was determined from a minimum of three measurements and the standard error from the observed growth rates was also derived from the linear regression in SYSTAT. Cultures were also measured on alternate days using a Coulter Counter (Beckman Coulter Ltd. High Wycombe, UK.) to measure cell numbers and cell volume. Replicate cultures were grown sequentially in the same position in the TGB. Between three and six replicates were grown.

2.1.5 Statistical analysis

Regression analyses, ANOVAs, Mann-Whitney (Rank Sum Test), Pairwise Multiple Comparison (Dunn's method) and T-tests (Student's and Paired) were conducted in Sigmaplot © Version 12.5.

2.1.6 Cell number and volume: Coulter counter

The Coulter Multisizer III is an accurate particle sizing and counting analyser which measures particles from size ranges of 0.4 µm to 1600 µm and the results are unaffected by refractive index, colour, size or shape of the particles. It uses electrical impedance (ratio of the voltage to the current in an alternating current (AC) circuit) to measure the volume of the particles (cells) that pass through an aperture. There are different aperture sizes available for a spectrum of different sized particles. For this research, a 100 µm diameter aperture was used. The sample (0.5 ml) along with 9.5 ml of electrolyte (0.2 µm filtered natural sea water) was placed into a cuvette and the suspended particles were drawn up through the aperture between two electrodes. The voltage between these electrodes creates the sensing zone via the electrical impedance. As the particles are pulled up (under vacuum), they displace a volume of electrolyte equivalent to the volume of the particles creating a measurable pulse allowing for discrete particle-by-particle analysis so cell number per ml can be identified (Beckman Coulter Counter, 2014); additionally the biovolume per ml was identified so that the average cell volume can be calculated by dividing the total biovolume by the cell number. Each analysis records the average of three replicate 0.5 ml subsamples.

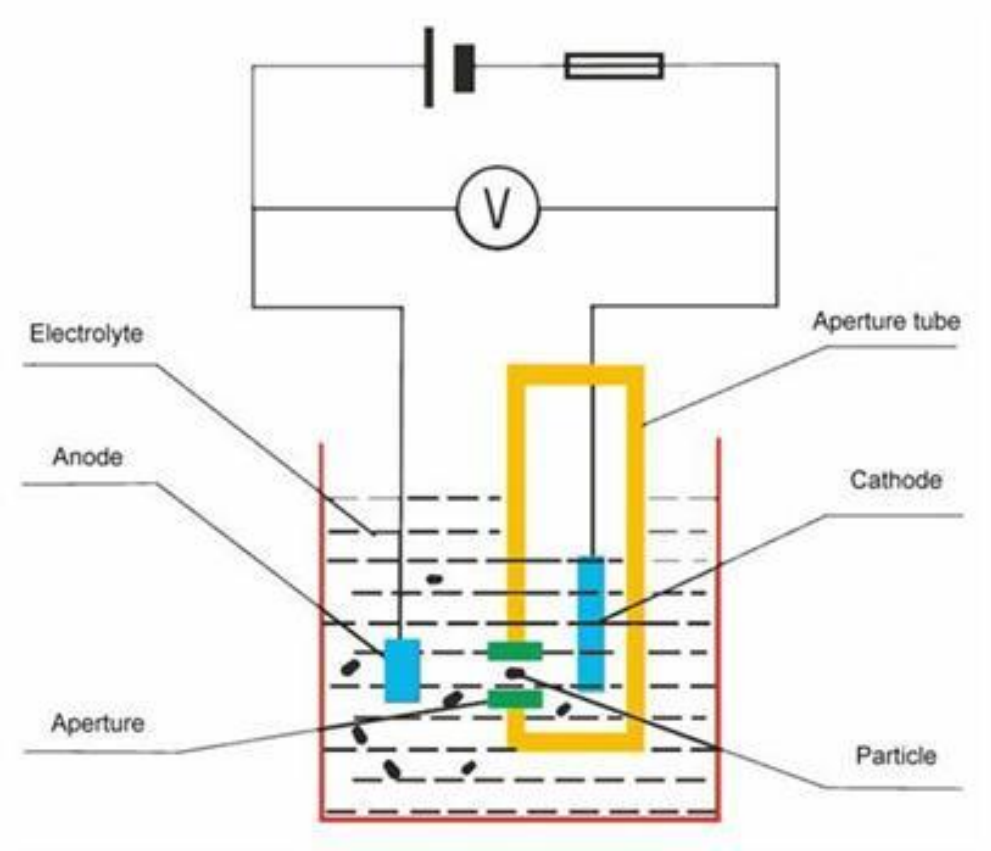

Figure 2.5 Schematic of the Beckman Coulter Counter. It shows the aperture with an internal and an external electrode with the sample vessel filled with electrolyte solution. Pre-determined subsamples of the original sample are pumped through the aperture (100 μm), where particles displace a volume of electrolyte and create voltage pulses which are processed through an analogue and a digital pulse processor converting them into data on cell concentration and volume in the sample.

2.1.7 Chlorophyll a

Samples for determining chlorophyll *a* concentrations were collected by filtering 8 ml of culture onto 13 mm diameter Whatman GF/F glass fibre filters (0.7 μm nominal pore size). They were filtered under a vacuum of approximately 10 inches of mercury and were immediately flash frozen in liquid nitrogen and then stored at -80°C prior to analysis (within 6 months). For the analysis, the chlorophyll *a* was extracted from the sample filters (along with blanks – blank filters and blanks with media) in the dark with 10 ml of 90% acetone in glass scintillation vials for 24 hours at 4°C and analyzed using the chlorophyll spectrophotometry acidification determination method

(Strickland *et al*., 1972; Aminot *et al*., 1999; Tada *et al*., 2004). The acidification method accounts for the chlorophyll derivatives. 8% HCl is added to the cuvette after each fluorescence reading and then measured again. The value of the acidified fluorescence reading is subtracted from the initial un-acidified reading. Fluorescence of the samples was measured in a LS45 Fluorescence Spectrometer (PerkinElmer, Waltham, USA). The excitation wavelength was 440 nm and the emission wavelength was 680 nm (Rebeiz 2002). A series of 5 chlorophyll standards (from spinach, SIGMA product C5753) was used to create the calibration curve (0, 50, 100, 250, 500 µg/L). Chlorophyll *a* standards were measured in triplicate before and after acidification, like the samples, using calculations from SCOR (U.N.E.S.C.O 1966) and Lorenzen (1967) methods. The linear regression from the calibration curve was used to calculate the concentration from absorbance.

2.1.8 Particulate organic carbon and nitrogen

Particulate organic carbon (POC) and particulate organic nitrogen (PON) were analyzed to allow for comparison with the Redfield ratio (the average molecular ratio of carbon, nitrogen and phosphorus in phytoplankton) (Redfield, 1934). Between 5 and 15 ml (30 ml for the light experiment) of culture was filtered for each sample replicate. The cultures were filtered under vacuum (10 inches of mercury) onto pre-ashed (4 – 6 hours at 450°C) 13 mm diameter Whatman GF/F filters. POC and PON are analyzed together using an Exeter 440 elemental CHN auto analyser (see section 2.8). The sample filters and blanks (blank filters and filters with media) were dried for approximately 24 hours at 60°C before being sealed in a container and stored in the dark until they were analysed. The filters were not rinsed with distilled water or NaCl to remove inorganic carbon (Goldman *et al*., 1985; Keller *et al*., 1999; Menden-Deuer *et al*., 2000; Collos *et al*., 2002; Sathyendranath *et al*., 2009). This was to avoid cell disruption which ultimately compensates for the small fraction of inorganic carbon content measured as POC (Collos, 2002). The absolute error from the POC correction from blank filters is 3.9 (or 6% relative error) and the absolute error from the POC correction from the media filters is 18.6 (or 29% relative error). To calculate the amount of organic carbon and nitrogen in the

samples, the CHN instrument was calibrated with acetanilide (C_8H_9NO) standards of known weight, as this substance has a similar C:N ratio (C:N = 8) to that of phytoplankton (C:N = 6.625 after Redfield 1934) (Nollet, 2007).

2.1.9 Exeter CE440 Elemental CHN auto analyser

The Exeter CE440 elemental analyzer uses combustion of weighted samples (usually between 1 – 3 mg) under static conditions in pure oxygen in order to analyse the organic and inorganic content of carbon, hydrogen and nitrogen within each sample.

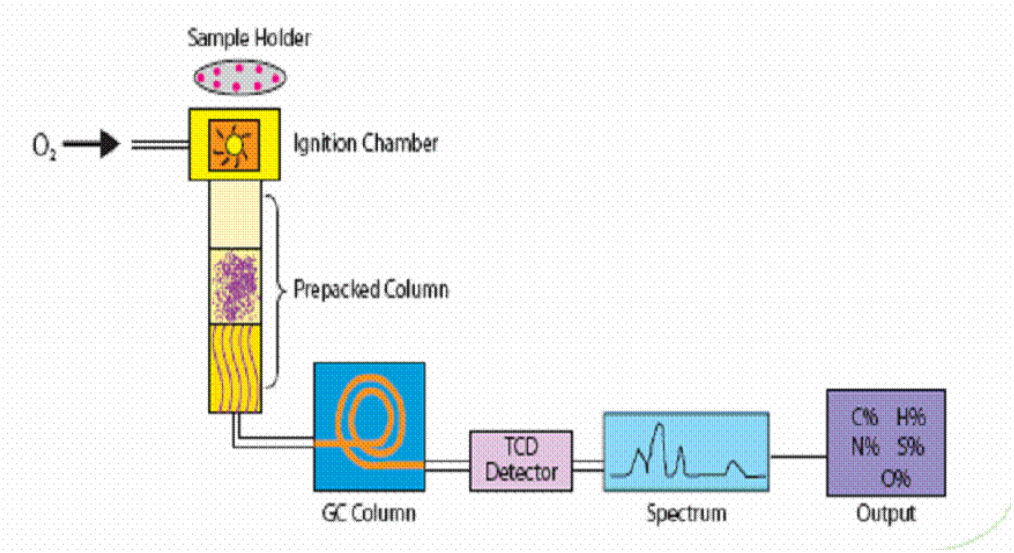

Figure 2.6 Schematic for the Exeter CE440 elemental analyser. (see below). IIT Bombay, 2014.

Helium carries the combusted products through the analytical system. Samples are combusted then transported to the prepacked column where the reagents ensure complete oxidation and by-product removal. The samples are carried to a mixing area for homogenization before entering the GC column for separation and a thermal conductivity detector where traps allow for differential signal readings. Through the analytical system, the combusted products are passed over reagents to assure complete oxidation and removal of by-products; here the oxidation process oxides the nitrogen and converts it to molecular nitrogen. This is then carried to a mixing area where it is homogenized under a specific temperature, pressure and volume and then

released into a thermal conductivity detector. In the thermal conductivity detector, a differential signal can read water content before the thermal conductivity cells remove it and then again afterwards, this water concentration differential determines the amount of hydrogen present in the combustion products. A similar process occurs subsequently, where another set of differential signals measure the carbon dioxide content before and after the thermal conductivity detector traps and removes it, the differential measurements of the concentration of carbon dioxide before and after the secondary thermal conductivity cells perform, gives the determination of the carbon content of the combustion products. By this stage, all that remains is the nitrogen and the helium used to transport the combustion products. This gas mixture then passes through another thermal conductivity cell and the output signal measured by the differential signal compares it with the reference cell through which only pure helium flows. Hence, determination of the nitrogen concentration can be determined.

The analyzer was calibrated using pre-weighed (between 1600 –2000 μg) standards of acetanilide. Weights of acetanilide standards are used to generate K factors (calibration factors); the analyser generates a signal that is directly proportional to the compounds that are being analysed (in this case, C, hydrogen (H_2) and N), so the following formula is employed by the Exeter analyser, where the K measurement is determined by the experimenter.

$$\text{Weight} = 1/K * 1/W * (R-Z-B) * 100$$

Where K is the calibration factor (acetanilide), W is the weight, R is the sample weight, Z is the zero reading of the instrument and B is the blank single generated by the instrument. The K factors of acetanilide for carbon are 71.09%, 6.71% for hydrogen and 11.84% for nitrogen (Exeter CHN manual available at: http://www.eai1.com/ce440.htm).

2.1.10 Particulate organic phosphorus

Particulate organic phosphorus (POP) was analyzed to enable comparison against the Redfield ratio. Analysis was achieved using the persulfate wet

oxidation method (Suzumura, 2008 – as detailed below). Culture aliquots (5 – 15 ml) were filtered under vacuum onto pre-ashed 25 mm diameter 0.7 μm pore size Whatman GF/F filters. The samples were stored at -20°C until analysis for no longer than 18 months. For the analysis, the filter samples, standards and blanks (filter blanks and filters with media) were placed into 50 ml Duran borosilicate glass bottles with 18 ml of 3% $K_2S_2O_8$ solution and autoclaved for 30 minutes at 120°C in order to hydrolyse the POP to orthophosphate (PO_4). Once cooled, the acidity of the solution is reduced using Milli-Q © water. Then 10 ml of mixed reagent is added according to Strickland and Parsons (1972) (see below) and then measured using a colorimetric analysis method (Strickland and Parson, 1972) (see below). The measurement of the standards gave a linear regression that was used to calculate the orthophosphate concentration in the samples.

2.1.10.1 Digestion protocol (Suzumura, 2008)

Reagents required:

- 3% Potassium persulfate solution [$K_2S_2O_8$]

Prepare 3% persulfate solution to the required volume.

Preparation and digestion:

Prepare 50 ml Duran bottles washed in 10% Decon 90 © and rinsed thoroughly with Milli-Q © water. Add the dried GF/F filtered samples, blanks and standards (standards prepared according to Strickland and Parsons, 1972). Then dispense 18 ml of the 3% $K_2S_2O_8$ solution and autoclave for 30 minutes at 120°C.

Once the samples are cool, reduce the acid solution to <2% and increase the pH to >1.5 by adding 18 ml of Milli-Q © water.

Add 10 ml of the mixed reagent according to Strickland and Parson (1972) (see below). Wait at least 10 minutes before measuring the absorbance but measure within two hours after the onset of mixing the samples with the mixed reagent.

2.1.10.2 Colorimetric analysis method (Strickland and Parsons, 1972)

Reagents required:

- Ammonium paramolybdate [$(NH_4)_6Mo_7O_{24}$]
- Sulphuric acid [H_2SO_4]
- Ascorbic acid [$C_6H_8O_6$]
- Potassium antimonyl-tartrate [$K_2Sb_2(C_4H_2O_6)_2$]
- Anhydrous potassium dihydrogen phosphate [KH_2PO_4]

Reagent preparation:

- $(NH_4)_6Mo_7O_{24}$: Dissolve 15 g in 500 ml of Milli-Q © water. Store in a dark plastic bottle. This solution is stable indefinitely.
- H_2SO_4: Add 140 ml of concentrated acid to 900ml of Milli-Q © water. Allow to cool and store in a glass bottle. The solution is stable indefinitely.
- $C_6H_8O_6$: Dissolve 27 g in 500 ml of Milli-Q © water and store in the freezer in a plastic bottle. Thaw for use, and then refreeze. The solution is stable for many months but should not be kept at room temperature for longer than one week.
- $K_2Sb_2(C_4H_2O_6)_2$: Dissolve 0.34 g in 250 ml of Milli-Q © water. Store in a glass or plastic bottle. The solution is stable for many months.

Mixed reagent: Mix together in a dark glass bottle:

- 100 ml of $NH_4)_6Mo_7O_{24}$; 250 ml of H_2SO_4; 100 ml of $C_6H_8O_6$ and 50 ml of $K_2Sb_2(C_4H_2O_6)_2$. This solution will remain stable for 6 hours. Ensure that the samples are cooled to room temperature before adding the mixed reagent. Use 1/10 of mixed reagent:sample.
- Stock solution (standard) KH_2PO_4: Dissolve 0.1361 g in Milli-Q © water – make final volume up to 1 litre. This equates to 1mM. This solution is stable for several months.

2.1.10.3 Colorimetric determination procedure:

Dilute the stock solution of the standard with 3% $K_2S_2O_8$ to make known concentrations to use for the calibration curve. For example: 0, 0.025, 0.5, 0.1 and 0.2 um. Digest these samples as above.

Measure the absorbance with a spectrometer at 885 nm. Calculate the concentration of the samples (Beer's Law) by using the calibration curve of the known concentrations.

3 Chapter 3: Temperature effects on physiology

3.1 Abstract

The growth rates of ten members of the nanophytoplankton over five taxonomic classes as a function of temperature have been measured. Among the chlorophytes (n = 4), *Pseudoscourfieldia cf. marina* grew fastest at tropical temperatures (μ_{max} = 0.94 d^{-1} at 30°C). The haptophytes (n = 4) were all largely consistent, all growing fastest in subtropical to tropical temperatures. Of the two remaining classes, the dinoflagellate (n = 1) had a temperature optimum of 20°C, and the chrysophyte (n = 1) at 15°C. These were all largely consistent with optimal growth rates at subtropical to tropical temperatures. Eppley's assumptions (1972) were statistically tested; his assumptions are that the response of a single species can be best described by an optimum function and that the mean community growth is better explained by an exponential fit. The nanophytoplankers measured here conform to the first but not the second of Eppley's assumptions. Temperature dependent growth of all species measured separately and the community fitted to an optimum function.

If Q_{10} values are used when considering members of the nanophytoplankton, with increasing climate change and warming of sea surface temperature (SST), they may be outcompeted by faster growing PFTs (or those with higher Q_{10} values). It is assumed in the literature that growth rates increase exponentially (Q_{10}) with temperature (Montagnes *et al*., 1994). Since nanophytoplankton does not follow the Eppley curve at warmer temperatures, the results may suggest that the Eppley assumptions cannot be used to describe nanophytoplankton or that these species are already distributed near to their geographical optima.

3.2 Introduction

With global climate change predicted to increase the sea surface temperature considerably, it becomes important to know how this will affect marine

organisms in order to predict future changes in marine ecosystems and ecosystem services.

Temperature is a key determinant of algal physiology and its effect on algal biology is well documented (e.g. Eppley, 1972; Foy *et al*., 1976; Vogel, 1981; Raven *et al*., 1988). A considerable amount of laboratory research has been done on plankton cultures that are known to be key players in the biogeochemical cycle, in particular the carbon cycle (Montagnes *et al*., 2001; Buitenhuis *et al*., 2008; Claquin *et al*., 2008). More emphasis has been given to larger organisms such as diatoms (2 – 200 μm), dinoflagellates (5 – 2000 μm) and coccolithophores (2 – 20 μm), and less attention has been given to non-calcifying members of the nanophytoplankton (2 – 20 μm) and the other smaller size class cultures such as picophytoplankton (< 2 μm) (Henson *et al*., 2011). It is necessary to have physiological data on a wide range of plankton functional types (PFTs) in order to model the effects of climate change on ocean ecosystems (Le Quère *et al*., 2005). This is becoming more apparent since literature reviews are suggesting that ecosystem structure is probably more important than size or ballasting effects for the carbon cycle (Henson, 2011; Francis *et al*., 2012) and that current regime shifts with changing climate are suggesting dominance towards smaller (eukaryotic) size classes (Beaugrand, 2004; Henson, 2011). However, this is not to suggest that temperature is the only, or the most important environmental factor affecting marine ecology.

Eppley (1972) compiled the maximum growth rates of approximately 130 species and strains between 2°C and 40°C and from this data set he suggested that:

1) The temperature dependent maximum growth rates of single phytoplankton species fit best to an optimum function.

2) The temperature dependent maximum growth rates of the whole phytoplankton community fit best to an exponential function.

Eppley (1972) did not verify these assumptions statistically. Montagnes e*t al*. (2003) showed that for individual species, a linear increase fitted better than an

exponential fit in the majority of cases. However, they did not test for an optimum function, nor did they test the whole phytoplankton community. Eppley estimated the maximum community growth but due to the high variability in physiological response of different PFTs to environmental conditions, PFT models need data from individual temperature parameters in order to more accurately determine their effects (Le Quéré *et al*., 2005).

In an attempt to address the relative sparseness of data on nanophytoplankton, the growth rates of ten nanophytoplanker species at thirteen temperatures ranging from 0°C to 32°C was determined, the latter being the predicted maximum sea surface temperature by the end of the century under the RCP8.5 scenario (Rayner *et al*., 2006; IPCC 2007). In addition, the cultures were sampled at these thirteen temperatures for cellular composition analysis; these results will be presented in Chapter 5.

3.3 Materials & Methods

3.3.1 Culture media

See sections 2.1.1 and 2.1.2 for strains and media. The cultures were grown as 45 ml batch cultures in 55 ml borosilicate glass (Pyrex Brand 9826) vials in the temperature gradient bar (TGB) and allowed to acclimate for two weeks. Each species was subcultured after one week of acclimation.

3.3.2 Light and temperature

Table 3.1 show light was maintained at 240 ± 21 μmol photons m^{-2} s^{-1} with a 14:10 light:dark (LD) cycle. The light intensities were measured using a Scalar PAR (QSL2101 Light Biospherical Instrument, San Diego, USA). Temperatures were measured using a Grant ® Squirrel (Grant instruments 1000 series).

Table 3.1 Mean light and temperature measurements (± the standard deviation) in the temperature gradient bar.

Column	Mean temperature °C	Mean light intensity µmol photons m^2 s^{-1}
1	3 ± 0.4	173 ± 13
2	5 ± 0.6	210 ± 8
3	8 ± 0.5	190 ± 9
4	10 ± 0.3	210 ± 7
5	12 ± 0.2	197 ± 11
6	15 ± 0.3	184 ± 9
7	17 ± 0.2	186 ± 9
8	20 ± 0.2	256 ± 9
9	22 ± 0.2	254 ± 7
10	25 ± 0.3	241 ± 3
11	27 ± 0.2	232 ± 8
12	30 ± 0.2	345 ± 53
13	32 ± 0.3	433 ± 24

3.3.3 Cell composition sampling

Samples for Chl, POC/PON and POP were taken at the end of the logarithmic growth phase. For analytical procedures see Chapter 2 (Sections 2.1.7; 2.1.8; 2.1.10).

3.3.4 Calculations and statistical analysis

Growth rates (µ) as a function of temperature (T) were fitted to three equations:

A linear fit (Lin) (Montagnes *et al*., 2001):

Equation 3.1 $\mu_{max} = \mu_{max,\ 0°C} + slope * T$

An exponential fit (Exp) (Bissinger *et al*., 2008):

Equation 3.2 $\mu max = \mu max,\ 0°C * Q_{10}(T/_{10})$

And finally an optimal function (Opt) (Schoemann *et al*., 2005):

Equation 3.3 $\mu max = \mu_{max} = \mu_{Opt} * \exp[-(T-T_{opt})^2/\ dT^2]$

Where $\mu_{max,\ 0°C}$ is the maximum growth rate at 0°C, Q_{10} is the increase in growth rate as a consequence of a 10°C increase in temperature, μ_{Opt} is the optimal growth rate, T_{opt} is the optimal temperature, and dT is half the width of the growth rate peak at μ_{opt}/e.

Each parameter and its asymptotic error (A.S.E) was determined with a non-linear model fitting function in SYSTAT. The goodness of fit was calculated using Akaike's Information Criterion (AIC). The AIC calculates the trade-off between the goodness of fit of the model and the complexity of the model (Burnham *et al*., 2004; Buitenhuis *et al*, 2008):

Equation 3.4 $AIC = n_{obs} \text{ Log } (\sigma 2) + 2n_{param}$

Where n_{obs} is the number of observations $\sigma^2 = 1/ (n_{obs} - n_{param}) * \sum (\mu_{obs} - \mu_{fit})$ and n_{param} is the number of parameters (i.e. the complexity of the model), μ_{obs} is the growth rate of each species at each temperature and μ_{fit} is the modeled fit to each of the above three equations (linear, exponential and optimal function). The best fit returns the lowest AIC value (including negative values) and the AIC for each fit is said to be significantly different if the difference between each one is greater than 2 (Burnham *et al*., 1998).

The μ_{opt} for all ten species was fit to the following equation (Sarthou *et al*., 2005):

Equation 3.5 $\mu_{opt} = x^* (v^y)$

Where v is cell volume.

The data were also compared to Eppley (Eppley equation converted into d^{-1}):

Equation 3.6 $\mu = 0.59 * 1.89^{(T/10)}$

The upper 99% quantile was estimated using the quantreg function in the software R © Version 3.1.0.

Statistical analyses were conducted in Sigmaplot © version 12.

3.3.5 Temperature gradient bar

The temperature gradient bar is an insulated zinc-plated steel device that was cooled at one end and heated at the other in order to generate a temperature gradient (Figure 3.1). It housed five rows and thirteen columns of wells and therefore could maintain sixty five cultures. The heated end comprised four thermostatically controlled heating pads (Omegalux SRFG-204/10-P) and the cold end was achieved with water mixed with antifreeze, circulated and thermostatically controlled with a refrigerated circulator (Haake DC50-K50). Each well was lit from below with an ultrabright LED (Winger WEPW1-S1 1W, 95 Lumen, white). The bar was insulated at the sides and top. A glass plate at the base of the TGB decreases condensation of water at the cold end of the TGB due to the temperature differential.

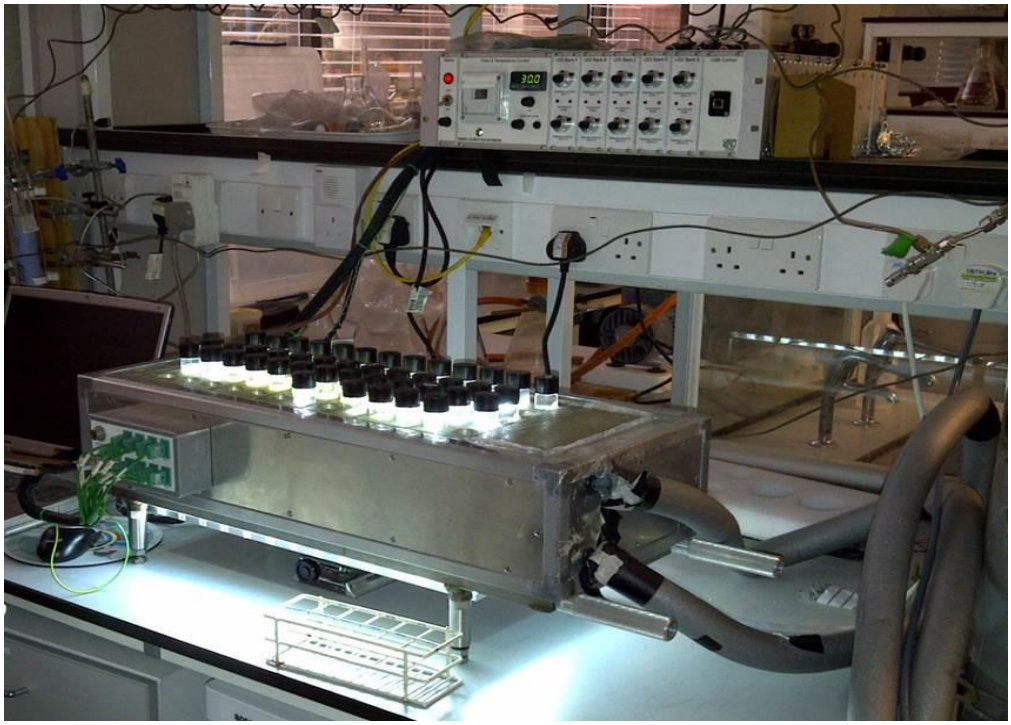

Figure 3.1 Photograph of the temperature gradient bar. The right end of the TGB is cooled by a water cooler, and the left end is heated. The insulated lid is not shown.

3.4 Results

3.4.1 Growth rates

Growth rate as a function of temperature was measured for ten species of nanophytoplankton. The first five cultures (1348, 1448, 261, 661 and 647)

were grown in f/2 media (Guillard, 1975; Guillard *et al*., 1962) and the second five (1406, 905, 916, 21 and 91) were grown in ESAW medium (Harrison *et al*., 1980; both available at: https://ncma.bigelow.org/). ESAW was chosen so that the fluctuations of trace constituents could be controlled. A comparison of the two media was conducted for the five species grown in ESAW at their optimum temperatures, which showed no significant differences (Student's T-test, n = 3, P = > 0.05, Table 3.2).

Table 3.2 growth rates at T_{opt} for cultures grown in ESAW as well as f/2 media.

Species RCC number	**1348**	**1448**	**905**	**261**	**661**
Mean μ at T_{opt} for f/2	0.73 ± 0.14	0.46 ± 0.23	0.58 ± 0.24	0.90 ± 0.18	0.59 ± 0.25
Mean μ at T_{opt} for ESAW	0.26 ± 0.10	0.52 ± 0.06	0.79 ± 0.83	0.72 ± 0.10	0.26 ± 0.01
P value	0.077	0.561	0.556	0.062	0.240

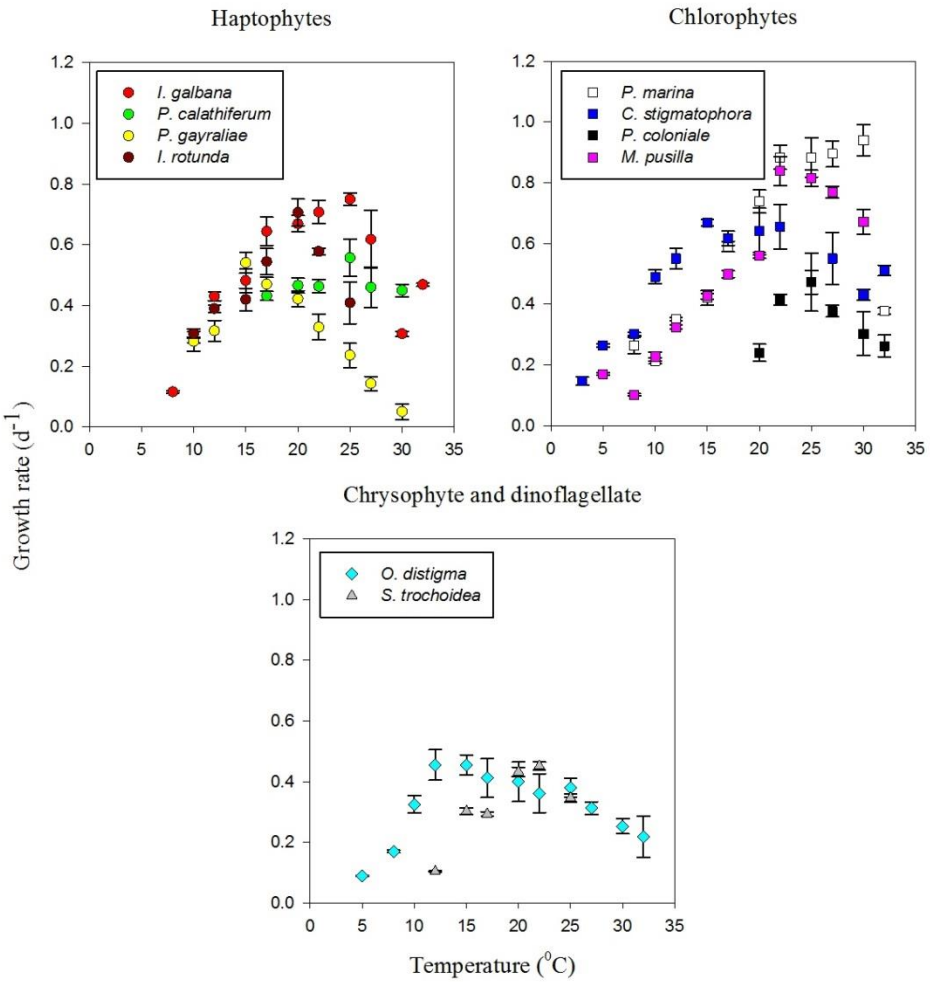

Figure 3.2 Mean growth rates of ten nanophytoplankton species as a function of temperature with standard error bars.

Nanophytoplanker growth rates increase with increasing temperature (Figure 3.2) up to maxima (μ_{Opt}) at their temperature optima (T_{opt}) where the growth rates begin to decrease with increasing temperature. Of the haptophytes, *I. galbana* showed growth across the larger temperature range (8 – 32°C), and. *P. calathiferum* across the smallest range (17 – 30°C). Of the chlorophytes, *C. stigmatophora* showed growth across the largest temperature range (3 – 32°C), and *P. coloniale* across the smallest range (20 – 32°C). The two species with the largest average cell volume (the chrysophyte at 84 μm^3/cell and the dinoflagellate at 258 μm^3/cell) showed the slowest growth rates ($\mu_{max} < 0.5\ d^{-1}$ *vs*.$\mu_{opt} = 0.90$ for *P. marina*).

The observed positive growth rates were fitted to three equations for growth rate as a function of temperature (linear, exponential and optimal function). The parameters for each of the fits can be seen in Table 3.3. The optimum function model did predict the broadest temperature range for growth (dT = 17.4) for *P. calathiferum* despite it being one of three species showing a low growth range (growth over 6 temperatures – mean is 9). This is because of the large standard error for this species. The species with the largest observed range of growth over the recorded temperatures was *C. stigmatophora* which showed the second broadest predicted temperature range (dT = 16.4).

The model best fit (Table 3.3) was the optimum function. The mean absolute observations were compared to that of the optimum function by calculating the error with the average error from the replicates. The optimum function showed a 22% deviation from the observations.

Table 3.3 model parameter fits (equations 3.1 – 3.3) and the AIC values (equation 3.4) fitted through the data sets (n = 92). The best model fit is indicated in red**.**

Species	n	Linear μ max, 0 °C	slope	Exponential μ max, 0 °C	Q10	Optimum function μ opt (d^{-1})	T opt (°C)	dT (°C)	AIC Lin	Exp	Opt
I. galbana	11	0.285	0.011	0.100	1.800	0.726	21.919	11.96 ± 1	**-11.8**	**-8.0**	**-17.8**
P. calathiferum	6	0.300	0.002	0.300	1.043	0.502	24.240	17.4 ± 6	**-5.7**	**-5.0**	**-10.6**
I. rotunda	7	0.120	0.014	0.120	1.276	0.611	19.386	10.3 ± 2	**-6.0**	**-2.0**	**-9.7**
P. gayraliae	9	0.100	0.005	0.100	1.440	0.444	17.856	13.6 ± 3	**-7.9**	**-8.0**	**-14.8**
P. coloniale	6	0.100	0.010	0.100	1.260	0.441	25.398	8.1 ± 1	**-6.9**	**-3.8**	**-9.3**
C. stigmatophora	13	0.327	0.009	0.368	1.166	0.653	20.309	16.4 ± 2	**-18.0**	**-17.6**	**-23.6**
P. marina	11	0.131	0.023	0.310	1.375	0.902	24.398	11.9 ± 2	**-10.6**	**-9.9**	**-13.9**
O. distigma	12	0.285	0.002	0.293	1.047	0.442	18.936	13.9 ± 2	**-18.1**	**-18.1**	**-23.3**
M. pusilla	11	-0.024	0.030	0.186	1.681	0.783	25.451	13.6 ± 2	**-17.1**	**-14.8**	**-19.8**
S. trochoidea	6	-0.054	0.020	0.119	1.691	0.441	21.174	8.2 ± 1	**-8.6**	**-8.1**	**-10.3**

Table 3.4 model parameter fits (equations 3.1 – 3.3) and the AIC values (equation 3.4) fitted through the data sets (n = 92 and n = 439). The best model fit is indicated in red**.**

	Linear				Exponential				Optimum function						AIC		
n =	μ max, 0 °C	A.S.E	slope	A.S.E	μ max, 0 °C	A.S.E	Q_{10}	A.S.E	μ opt (d^{-1})	A.S.E	T_{opt} (°C)	A.S.E	dT (°C)	A.S.E	Lin	Exp	Opt
92	0.25	0.051	0.010	0.002	0.45	0.035	1.06	0.035	0.56	0.025	22.4	0.823	15.5	1.50	-131.40	-125.441	-142.014
439	0.42	0.030	0.005	0.001	0.429	0.026	1.09	0.03	0.57	0.018	21.4	1.020	23.8	2.71	-523.77	-523.328	-529.941

Figure 3.3 shows that there is no relationship between T_{opt} and isolation latitude (P = 0.06. The two species with the narrowest growth width were of the most tropical isolates coming from an isolation latitude of 8°20'S and 14°64'N respectively (Table 2.1). There is a statistically significant relationship between dT and isolation latitude (P = 0.008) however, none of the results from the dT parameter were statistically significantly different from one another across the range of species (Student's T-test, P = > 0.05; n = 10). There is no significant difference between mean optimum growth temperatures (T_{opt} = a ± b, P = 0.53) or the optimum growth rates (μ_{opt} = a ± b, P = 0.5).

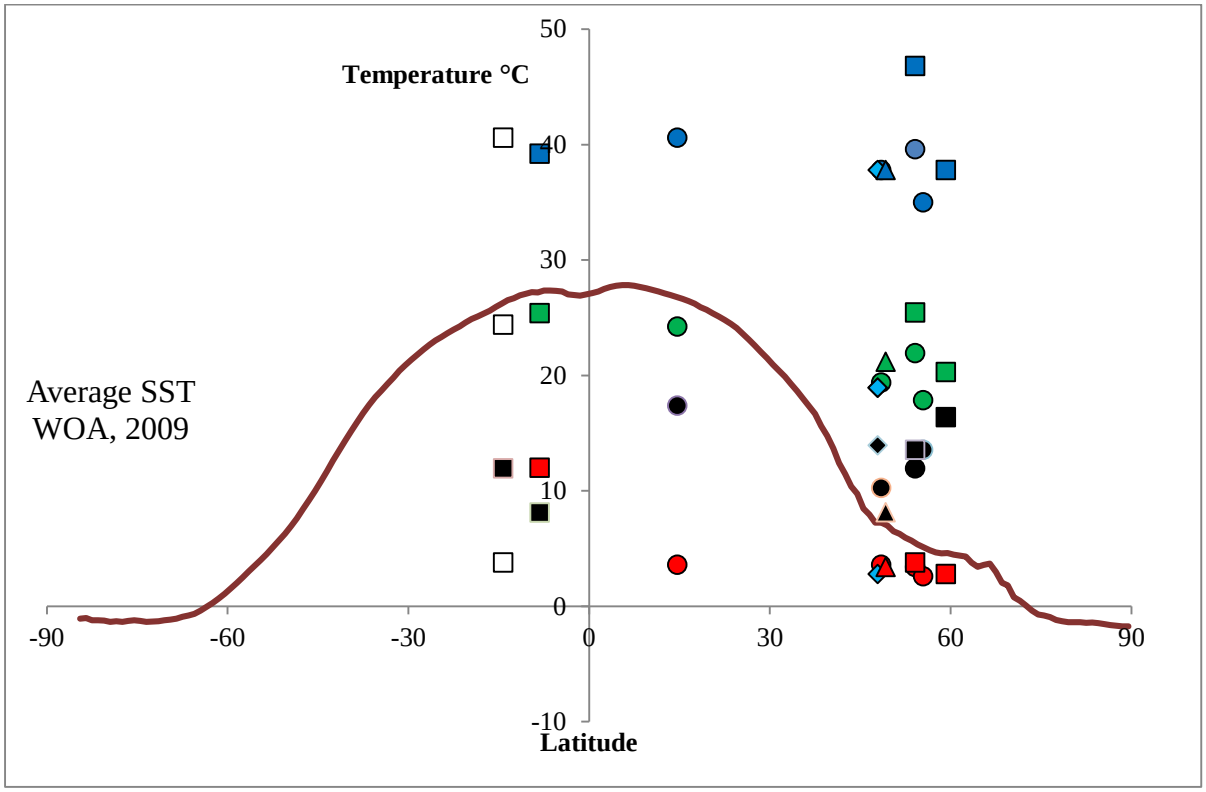

Figure 3.3 T_{max}, T_{opt} and T_{min} *vs.* isolation latitude. The haptophytes are represented by filled circles. The chlorophytes are represented by filled squares, the chrysophyte is represented by filled diamonds and the dinoflagellate is represented by an up facing filled triangle. Blue shows T_{max}, green shows T_{opt}, red shows T_{min} and black shows dT. T_{opt} was taken from the optimal fit. T_{min} and T_{max} were taken as the last observations with positive growth rates. The line is the zonally averaged sea surface temperature (SST) from the World Ocean Atlas, 2009 (NOAA, 2009).

The AIC values clearly indicate that for all the data (presented as individual species or collectively as a PFT) the optimal function is consistently better (more negative) (Table 3.3). For the dinoflagellate *S. trochoidea* the linear model was not significantly worse than the

optimum function. The linear and the exponential models have similar results (ΔAIC < 2) for 60% of the species (*P. calathiferum*, *P. gayraliae*, *C. stigmatophora*, *P. marina*, *O. distigma* and *S. trochoidea*). In the other species the exponential model gave the worst fit.

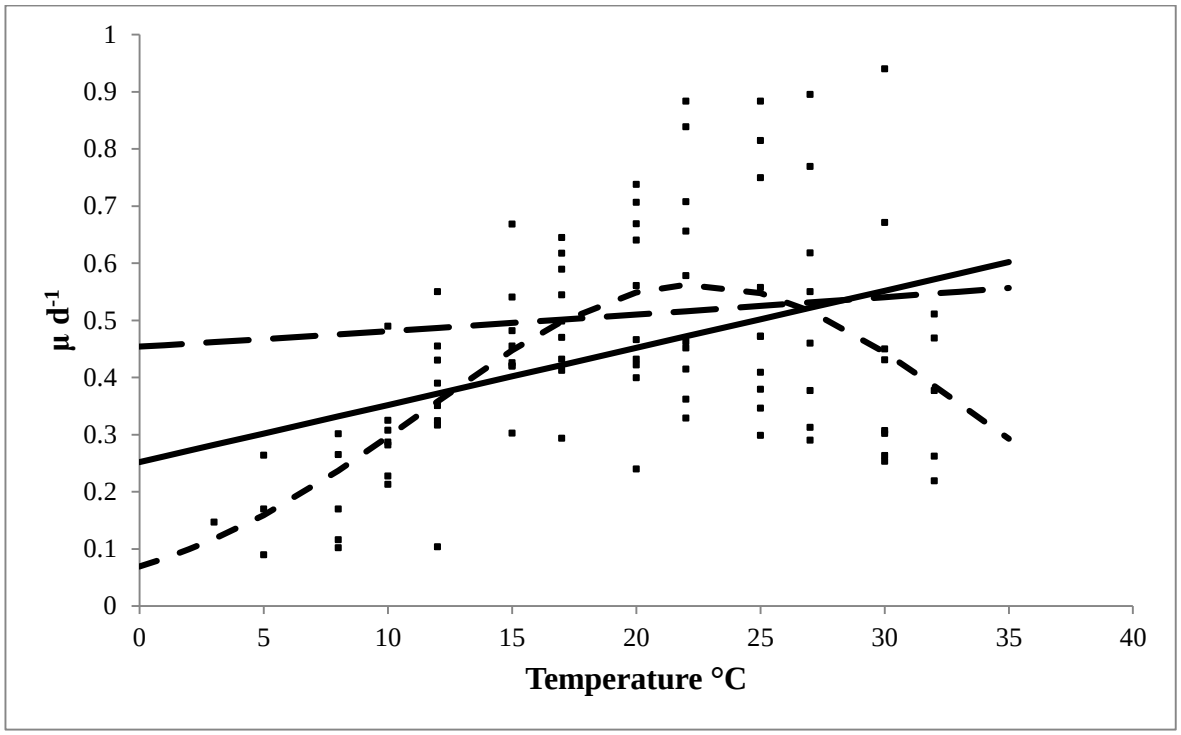

Figure 3.4 Observed mean growth rates of all the species (n = 92) (dots) with standard error bars, fitted with the three equations for measuring growth rate as a function of temperature. Linear – straight lines; exponential – long dash and optimal function – short dash.

Figure 3.4 shows the three model equations fitted to the mean growth rates of all species (n = 92). The optimum function is the best fit (AIC = -142) compared to the fits for the linear and exponential models (AIC = -131 and AIC = -126 respectively).

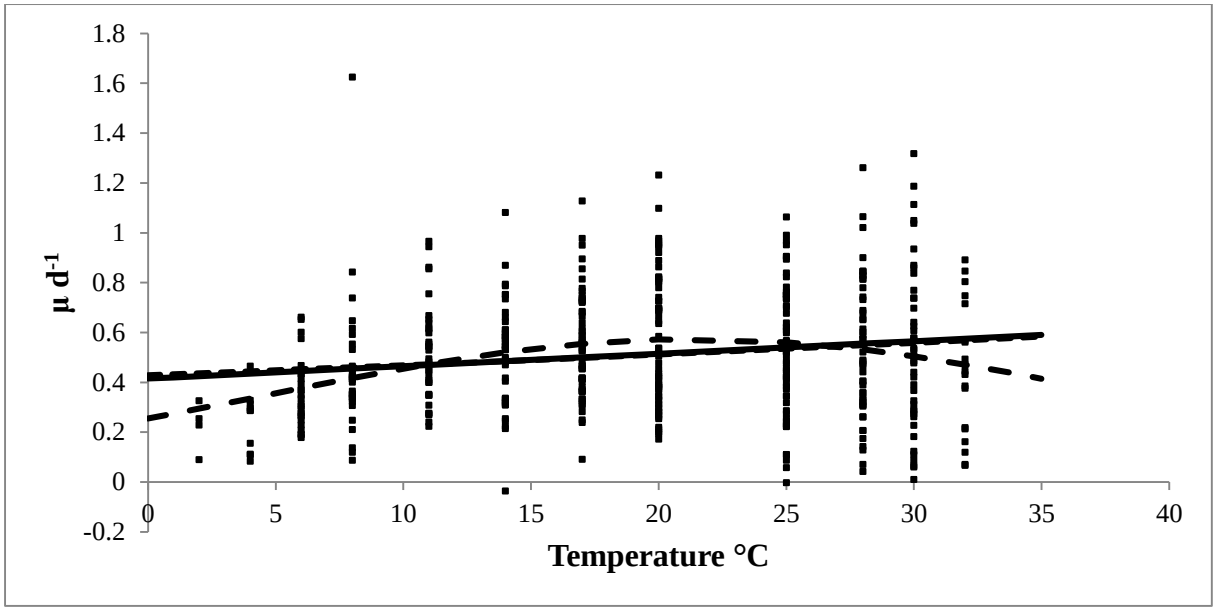

Figure 3.5 Observed growth rates of all the species (n = 438) (dots) fitted with the three equations for measuring growth rate as a function of temperature. Linear – straight lines; exponential – long dash and optimal function – short dash.

Figure 3.5 shows the three model equations fitted to the entire data set (n = 438). The optimum function is the best fit (AIC = -530) than both the linear and exponential models (AIC = -524 and AIC = -523 respectively).

3.4.2 PFT comparison

Table 3.5 Regression coefficients with their standard errors for the log transformed growth rate data for a linear 99% quantile.

	Intercept	Standard Error	Slope	Standard Error
Nanophytoplankton	-0.076	0.19	-0.403	0.69

The 99% quantile regression for all nanophytoplankers (n = 438) gives a low Q_{10} of 1.1 (Equation 3.6). The average Q_{10} for the individual nanophytoplanker species was 1.68 ± 0.5 (n = 10). A few species showed much lower Q_{10} values (*P. gayraliae* with a Q_{10} of 0.87 and *P. coloniale* at 0.95).

Equation 3.7 $\mu_{Nano} = 0.93 * 1.1 (T/^{10})$

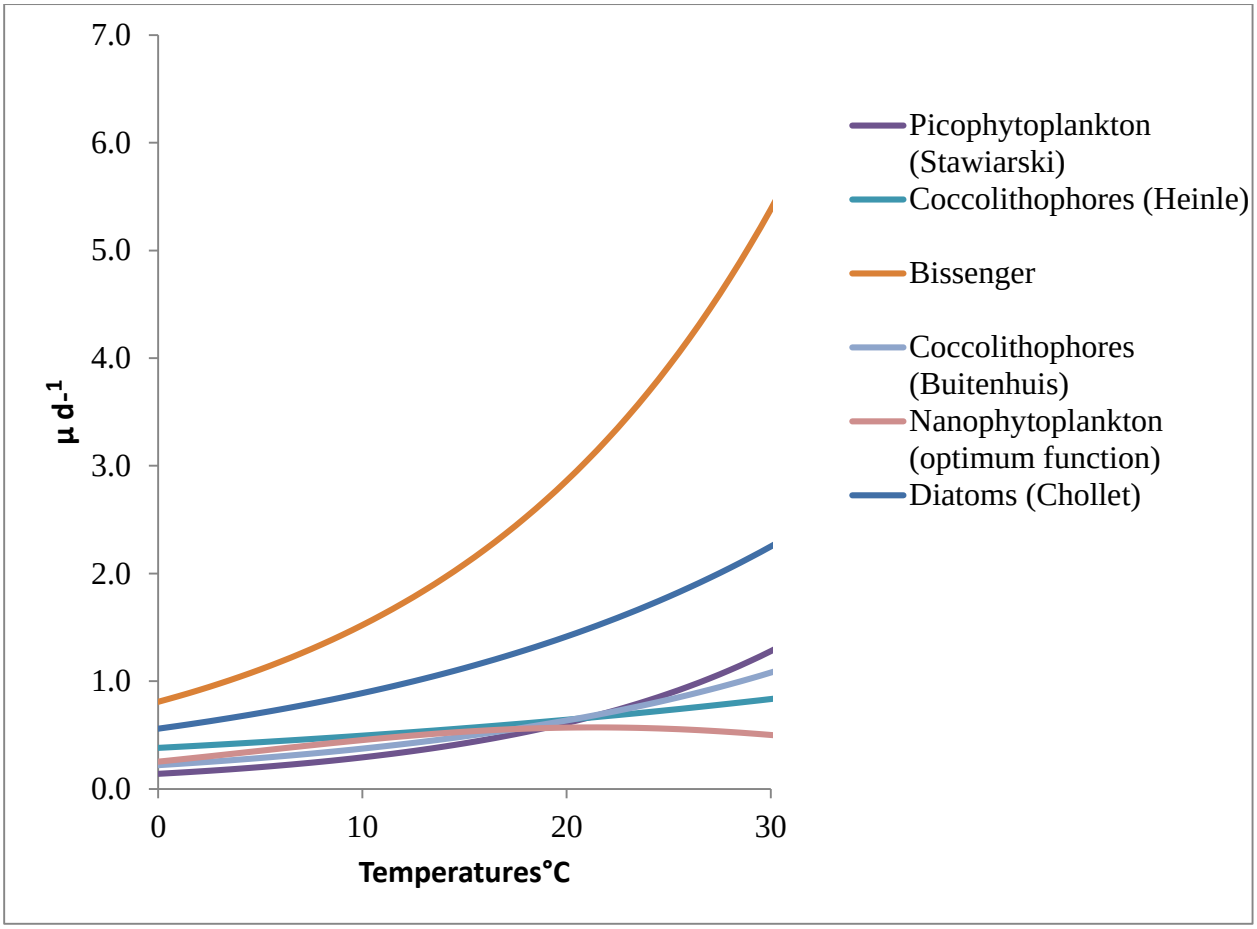

Figure 3.6 Nanophytoplankton best community fit (optimum function) (pink) compared to exponential best fits from other PFTs (through the data). In size order - diatoms (Chollet, 2013); coccolithophores (Heinle, 2014); coccolithophores (Buitenhuis *et al*., 2008); picophytoplankton (Stawiarski, 2014). The orange line is the comparison to the 99% quantile from Bissinger *et al*., 2008.

Figure 3.6 shows 99% quantiles for several PFTs. Picophytoplankton have low maximum growth rates at lower temperatures up until approximately 23°C where their growth rates are much higher than all other PFTs except for the diatoms. Picophytoplankton are well adapted to higher temperatures. Diatoms have higher growth rates at all temperatures, possibly because they uniquely have vacuoles for energetic storage and to increase their surface to cytoplasm volume ratio. The coccolithophores (Heinle, 2013 and Buitenhuis *et al*., 2008) and the nanophytoplankton all have similar growth rates up until approximately 20°C. The plot shows PFT data compared to the 99% quantile from the Bissinger paper (Bissinger *et al*., 2008). This database has all these PFTs (as well as more) and includes a database of 1501 observations. The Bissinger curve is actually higher that the Eppley curve for all measured temperatures (Bissinger *et al*., 2008). For temperatures below 19°C, the Eppley curve falls

below the 95% confidence internal of the Bissinger curve. The Q_{10} value from the Bissinger curve is actually exactly the same as the estimate from Eppley (1.88) (Eppley, 1972); therefore they conclude that it supports the use of models that incorporate Q_{10} estimates of phytoplankton growth-rate response to temperature change (Bissinger *et al.*, 2008), but presumably only for larger databases.

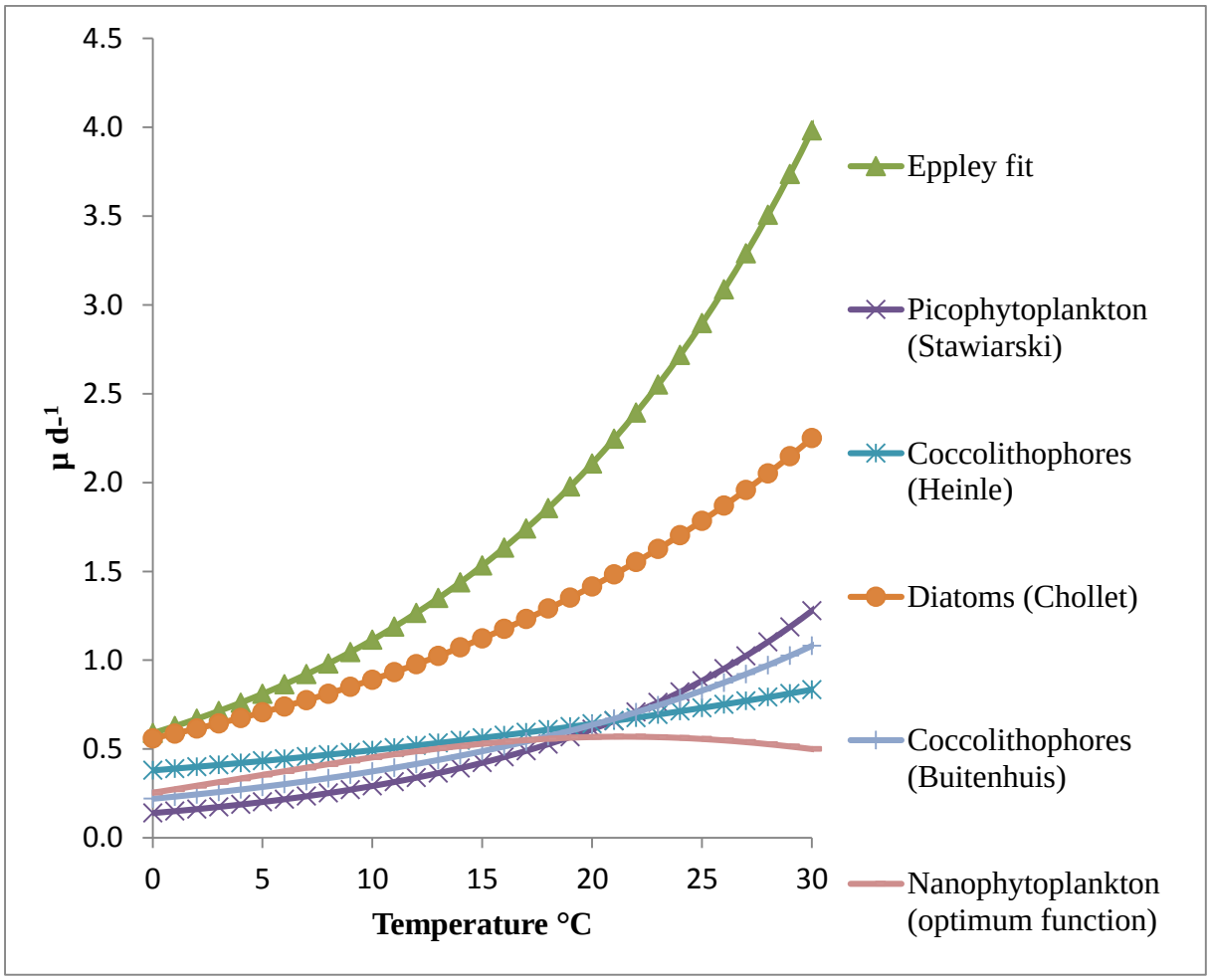

Figure 3.7 Nanophytoplankton best community fit (optimum function) (pink) compared to exponential best fits from other PFTs (through the data). The green line is the Eppley fit (1972).

When Figure 3.7 is compared with Figure 3.6 it can be seen that the Bissinger *et al.*, 2008 fit is not realistic when compared to the empirical data for this smaller data base. Growth rate estimates are 36% higher in the Bissinger fit compared to Eppley. Moreover, the Eppley fit is also not realistic when compared to the empirical data for these PFTs. Collectively, these PFTs differ from Eppley by 63% and differ from Bissinger by 73%.

3.4.3 Cell volume

At low rates of growth literature reviews state phytoplankton has more time and energetic resources to build up biomass; this is generally reflected in their cell volume (Brown *et al*., 2004). A regression analysis was performed with 30% of the tested nanophytoplankers having a statistically significant inverse relationship of cell volume *vs*. temperature dependent growth rate (Figure 3.8). For *I. galbana* – r^2 = 0.92, *P. gayraliae* – r^2 = 0.91 and *O. distigma* – r^2 = 0.99.

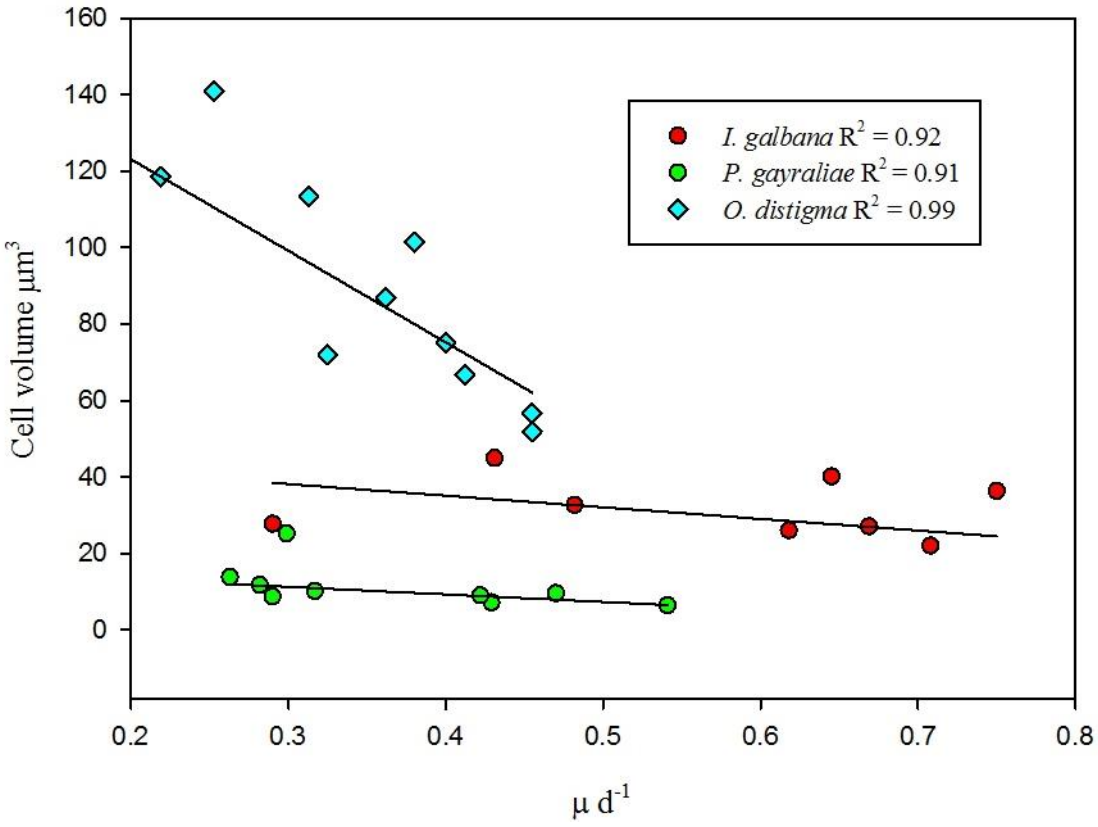

Figure 3.8 30% of nanophytoplankers showing an inverse relationship between cell volumes *vs*. temperature dependent growth rates. Haptophytes are in circles. Chlorophytes are in squares. The chrysophyte (*O. distigma*) is a cyan diamond. The r^2 value is shown in the legend.

On an individual level members of the nanophytoplankton show exceptions; 30% of nanophytoplankers tested (*P. marina* – r^2 = 0.99, *S. trochoidea* – r^2 = 0.99 and *C. stigmatophora* – r^2 = 0.94) show a statistically significant relationship between temperature dependent cell volume and growth rate (Figure 3.9). The other 40% either showed a weak relationship, or no statistical significance.

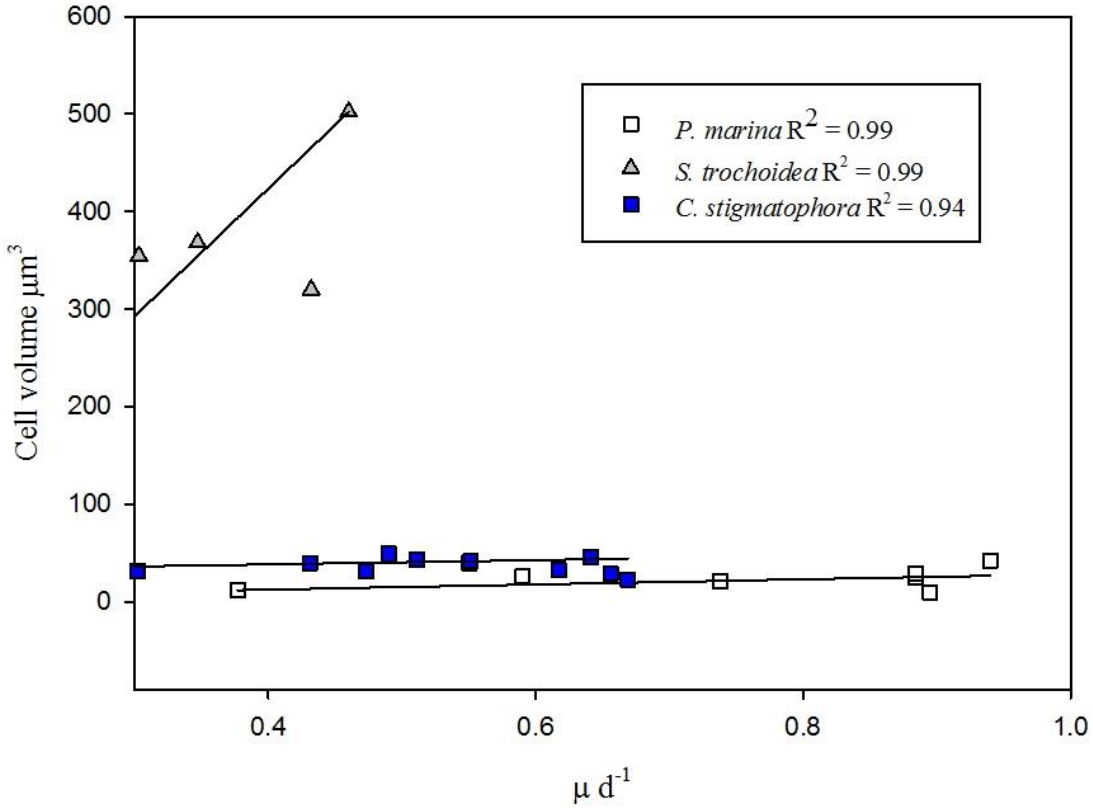

Figure 3.9 30% of nanophytoplankers showing a statistically significant relationship between cell volumes and temperature dependent growth rates. Chlorophytes are in squares. The grey triangle (*S. trochoidea*) is the dinoflagellate. The r^2 value is shown in the legend.

Between different species, cause and effect run the other way, and there is an expected inverse relationship in the literature of growth rate with cell volume. Large cells have a lower surface to volume ratio, which leads to lower volume specific nutrient uptake rates. Figure 3.10 shows the optimum growth rate μ_{opt} decreases as a function of the cell volume. The fit to Equation 3.5 shows a relatively small dependence on cell volume with an exponent of -0.095 (*vs.* -0.13 Sarthou *et al*., 2005 and -0.32 Buitenhuis *et al*., 2008).

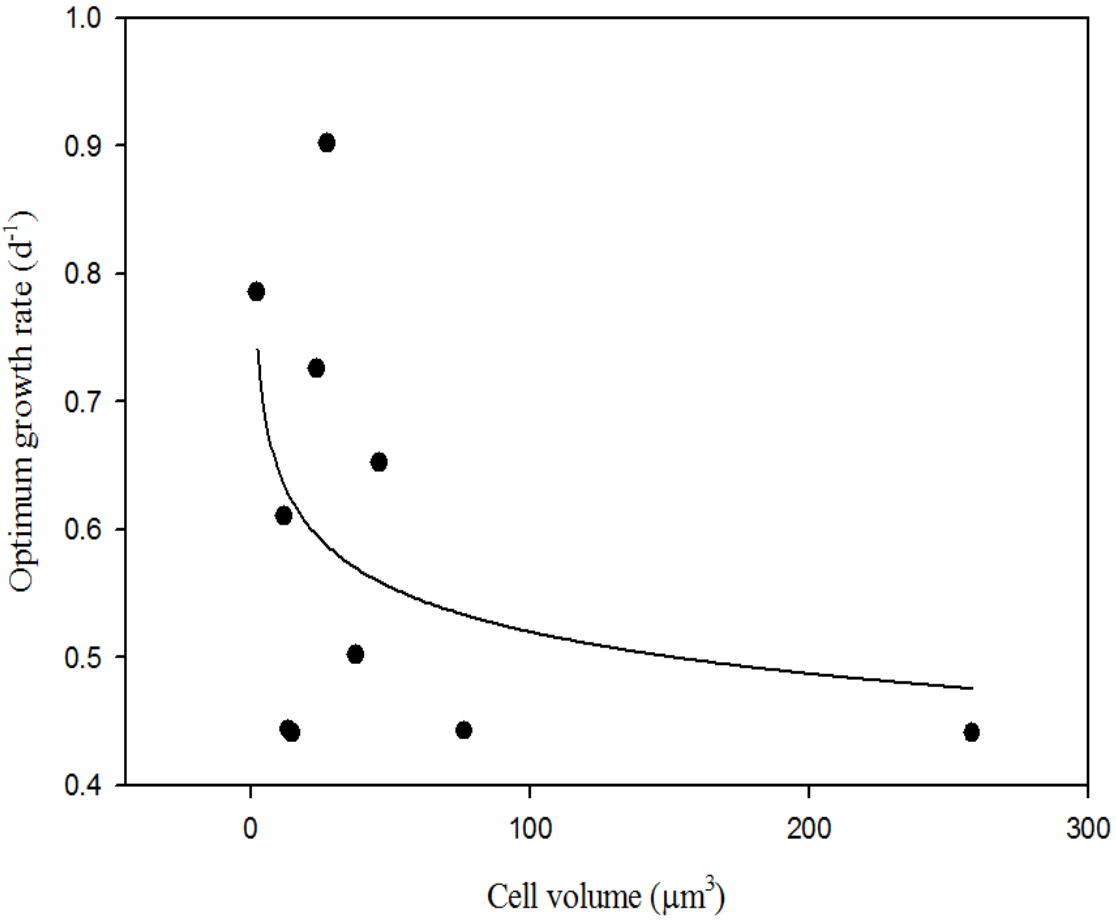

Figure 3.10 Mean optimum growth rate as a function of cell volume for all species. The line is fitted to equation 3.5:μ_{max} = 0.85 * (v^-0.095).

3.5 Discussion

3.5.1 The temperature dependent maximum growth rates of single nanophytoplankton species fit best to an optimum function

For all ten nanophytoplankton species the optimum function gives the best fit. Only for *S. trochoidea* was there also significant support for the linear equation. This is consistent with Eppley's assumption that for individual species the best way to describe the relationship between maximum growth rate and temperature is with optimum growth rates, optimum temperature and temperature tolerance ranges (Versteegh *et al*., 2001; Zhu *et al*., 1997; Molina Grima *et al*., 1994). Most of the temperature dependant growth rates determined here are for novel species apart from data for *M. pusilla* (Mc Rose, 2008) which shows the growth

rates of three (other) strains with 0.5-0.7 d^{-1} 0.2 at 12ºC; 0.5-1 0.5 d^{-1} at 18ºC and 0.5-1.2 0.7 d^{-1} at 21ºC. These results are in good agreement with the growth rate results shown here (0.5 d^{-1} for 17ºC and 0.84 d^{-1} for 20ºC); with the exception of the growth at 12ºC which was slighter lower at 0.33 d^{-1}.

In order to draw the conclusion that the optimal function shows the best fit to this data set one must be sure that the maximum growth rate data are reliable. The standard coefficients for all the mean maximum growth rates are always within 2% (n = 1) and more often within 1% (n = 91). Additionally, the standard errors were generally low with the highest being 0.09 and the lowest being 0.002. Growth rates used an average of five replications per culture (n = 22) and with a minimum of two replicates (n = 6) and a maximum of eight replicates (n = 2). Taken collectively this suggests that the maximum growth rates used in this data set are reliable and that the best fits to the optimal function are justified (22% deviation from observations). However, the relatively invariant growth rates near the optimum temperatures for some of the cultures suggest it is likely that deviations out with the T_{opt} lead to deviations of growth rate. It may be possible that these could have been light limited rather than temperature limited, since all of the cultures were grown at the same light intensity (240 ± 21 μmol photons m^{-2} s^{-1}). It is therefore possible that in some of the cultures with a preference for high light conditions the optimum growth rate may have been underestimated.

3.5.2 Temperature dependent maximum growth rates of a nanophytoplankton PFT fit best to an optimum function

Table 3.3 shows reasonable results for the optimum function compared to the empirical results for its parameter estimates. The $\mu_{max,\ 0°C}$ estimates are really high for both the linear and the exponential fits and for both the mean and entire data sets (n= 92 and n= 438 respectively), while the Q_{10} values for the exponential equation are low, presumably because the Q_{10} is inhibited by values above the T_{opt}. This could prove difficult for biogeochemical modelling, since this is one of the parameters calculated for temperature response in PFTs.

Where the use of the Q_{10} value assumes that of an Arrhenius relationship of temperature dependent reaction rates – a generalization is that for common chemical reactions at room temperature, the reaction rate doubles for every 10°C rise in temperature (Berges *et al*., 2002). The relationship between rates of chemical reactions and temperature therefore assumes chemical kinetics control the observations; as such, biological processes are

expected to have a Q_{10} near to 2. Unlike the exponential equation, the steepness of the Arrhenius equation is controlled by the activation energy (which varies between chemical reactions) that may limit growth and Q_{10} values may be higher than those of an exponential equation. A literature review has revealed that the Q_{10} value for the maximum specific growth rate (μ_{max}) for algal cultures grown in nutrient replete cultures with optimal growth temperatures between 5 and 40˚C is 1.88 (Eppley 1972). However, this value is often a lot higher in nutrient limited continuous cultures (Raven *et al*., 1988). Cultures grown at sub optimal temperatures also tend to show a Q_{10} value in excess of 1.88 (Raven *et al*., 1988).

The optimum fit for nanophytoplankton as a whole is in contrast with the Eppley whole community function. These results are in agreement with the results for coccolithophores in Heinle (2013), but in contrast to the results for coccolithophores in Buitenhuis *et al*. (2008) and for picophytoplankton in Stawiarski (2014). In diatoms there was about equal support for the optimum and exponential functions (Chollet, 2013). The contrast to the Buitenhuis *et al*. (2008) results could have been because the Buitenhuis study was conducted only to a maximum temperature of 25°C.

Eppley suggested that phytoplankton assemblages could be defined by an exponential relationship even though individual species better fit to an optimum function (Eppley, 1972). Since this time, this exponential relationship has been used widely in biogeochemical modelling. Other researchers have suggested that other relationships may be best suited to represent the general relationship of temperature dependent growth rates. For example, Raven *et al*., (1988) and Montagnes *et al*., (2001) suggested a linear relationship; and Schoemann *et al*., 2005 suggested an optimum function. For some PFTs, studies have shown a more linear increase in growth rate with increasing temperature, but over a narrower range of temperatures (Sorrosa *et al*. 2005, Schouten *et al*., 2006, Sarthou *et al*., 2005). Buitenhuis *et al*., (2008) determined which growth fit would best represent the temperature dependent growth rates in coccolithophores. All three fits were compared (exponential, linear and optimum function) and the study found that the exponential and the linear fits best reproduced the results from empirically derived data on coccolithophores. Chollet (2013) found no difference between the optimum function and the exponential fit to a large (> 648) database of diatoms. Heinle (2014) found that the optimum function fit best to cocolithophore growth rates whereas Stawiarski (2014) found that the exponential function fit best for picophytoplankton growth rates.

Further to the work of Eppley, Bissinger (2008) used a 99% quantile regression to determine maximum community growth rates. The Q_{10} estimates from the quantile regression is quite low (1.1). Nanophytoplankton is often characterized as a mixed group – non-calcifying and non-silicifying, and due to its smaller cell size compared to many diatoms and dinoflagellates its growth rates might be expected to be relatively high. However, the experimental results do not support this expectation, and overall growth rates for nanophytoplankton is substantially lower than diatom growth rates and comparable to those of other PFTs. Between 3 – 12°C there is a good fit to Eppley, but above the 12°C temperature range there is no longer an observed steep increase in growth rate with increasing temperature. So, for the nanophytoplankton PFT here, they may compete well at lower temperatures, but be outcompeted above and beyond 12°C – this makes for an interesting observation when compared to the temperature dependent niche for this PFT based on latitude and expected SST with current climate change. However, given a larger data set the nanophytoplankton PFT may show a better fit to Eppley above 12°C. The paper from Bissinger *et al*., (2008) uses a dataset of > 1500, including nanophytoplankers. The results from this paper show that the 99% quantile best fits to an exponential fit, in line with the Eppley assumptions for community growth (Figure 3.6).

3.5.3 The temperature dependent cell volume of nanophytoplankers shows a positive or weak relationship to growth rate

There is a statistically significant positive trend between temperature and cell volume (except for three species which show an inverse relationship). The general trend is an increase in cell volume with decreasing growth rate. Figure 3.10 shows a relatively small dependence of growth rate on cell volume with an exponent of -0.095. In the literature, the general expectation is an inverse relationship of cell volume to growth rate; at low temperatures species tend to grow more slowly allowing time to build up biomass reflected as larger cell volumes. Larger cells tend to show a decrease in μ at any given temperature. This is not the case for nanophytoplankton, there is a weak relationship between temperature and cell volume.

3.5.4 Implications for future distribution with climate change

Overall, nanophytoplankton shows a relatively wide range of growth temperatures, but the individual species here, generally struggle to grow below 8°C. The chlorophytes have a mean optimum growth rate at 24°C; the haptophytes have a mean optimum growth rate at 21°C and collectively the mean optimum growth rate for all the nanophytoplankers in this thesis is 21°C, suggesting a temperate to sub-tropical distribution.

With regard to temperature dependent growth and average sea surface temperature with climate change, Figure 3.3 demonstrates no relationship between temperature dependent growth rates and isolation latitude, and that for their relative isolation latitude the high latitude northerly isolates 661, 1406, 1348, 647 (Table 2.1) have their T_{opt} well outside the SST estimates and their T_{min} are dangerously close to the line. To an extent, the calculated T_{max} values are irrelevant since the maximum predicted temperature range are well above what would happen in nature. Algae tend to grow well below their T_{opt} because there is such a big decrease in growth rate above T_{opt}, and with temperature variations this margin allows for interspecific competition (Eppley, 1973). As seen from Figure 3.2 and confirmed from literature reviews there would be a decreasing growth rate with decreasing temperature, above and below the optimum temperature probably due to resource reallocation (Raven *et al*., 1988; Eppley, 1972) and that individual species tend to grow at their highest growth rates rate (μ_{max}) under optimal conditions (Eppley, 1972), which would suggest that PFTs subject to SST near to their optima would struggle to maintain a niche when other factors such as competition are factored in.

3.6 Conclusions

Nanophytoplankton follows an optimum function at both species and PFT level – the latter contradicting Eppley's (1972) assumptions. The Q_{10} value is also much lower than Eppley. Therefore for nanophytoplankton – optimum growth rates, optimum temperature and temperature tolerance ranges are the best parameters to identify nanophytoplankton temperature dependent physiological responses. This is in contrast to the use of the Q_{10} and μ_{max0} for biogeochemical modelling (parameters to describe PFTs).

The increase in global SST with increasing climate change may have a negative effect on nanophytoplankton, especially for those geographically distributed close to their T_{opt}. With global warming existing temperature niches will likely move north, and newly created niches in the tropics might not be suitable for nanophytoplankton. Although there was no

relationship between optimum growth rate and optimum temperature, there was a statistically significant relationship between dT and isolation latitude ($P = 0.008$). From Figure 3.6 it can be seen that members of the nanophytoplankton are not well adapted to higher temperatures and therefore are likely to be outcompeted by other phytoplankton. While there is no relationship between Topt and isolation latitude there is a relationship between dT and isolation latitude. However, a caveat of this conclusion is that only ten nanophytoplanker species were tested. Further data are required for a more accurate overview of nanophytoplankton physiology.

4 Chapter 4: Light effects on physiology

4.1 Abstract

The acclimated and dynamic responses of five species from two classes of nanophytoplankton to various light intensities were measured. Using a dynamic photosynthesis model five phytophysiological parameters were derived including the maximum photosynthesis rate (P_m^C,), respiration rate (resp), the initial slope of the line (*a*chl), light inhibition (β^{chl}) and the maximum chlorophyll to carbon ratio (θ_{max}). The first four parameters were also defined directly from curve fits to the (photosynthesis *vs*. irradiance) PE curves.

The parameters from the two methods are comparable for P_m^C, resp and θ_{max} but show significant differences for α^{chl} and β^{chl}.

The photoinhibition was significantly lower for the haptophytes than for the chlorophytes (P = 0.002). The maximum carbon-specific rate of photosynthesis is similar for chlorophytes and haptophytes (P_m^C = 2.66 d^{-1} *vs*. 1.15 d^{-1}), with no significant difference between them. The initial slope of α^{chl} from the photosynthesis *vs*. irradiance curve is similar for the chlorophytes and haptophytes (8.6 g C m^2 (mol photons g Chl *a*)$^{-1}$ *vs*. 5.84 g C m^2 (mol photons g Chl *a*)$^{-1}$). Respiration rates are also similar for the chlorophytes and haptophytes (0.5 d^{-1} *vs*. 0.23 d^{-1}). There is no difference between θ_{max} for the two groups.

4.2 Introduction

Light is an important limiting factor for photosynthesis, and the relationship between light intensity and photosynthesis has been described for a number of species comprising various PFTs, resulting in empirically derived relationships between these quantities (Ryther, 1956; Jassby *et al*., 1976; Falkowski, 1981).

The physiological relationship between these parameters (photoacclimation) is determined using photosynthesis (P) *vs*. irradiance (E) curves (PE curves). PE curves increase asymptotically from oxygen consumption in the absence of light (respiration), to a light saturated maximum production level (P_m^C). Under light-limited conditions, the initial slope of the curve (α^{chl}) indicates the affinity for light which is dependent on the Chl *a*:C ratio (θ) (Geider *et al*., 1998). The Chl *a*:C ratio reaches a maximum at low light (θ_{max}). Above the point where light saturation is reached (I_{opt}), the photosynthesis rate is reduced by a light inhibition parameter (β^{chl}) (Platt *et al*., 1980). These parameters are species-specific (Table 4.1).

Table 4.1 Photosynthetic model parameters.

Parameter	Definition	Unit
α^{chl}	Chlorophyll specific initial slope of the photosynthesis *vs*. irradiance curve	g C g^{-1} Chl *a* m^2 mol^{-1} photons (m^2 = metres squared)
β^{Chl}	Chlorophyll specific light inhibition parameter	g C g^{-1} Chl *a* m^2 mol^{-1} photons
P_m^C	Carbon specific maximum rate of photosynthesis	d^{-1}
P^C	Carbon specific instantaneous rate of photosynthesis	d^{-1}
$resp$	Respiration rate	d^{-1}
Θ	Chlorophyll: carbon ratio	g Chl *a* g^{-1} C
θ_{max}	Maximum chlorophyll: carbon ratio	g Chl *a* g^{-1} C
μ_{max}	Maximum growth rate	d^{-1}
I_{opt}	Light intensity of growth saturation	µmol photons $m^{-2}s^{-1}$

Photoacclimation is the description of phytoplankton physiological responses to variations in irradiance and is expressed by changes in pigment content and elemental composition (Suggett *et al*., 2007). There are two types of photoacclimation (short and long term). This chapter will only deal with long term photoacclimation, which occurs on timescales of hours to days, and involves chlorophyll synthesis changes, growth rate changes and changes in

elemental composition (Geider, 1993). Modeling this process is essential to understand algae productivity as a function of irradiance in relation to net primary productivity (NPP).

4.2.1 Optimum cell volume and the package effect

Cell volume is thought to be an adaptive trait under some environmental conditions (Verdy *et al*., 2009); but obviously algae are restricted to how much their cell size can vary based on their allometry. Literature is often divided as to whether small size, or large size cells are optimal; for example, it is generally understood that small cells should dominate under steady state conditions and in the absence of grazing pressures (Verdy *et al*., 2009); and that scaling dictates that the best evolutionary strategy is to minimize cell volumes to maximize surface to volume ratio and reduce sinking loss (Raven, 1998; Verdy *et al*., 2009). Growth and grazing rates are thought to decrease with increasing size in most PFTs (Hansen *et al*., 1997; Verdy *et al*., 2009), but picophytoplankton seem to follow different patterns (Raven, 1994).

Carbon-specific rates of photosynthesis are thought to peak at intermediate cell sizes. Larger cells need larger Chl *a*:C due to the package effect (Nelson *et al*., 1993; Finkel *et al*., 2000) which makes chlorophyll less effective in larger cells. This package effect implies that with a constant ratio of chlorophyll molecules to volume, each chlorophyll molecule has less chance of absorbing light in a larger cell than in a smaller cell (Nelson *et al*., 1993; Finkel *et al*., 2000). The package effect modifies the size-scaling of light-limited metabolic rates by changing carbon-specific photosynthetic efficiency (Finkel *et al*., 2001) An increase in cell size and/or cellular pigment concentrations (e.g. chlorophyll *a*) can result in a decrease in photosynthetic efficiency.

4.2.2 Mixed layer

Physical factors (e.g. temperature and light availability) can limit primary production. The mixed layer is the homogenous upper sunlit layers that are well mixed by wind turbulence. Due to their small size, phytoplankton is mixed and transported by water movements within the mixed layer. With increases in

temperature and a consequent increase in stratification, the maximum depth to which the phytoplankton is mixed gets shallower and thus the mean light intensity available to the phytoplankton increases (Huisman *et al*., 2004; Sommer *et al*., 2008).

Optimum cell volumes can vary with the mixed layer depth. Net growth rates of cells larger than 10^5 are largely determined by sinking losses. Phytoplankton cells smaller than 10^4 have a trade-off between production efficiency and respiration. When the mixed layer depth is shallower and light intensity is higher, production efficiency increases, and respiratory losses are less important. Under these conditions maximum growth rates occur at smaller cell sizes (Laws, 2000).

4.2.3 Chlorophyll a:Carbon ratios

Chlorophyll pigment content decreases in the presence of higher light intensities. This is because at low light, more chlorophyll is required in order to achieve the same level of photosynthetic activity as at a high light intensity, while at high light chlorophyll content is reduced, initially this is a reallocation of resources, while at higher light it is to prevent excess light from being harvested and reduce the potential for photo inhibitory damage at high light (Geider, 1987; Raven *et al*., 1988). This generalization should be easily seen when one analyses the elemental stoichiometry of chlorophyll *a* to (particulate organic) carbon. Higher ratios should indicate phytoplankton physiological acclimation to low light intensities and the inverse to high light intensities.

Phytoplankton physiological states have often been assessed by analysing the carbon:chlorophyll *a* ratio which changes with temperature, light intensity and nutrient availability (Armstrong, 2006; Behrenfeld *et al*., 2002, 2005; Geider *et al*., 1996, 1997, 1998). The Chl *a*:C ratio has been shown to increase exponentially with increased temperature at constant light (Raven *et al*., 1988). The Chl *a*:C decreases linearly with increasing light intensity at constant temperature (Geider, 1986) supporting the general theory for phytoplankton that more chlorophyll is produced at low light intensity to take full advantage of the light that is available (MacIntyre *et al*. 2002).

4.3 Materials & Methods

4.3.1 Cultures and media

Five species were used from the Roscoff Culture Collection (RCC) http://www.sb-roscoff.fr/Phyto/RCC/. These included three haptophytes: RCC 1348 *Isochrysis galbana*; RCC 1448 *Prymnesium calathiferum*; and RCC 905 *Imantonia rotunda*; and two chlorophytes: RCC 261 *Pseudoscourfieldia cf. marina* and RCC 661 *Chlorella stigmataphora*. All of the cultures were unialgal but probably not axenic.

The cultures were maintained as batch cultures in ~ 200 ml of media in 500 ml Erlenmeyer glass flasks in a Sanyo MLR-351 Versatile Environmental Test Chamber and allowed to acclimate for two weeks (or longer for slower growers to achieve at least 5 divisions). Fresh medium was given after one week of acclimation. All cultures were grown in nutrient replete Enriched Seawater Artificial Medium (ESAW) (Harrison *et al*., 1980; Berges *et al*., 2000; available at: https://ncma.bigelow.org/). The incubator was maintained at 20°C ± 0.05. The temperature was confirmed with a Grant ® Squirrel (Grant instruments 1000 series).

4.3.2 Light

Cultures were grown in a 14:10 light:dark (LD) cycle. The light source was from fluorescent tubes (Mitusbishi/Osram FC40ss. W/37). Each species was incubated at five different light intensities within the same incubator. The variations of the light intensity were achieved by using Lee 0.3 neutral density light filters (Viking Stage Lighting, Norwich, UK). Light intensities were measured using a Scalar PAR (QSL2101 Light Biospherical Instrument, San Diego, USA). The light intensities were 430, 260, 125, 30 and 15 µmol photons m^{-2} s^{-1} (Table 4.2). Growth rates were measured at each light intensity (see section 3.3.3).

Table 4.1 Light intensities in the cultures.

Filters 0.3 neutral	Mean light intensity

density	µmol photons m^2/s^{-1}
Full light	430 ± 1.7
1 layer	260 ± 2.3
2 layers	125 ± 1.8
4 layers	30 ± 0.3
5 layers	15 ± 0.3

4.3.3 Oxygraph, PE curves and analysis

Instantaneous photosynthetic activity was measured during the exponential phase of the acclimated light cultures after five to eight hours from the onset of the light cycle, using oxygraphs (Hansatech Instruments, King's Lynn, UK) to measure dissolved oxygen in the reaction vessel of the liquid-phase chamber. The electrode comprises an anode and a cathode, with a layer of electrolyte (potassium chloride) between the two electrodes which are covered with a sealed, oxygen-permeable membrane so that when an electrical voltage is applied it can stoichiometrically determine oxygen consumed at the cathode. The light source was a 3 watt white LED lamp (Deltech GU10-1HP3W); light was dimmed using neutral density filters (0, 2, 25, 65, 150, 315, 600, 1300 and 2000 µmol photons m^2 s^{-1}). Temperature was controlled at 21°C by a water jacket connected to a temperature controlled water bath. Each light intensity was measured for at least 10 minutes so that the disturbance between switching filters can be disregarded and the oxygraphs have time to readjust to the new light environment, and the final 5 minutes were used to determine photosynthesis rates. Blanks were measured using sterile medium and GFF filtered cultures to measure oxygen consumption by the electrodes and bacterial respiration. PE curves were corrected to cells/ml to give fmol/cell from each of the oxygraphs run in series.

Cultures were sampled for cell concentration (see section 3.3.3), POC/PON (see section 2.1.6) and POP (see section 2.1.8) as well as Chl *a* (see section 2.1.5).

4.3.4 Calculations

Oxygen concentration was corrected for temperature and salinity according to Benson *et al*., 1984. Corrected oxygen concentrations were converted to carbon using a photosynthetic quotient of 1.4 mol O_2 mol^{-1} CO_2 (Laws, 1991) for growth on nitrate as the nitrogen source. The instantaneous rates of photosynthesis were normalized to the measured cell densities, to cellular organic carbon content and up scaled to daily rates (light intensity µmol photons m^2s^{-1} to mol photons m^2s^{-1} $=/10^5*60*60*24$) to calculate specific photosynthetic production (P^c, d^{-1}).

Two models were used to estimate the photosynthetic parameters α^{chl}, β^{chl}, P^C_m, resp, θ_{max}. The first model was the acclimated model. It uses the measurements of P^C and estimates 4 parameters (α^{chl}, β^{chl}, P^C_m, resp) for each PE curve by minimizing the residual sum of squares (RSS) between the model and the individual PE curves using the Excel solver function. Parameters for each species were calculated as the mean result for each PE curve. θ_{max} was estimated from linear regression of $\frac{1}{\theta}$ versus I.

The second model was the dynamic model, where estimates of all five parameters were calculated using a random parameter generation combined with a golden section optimization to minimize the RSS between the model and the observations of P^C, θ, and μ_{max} (Buitenhuis *et al*., 2010). A new dynamic photosynthesis equation was developed which predicts the dependence of P^c on θ and irradiance (I). This model is based on the equation developed by Geider *et al*., 1997, but it was extended by a light inhibition term which is a reformulation of the steady-state light inhibition equation from Platt *et al*., 1980, in order to match the dependence on variable θ. The equation is as follows:

Equation 4.1 $Pc = P^C_m[1-\exp(\frac{-\alpha^{chl}*I*\theta}{P^C_m})]\exp\left(\frac{-\beta chl*I*\theta}{P^C_m}\right)$

The chlorophyll synthesis was formulated as per Geider *et al*., 1997. To compensate for the fact that there were more replicates of P^C but they were less reproducible, growth rate was weighted 50 times more in the RSS and θ was weighted 30 times more in the RSS.

Mean standard error for empirically measured triplicate growth rate, triplicate theta and sextuplet PE curves is SE = 17 for haptophytes and SE = 16 for chlorophytes. Compared to the acclimated model, the errors were SE = 22 for haptophytes and SE = 84 for chlorophytes; and finally the dynamic model, the errors were SE = 271 for haptophytes and SE = 490 for chlorophytes.

Maximum growth rates were calculated using the following equation:

Equation 4.2 $\mu_{max} = P_m^C * (\frac{14}{24}) - resp$

The goodness of fit between the two models was calculated using Akaike's Information Criterion (AIC). The AIC calculates the trade-off between the goodness of fit of the model and the complexity of the model (Burnham *et al*., 2004; Buitenhuis *et al*, 2008):

Equation 4.3 $AIC = n_{obs} \text{ Log } (\sigma 2) + 2n_{param}$

Where n_{obs} is the number of observations $\sigma^2 = 1/ (n_{obs} - n_{param}) * \sum (_{obs} - _{fit})$ and n_{param} is the number of parameters (i.e. the complexity of the model). The best fit returns the lowest AIC value (including negative values) and the AIC for each fit is said to be significantly different if the difference between each one is greater than 2 (Burnham *et al*., 1998).

4.3.5 Statistical analysis

P values for normality were conducted in Sigmaplot © version 12 or Mystat ©. Standard error and standard deviation were calculated in Microsoft Excel 2010 ©. Linear regression analyses were conducted in Sigmaplot © version 12.5.

4.4 Results

4.4.1 Growth rates

Figures 4.1 and 4.2 show the measured growth rates of the haptophytes and chlorophytes respectively as well as the estimated growth rates from the dynamic photosynthesis light response model. Growth increases with increasing light intensity until species reach light saturation (I_{opt}); once this

point is reached light inhibition will cause a decline in growth rate. The maximum measured growth rates were from *I. rotunda* (0.72 d^{-1} ± 0.12, Figure 4.1) which also showed the steepest decline in growth rates at higher light levels (0.19 d^{-1} ± 0.05 at 430 µmol photons m^2 s^{-1} *vs*. 0.60 d^{-1} ± 0.29 at 260 µmol photons m^2 s^{-1}). Light inhibition was observed across all nanophytoplankers. The percentage bias between the measured growth rates and those estimated by the dynamic model ranged from 6% – 20% and there was a tendency towards negative bias at high light and positive bias at low light. Of the haptophytes, two of the three species showed negative bias at each light intensity. *P. calathiferum* only showed negative bias at the highest light intensity. Of the chlorophytes, both species showed positive bias.

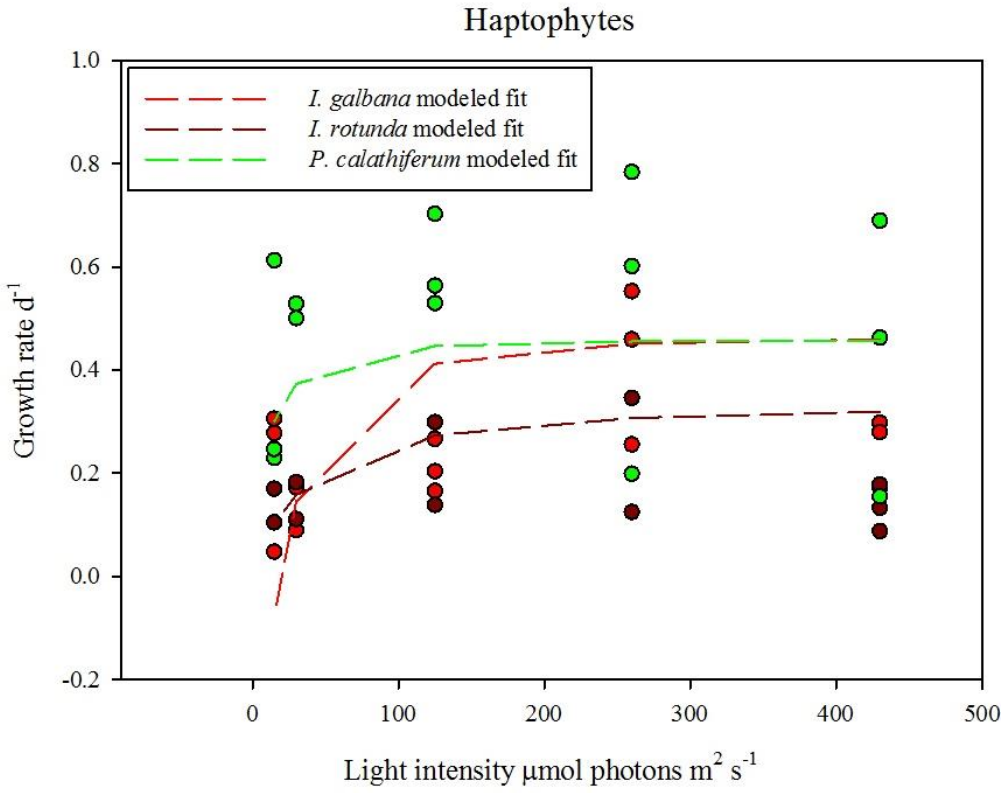

Figure 4.1 Light dependent growth rates of the haptophytes. Circles show the empirical data; lines show the dynamic model fits.

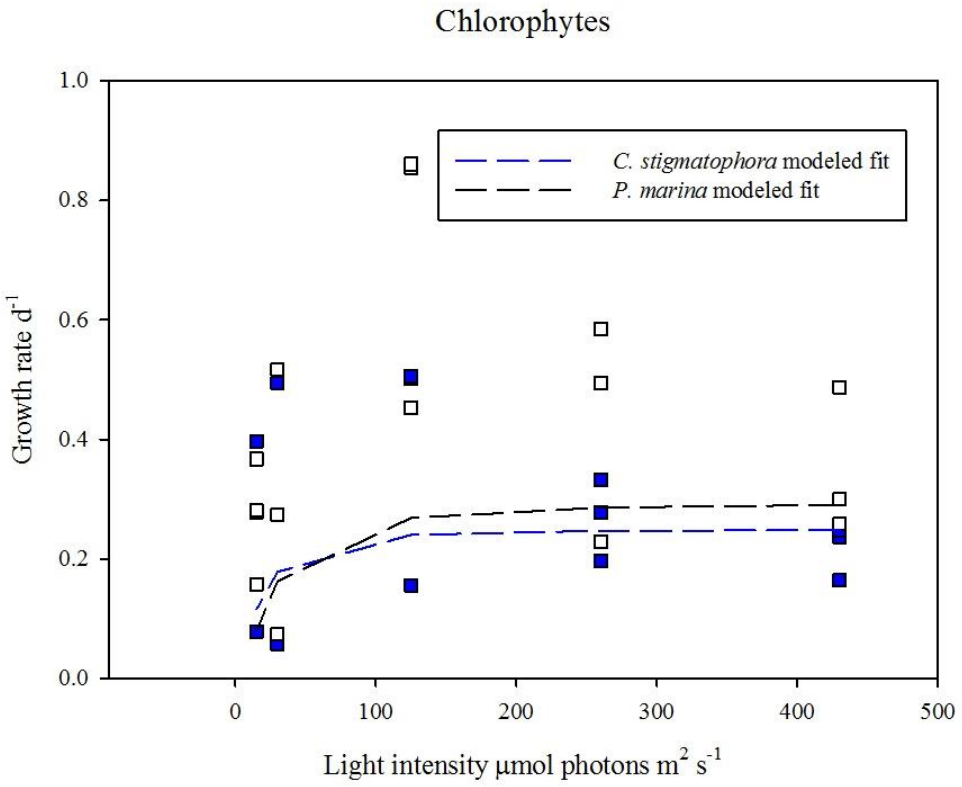

Figure 4.2 light dependent growth rates of the chlorophytes. Squares show the empirical data; lines show the dynamic model fits.

4.4.2 Cell volume

Mean cell volume for the nanophytoplankers was 40 µm^3; maximum was 101 µm^3 (*C. stigmatophora*) and minimum was 18 µm^3 (*I. rotunda*). The haptophytes had a larger mean maximum cell volume (43 µm^3 *vs*. 37 µm^3 than the chlorophytes).

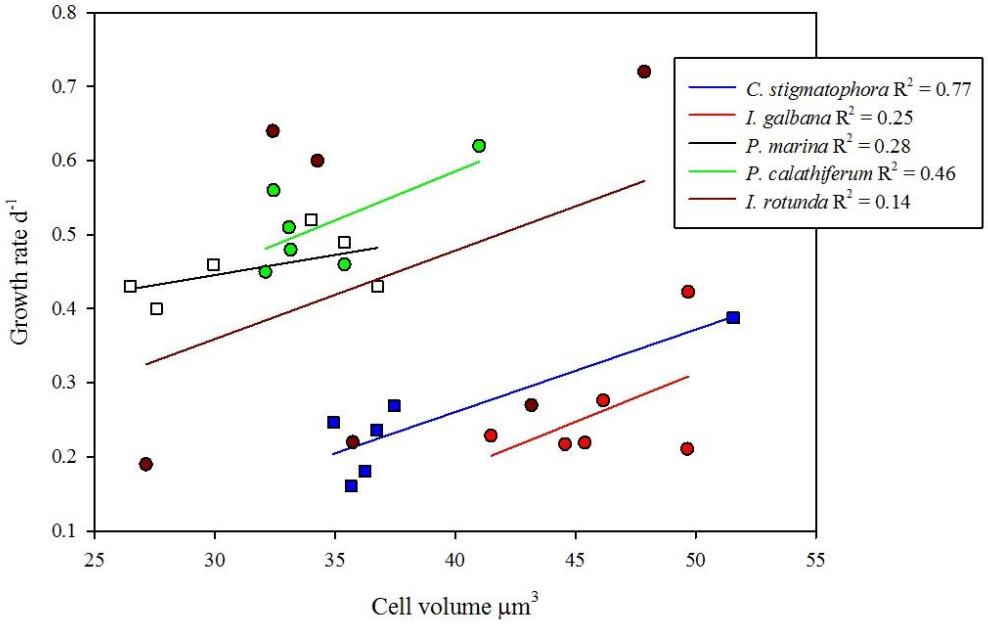

Figure 4.3 mean measured growth rates at each acclimated light intensity as a function of cell volume. Circles show the haptophytes, squares show the chlorophytes. The lines are the linear regressions through the data, r^2 values are shown in the legend.

There is a statistically significant trend (ANOVA) in that the maximum growth rates increases with increasing cell volume for all of the species. Among the haptophytes for *I. galbana* P = 0.02, for *P. calathiferum* P = 0.02 and for *I. rotunda* P = 0.02; among the chlorophytes for *C. stigmatophora* P = 0.02 and for *P. marina* P = 0.02.

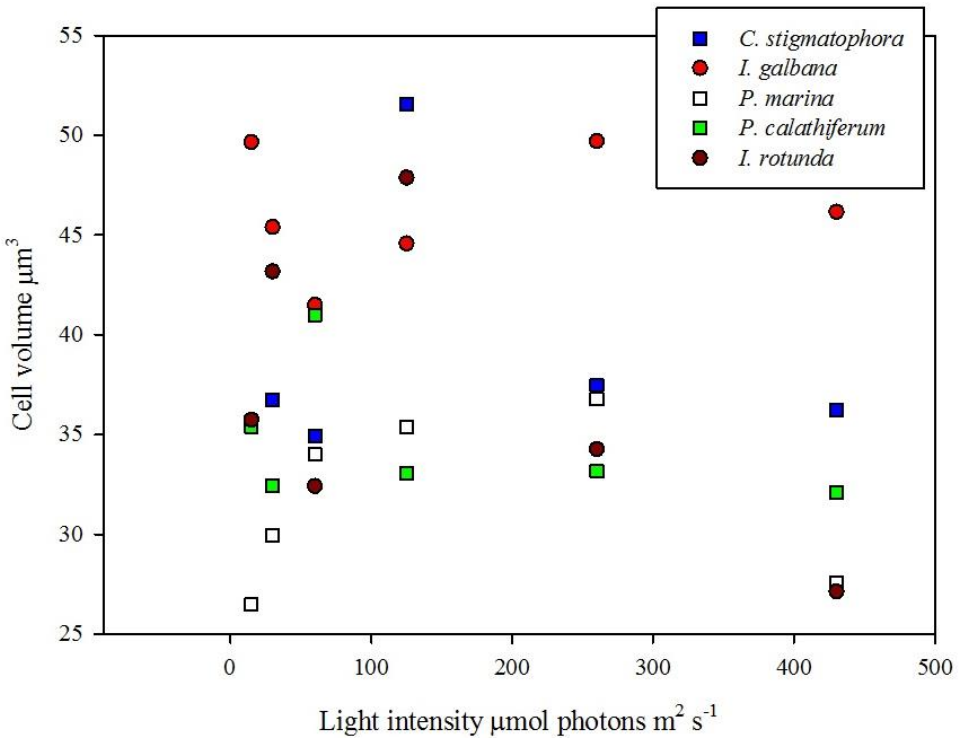

Figure 4.4 Mean measured cell volume as a function of I. Circles show the haptophytes, squares show the chlorophytes. Red is *I. galbana*; green is *P. calathiferum* and dark red is *I. rotunda*. Blue is *C. stigmatophora* and white is *P. marina*.

Cell volumes increase with increasing light intensity up to light saturation. There was a statistically significant relationship between cell volume and (as a function of) light intensity for *I. galbana* – P = 0.02, r^2 = 0.87, *I. rotunda* – P = 0.005, r^2 = 0.97 and for *P. marina* – P = 0.02, r^2 = 0.86.

4.4.3 Chlorophyll a to carbon ratios

The Chl *a*:C (Θ) ratios decrease reciprocally with increasing light intensity in nanophytoplankton. For haptophytes Θ increases from 0.09 g g^{-1} at 15 µmol photons m^2 s^{-1} and 0.008 at 430 µmol photons m^2 s^{-1} (Figure 4.5). *I. galbana* showed the highest ratio (0.09 g Chl *a* g^{-1} C) at lowest light intensity (15 µmol photons m^2 s^{-1}). *I. rotunda* had the lowest overall ratios of the haptophytes, suggesting it was the least light limited of all the nanophytoplankers. Generally the Chl *a*:C ratio should be highest at low light because more chlorophyll is required for photosynthesis. All haptophytes showed statistically significant results for Θ decreasing with increasing light intensity (Figure 4.5).

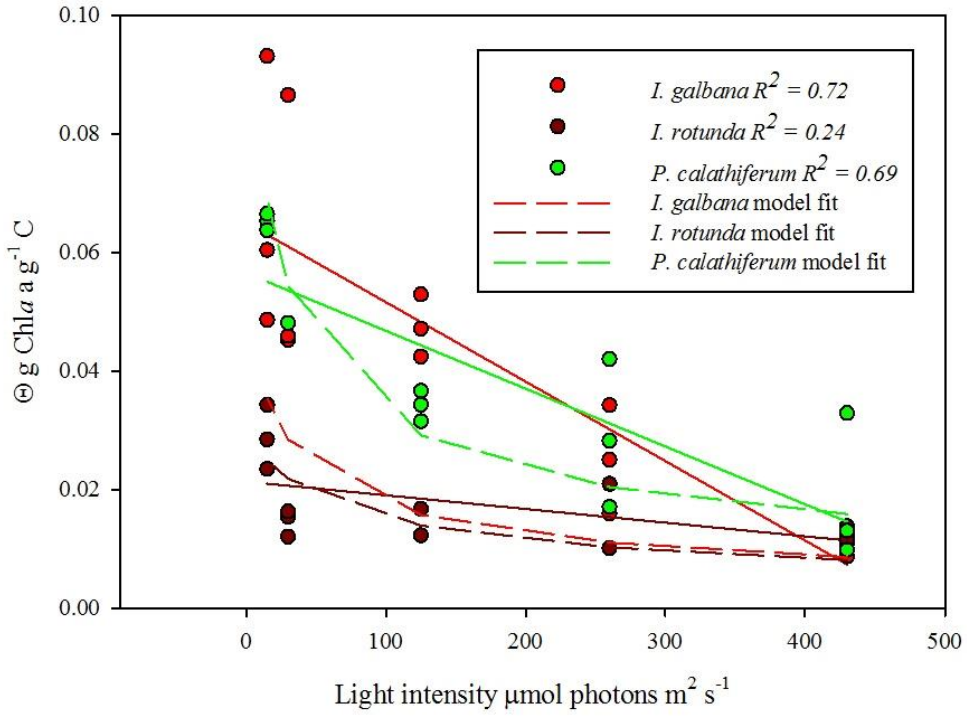

Figure 4.5 Chl *a*:C (g g^{-1}) as a function of light for haptophytes. Circles show measured ratios with straight lines representing a linear regression – r^2 values are shown in the legend, and dashed lines show those estimated by the dynamic model. The mean percentage bias between the measured ratios and model fit is 1%.

The Chl *a*:C ratios also decreased reciprocally with increasing light intensity for chlorophytes, but were not statistically significant. Θ decreased from 0.14 g g^{-1} at 15 µmol photons m^2 s^{-1} and 0.005 at 430 µmol photons m^2 s^{-1} (Figure 4.6). *C. stigmatophora* showed the highest overall ratio of 0.14 g g^{-1}; but with anomalous results at high light.

Figures 4.5 and 4.6 show Θ compared to the model fit estimates for haptophytes and chlorophytes. There is no statistically significant difference between the measured values of Θ and those estimated by the model.

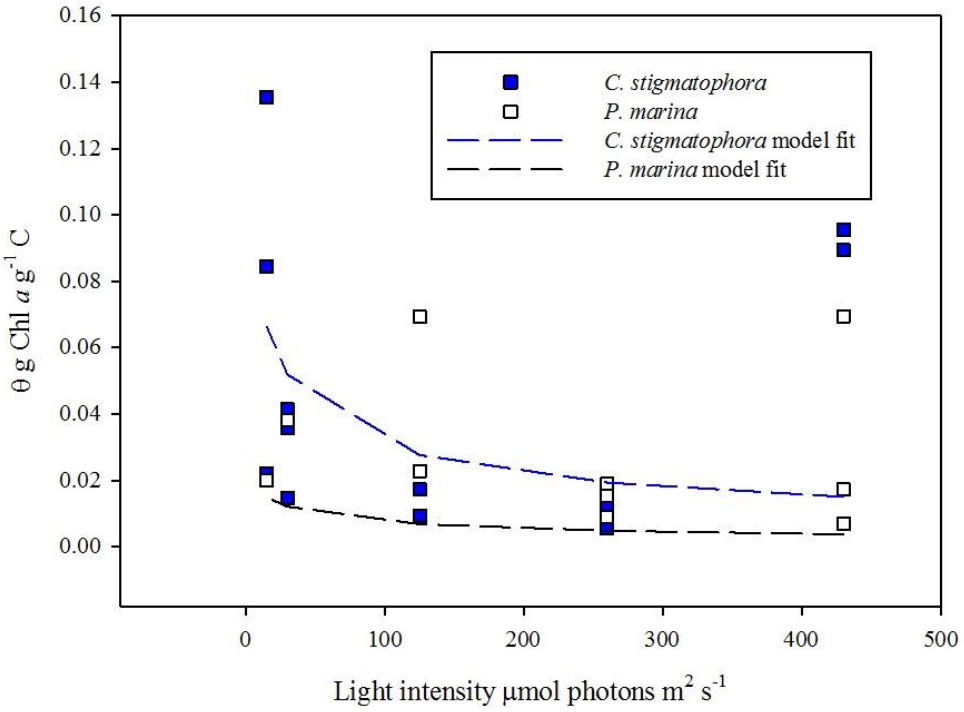

Figure 4.6 Light dependent Chl *a*:C (g g^{-1}) from acclimated cultures squares show the chlorophytes. Blue is *C. stigmatophora* and white is *P. marina*. Squares show the empirically measured ratios and lines show those estimated by the dynamic model. The mean percentage bias between the measured ratios and model for is 1.5%.

4.4.4 Photosynthetic parameters

The parameterization of the acclimated photosynthesis response model to steady state chlorophyll *a* to carbon ratios showed significant differences (Student's T-test P = 0.002) between the haptophytes and chlorophytes for photoinhibition (β^{chl}), but not for any of the other parameters. The chlorophytes have stronger light inhibition (mean β^{chl} = 0.72 g C m^2 (mol photons g Chl *a*)$^{-1}$) than the haptophytes (mean β^{chl} = 0.34 g C m^2 (mol photons g Chl *a*)$^{-1}$) suggesting the haptophytes prefer higher light intensities. The maximum chlorophyll to carbon ratios were calculated (Table 4.4) by a linear regression of $\frac{1}{\theta}$ which gave a maximum range between 0.02 and 0.04 g Chl *a* g^{-1} C the lowest of which was *I. rotunda*.

Table 4.2 Acclimated model parameters.

Species (RCC)	Size µm	P_m^C d^{-1}	α^{chl}g C m^2 (mol photons g Chl *a*)$^{-1}$	β^{chl}g C m^2 (mol photons g Chl *a*)$^{-1}$	Respiration d^{-1}	θ_{max} g Chl *a* g^{-1} C
1348	5	0.55 (0.19)	7.92 (1.6)	0.35 (0.10)	0.18 (0.1)	0.04 (0.01)
1448	5	2.46 (1)	5.35 (1.8)	0.27 (0.1)	0.46 (0.4)	0.04 (0.01)
905	4	0.45 (1.3)	4.25 (0.9)	0.39 (0.1)	0.06 (0.1)	0.02 (0.003)
661	4	1.93 (0.8)	9.63 (5.1)	0.75 (0.2)	0.18 (0.3)	0.03 (0.01)
261	4	3.39 (1.2)	7.58 (3.9)	0.68 (0.3)	0.82 (0.9)	0.03 (0.01)

Table 4.3 Dynamic model parameters.

Species (RCC)	Size µm	P_m^C d^{-1}	α^{chl}g C m^2 (mol photons g Chl *a*)$^{-1}$	β^{chl}g C m^2 (mol photons g Chl *a*)$^{-1}$	Respiration d^{-1}	θ_{max} g Chl *a* g^{-1} C
1348	5	2.22	42.4	$1.85*10^{-12}$	0.83	0.05
1448	5	0.79	9.41	$1.15*10^{-10}$	$4.9*10^{-6}$	0.11
905	4	0.57	6.89	$5.01*10^{-10}$	0.01	0.03
661	4	0.71	9.28	$1.08*10^{-12}$	0.16	0.11
261	4	0.79	32.5	$1.59*10^{-10}$	0.17	0.02

Comparing the acclimated model with the dynamic model; there is a significant difference for α^{chl} and β^{chl} (Student's t-test P = < 0.05). For P_m^C the haptophytes had a mean value of 1.15 d^{-1} for the acclimated model and 1.19 d^{-1} for the dynamic model; the chlorophytes had a significant difference (P = < 0.05) between the two models with 2.66 d^{-1} for the acclimated model and 0.75 d^{-1} for the dynamic model. The highest P_m^C for the acclimated model was for *P. marina* at 3.39 d^{-1} ± 1.2 and 2.2 d^{-1} for *I. galbana* in the dynamic model. The initial slope of the PI curve was highest in *C. stigmatophora* in the acclimated model at 9.63 ± (5.1) g C m^2 (mol photons g Chl *a*)$^{-1}$ and highest for *I. galbana* at 42.2 g C m^2 (mol photons g Chl *a*)$^{-1}$ in the dynamic model. Photoinhibition

was significantly lower in the dynamic model. In the acclimated model, the haptophytes had the lowest values. A chlorophyte (*C. stigmatophora*) had the highest value at 0.68 g C m^2 (mol photons g Chl *a*)$^{-1}$ ± 0.3. Mean respiration for the haptophytes in the acclimated model were 0.23 d^{-1} ± 0.02 and 0.28 for the dynamic model; and for the chlorophytes resp = 0.5 ± 0.06 d^{-1} for the acclimated model and 0.17 d^{-1} for the dynamic model. The mean Chl *a*:C for the acclimated model for haptophytes is 0.03 g Chl *a* g^{-1} C and 0.06 g Chl *a* g^{-1} C for the dynamic model; for the chlorophytes it is 0.03 g Chl *a* g^{-1} C for the acclimated model and 0.07 g Chl *a* g^{-1} C for the dynamic model.

The mean percentage error between the acclimated model and the empirical data for the combined parameters is less than the percentage error between the dynamic model and the empirical data for only two species – *P. calathiferum* (7% *vs*. 11%) and *C. stigmatophora* (negative percentage error *vs*. 6%). The dynamic model was lower for the other three species - *I. galbana* (35% *vs*. 621%), *I. rotunda* (20% *vs*. 55%) and *P. marina* (27% *vs*. 207%).

In the dynamic model, the average contributions to the RSS for growth rates was 69%; for instantaneous photosynthesis rates it was 28% and for θ it was 3% (lower error likely due to much smaller numerical values).

To definitely compare the two models) against the observations, the AIC was calculated (equation 4.3). The acclimated model returned an AIC value of -3.75, and the dynamic model returned an AIC value of -0.95.

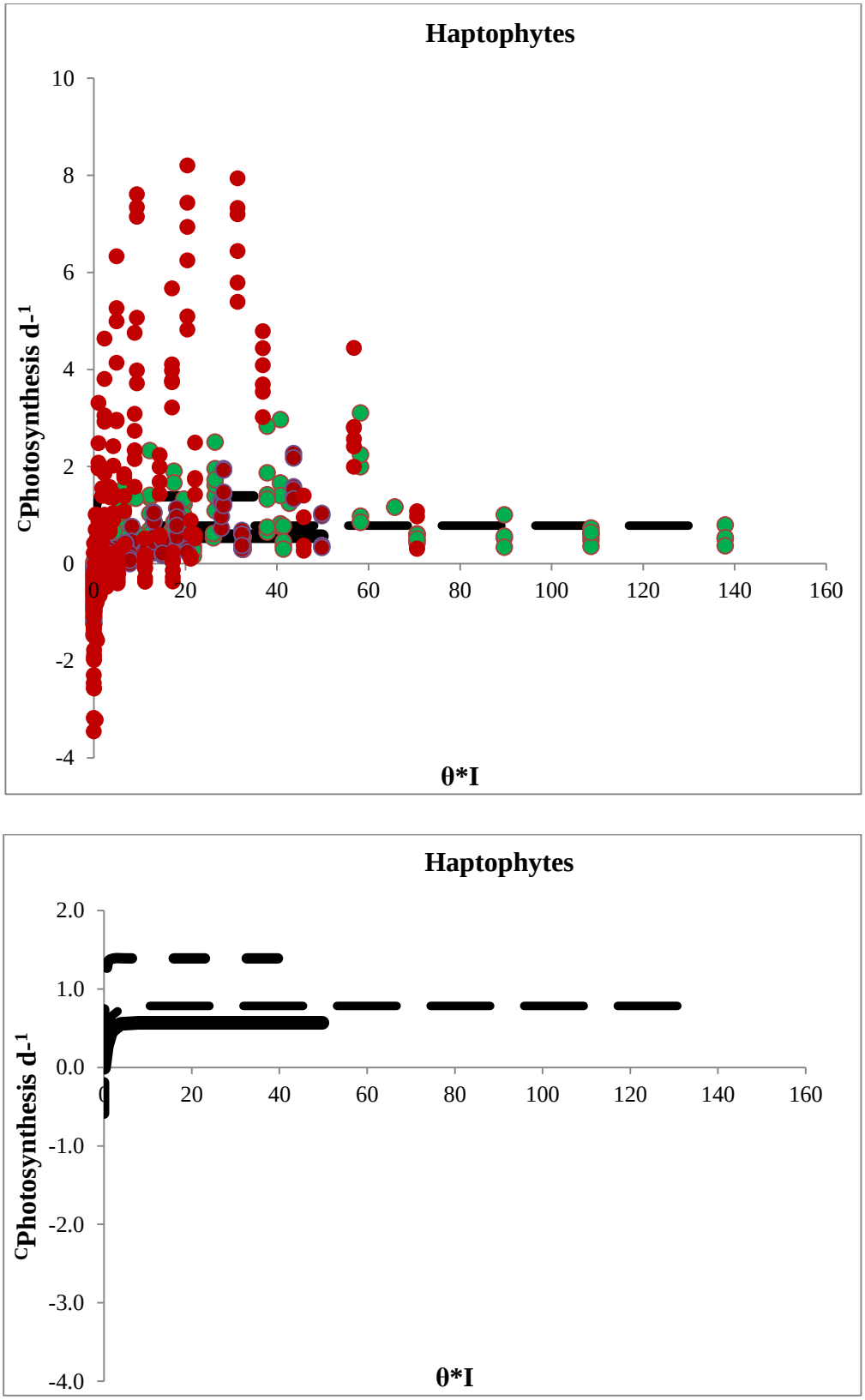

Figure 4.7 Photosynthesis to light response of the haptophytes normalized to Chl *a*:C. The circles in the top plot show the measured individual haptophyte species; red is *I. galbana*; green is *P. calathiferum* and dark red is *I. rotunda*. The lines show the dynamic model fits. For

clarity, the model fits are shown separately in the bottom plot. Short dashed line is *I. galbana*; long dashed line is *P. calathiferum* and unbroken line is *I. rotunda.*

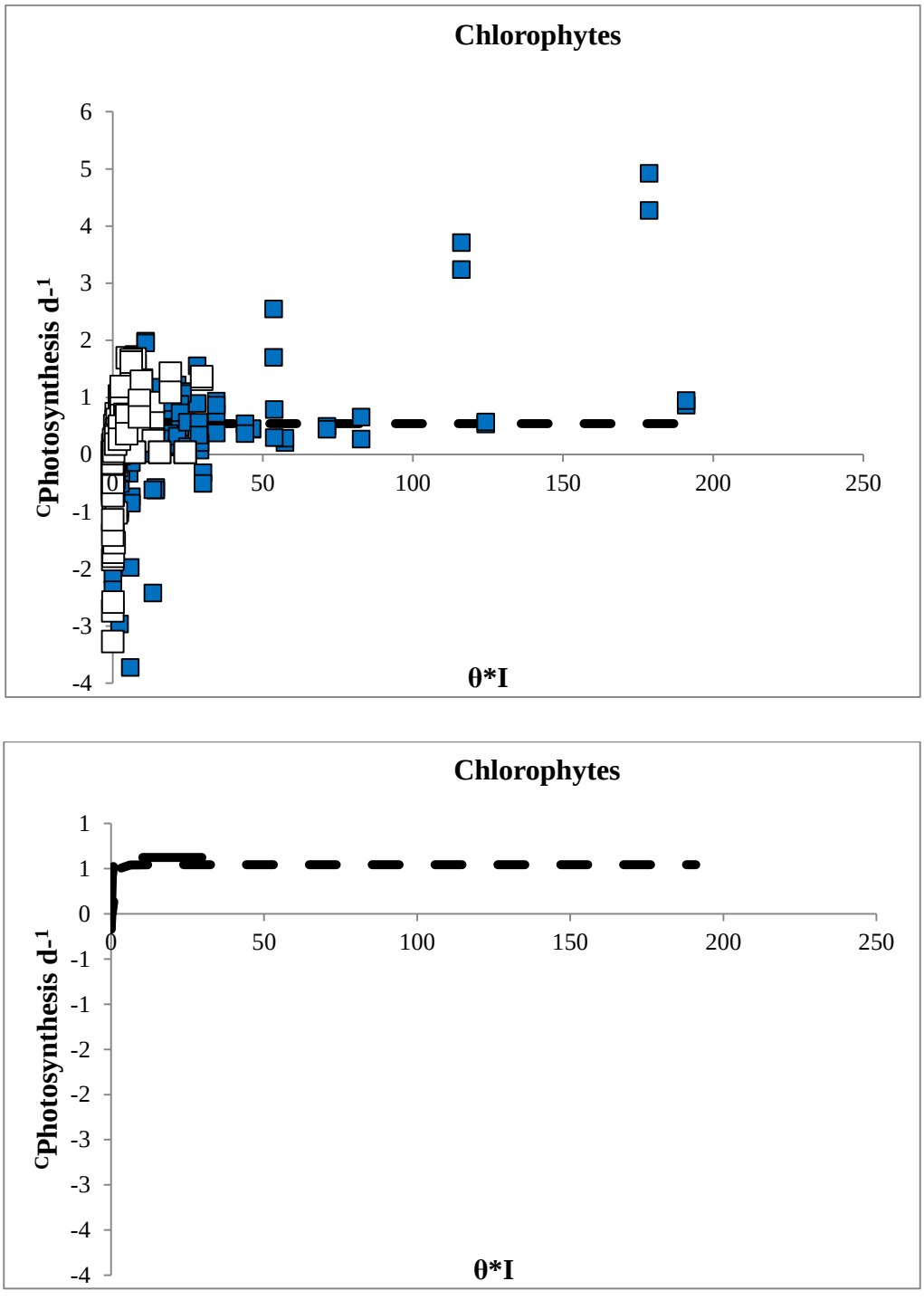

Figure 4.8 Photosynthesis to light response of the chlorophytes normalized to Chl *a:*C. The squares in the top plot show the measured individual chlorophyte species; blue is *C. stigmatophora* and white is *P. marina*. The lines show the dynamic model fits. For clarity, the model fits are shown separately in the bottom plot. Short dashed line is *C. stigmatophora* long dashed line is *P. marina.*

The instantaneous response of photosynthesis to light was plotted *vs*. θ*I (Figures 4.7 - 4.8) and shows responses predicted by Equation 4.1. The normalization to θ is used because there is a decrease in light requirement with increasing θ. This equation means that with normalization all the PE curves from one species acclimated to a specific light intensity but measured at different light intensities should match.

4.5 Discussion

4.5.1 Growth rates and cell volume

From the results, we can see that growth rate is a saturating function of I, in exponentially growing, constant temperature, nutrient-saturated cultures. However, there are few light-limited growth rates in the literature for nanophytoplankton to make a comparison. One study had growth rates between 1.3-1.8 d^{-1} for 10 μ mol photons m^2 s^{-1} (Alpine *et al*., 1988). Maximum growth rate at lowest light intensity in this thesis was 0.46 d^{-1} ± 0.08 at 15 μ mol photons m^2 s^{-1} for *P. calathiferum*.

Nanophytoplankton tends to dominate in temperate regions (temperatures around 10°C) where algal communities tend to be low-light adapted; with light saturation occurring at 25 – 75 μmol photons m^{-2} s^{-1} (Anderson *et al*., 1994).

There are statistically significant species-specific differences between the growth rates within the haptophytes; with *I. galbana* and *P. calathiferum* (P = 0.001) and *I. rotunda* (P = 0.03); and between *P. calathiferum* and *I. rotunda* (P = 0.00002). There is also a statistically significant species-specific difference in growth rates between the chlorophytes (P = 0.03); but no significant difference when taken collectively.

Nanophytoplanker maximum growth rates increase with increasing cell volume. However, there is only a statistically significant difference between cell volume as a function of light intensity for *P. marina*. In the literature, it is stated that the relationship between cell size and maximum growth rate is negatively correlated over a wide range of phytoplankton size classes

(Marañón *et al*., 2013). The Marañón study states that the maximum population growth rate peaks around cell volumes of 100 μm^3 and declines sharply as cell become either larger or smaller (Marañón *et al*., 2013). In other words, maximum growth rate and carbon-specific photosynthesis peaks at intermediate cell sizes (Marañón *et al*., 2013), it is stated that nutrient kinetics (uptake, requirement and assimilation) are limited to taxon-dependent size scaling of growth. Cell volumes in this chapter only reach up to ~50 μm^3, with a μ_{max} of 1.2 d^{-1}.

Of the two models, the dynamic model gives a better estimate of μ_{max}. The percentage bias between the measured μ_{max} and the acclimated model is -36%; whereas the percentage bias between the measured μ_{max} and the dynamic model is much lower at 13%. This is likely a consequence of including growth rate measurements in the data that were used to estimate the photosynthetic parameters of the dynamic model.

For growth rates, the dynamic model takes into consideration measurements of photosynthesis which is useful when used to consider growth rates *vs*. cell size. Generally, smaller cells have a lower C:N ratio; but a greater nutrient demand; whereas larger cells have higher ratios of respiration to photosynthesis (Marañón *et al*., 2013). The dynamic model also agrees better with the measured growth rates and maximum growth rates than does the acclimated model estimates (from Equation 4.2). However, the growth rate estimates for the chlorophytes are a little low.

4.5.2 Chlorophyll a:C

The Chl *a*:C ratio is an indicator of the physiological state of phytoplankton. Light-saturated photosynthesis is assumed to be proportional to POC concentration and light-limited photosynthesis is assumed to be proportional to Chl *a* concentration and I (Geider *et al*., 1997). In the literature the dependence of θ on I and temperature in exponentially growing, nutrient-saturated cultures has been described by four photosynthetically relevant parameters in an empirical equation (Geider, 1987; Geider *et al*., 1997).

Further to the impact of cell volume; larger cells are advantaged by larger Chl *a*:C due to the package effect (Nelson *et al*., 1993; Finkel *et al*., 2000). In the literature, diatoms (~2 – 200 μm in diameter) tend to show higher Chl *a*:C than do dinoflagellates (~5 – 2000 μm in diameter). High α^{chl} (mean 6.95 g C m^2 (mol photons g Chl *a*)$^{-1}$) in nanophytoplankton could be indicative of the small package effect, which can lead to an increased efficiency in light acquisition (Raven, 1988). On a positive note, higher α^{chl} can mean lower light saturation levels and therefore continued success in low-light regions; but inversely, it can mean that nanophytoplankton is prone to photo damage. For nanophytoplankton there may also be a trade-off between high alpha and high respiration.

4.5.3 Photosynthetic parameters

The results from the photosynthetic parameters suggest that more physiological data is required for nanophytoplankton in terms of modelling. Biogeochemical models use a dynamic model rather than an acclimated model despite, in this instance, the acclimated model being a better fit for nanophytoplankton.

Overall, the instantaneous physiological response of nanophytoplankton photosynthesis to light was calculated using two separate methods which showed agreement for some photosynthetic parameters (P_m^C, resp and θ_{max}), but not for photoinhibition (β^{chl}) and the initial slope (α^{chl}). The negative bias of photosynthesis at high light is an indication of underestimated photoinhibition at high light in the dynamic model. Further to this, β^{chl} is much lower in the dynamic model estimates (Table 4.3) than in the acclimated model (Table 4.2).

Both models have merit; the dynamic model allows for better representation of the conditions for photoacclimation in the natural environment because the acclimated model requires conditions to retain balanced growth and empirically measured Chl *a*:C. The photosynthetic parameters that these models calculate are required to assess chlorophyll *a* data from the natural environment so that it may be translated into phytoplankton biomass and/or primary production. Therefore, it is sensible to continually improve these models by validating them with more empirical data.

Between the chlorophytes and the haptophytes, there is a statistically significant difference in the physiological response to photoinhibition, but not for any of the other photosynthetic parameters. Photoinhibition was strongly reflected in the acclimated model (which only uses these instantaneous photosynthesis measurements), but not so strongly reflected in the dynamic model which gives much lower β^{chl} . It is possible that this may be a shortfall in the dynamic model; where irreversible photo damage can perhaps occur over longer time scales while the model only represents short term reversible inhibition as a function of θ. I.e. growth rates are a measurement that are represented on a time-scale of days; but photosynthesis measurements are over a time-scale of minutes. The chlorophytes showed stronger photoinhibition than the haptophytes, but overall β^{chl} was 0.49 g C m^2 (mol photons g Chl *a*)$^{-1}$for nanophytoplankton.

4.6 Conclusions

Within nanophytoplankton there is a statistically significant species-specific difference between the growth rates within the haptophytes, and between the two chlorophytes; however, there is no significant difference when taken collectively.

Results indicate that the light dependent maximum growth rates increase with increasing cell volume for nanophytoplankers.

Between the chlorophytes and the haptophytes, there is a statistically significant difference in photoinhibition.

Both models have merit. However, the acclimated model was a better overall fit (AIC = -3.75 *vs*. -0.95 for the dynamic model).

4.7 Appendix

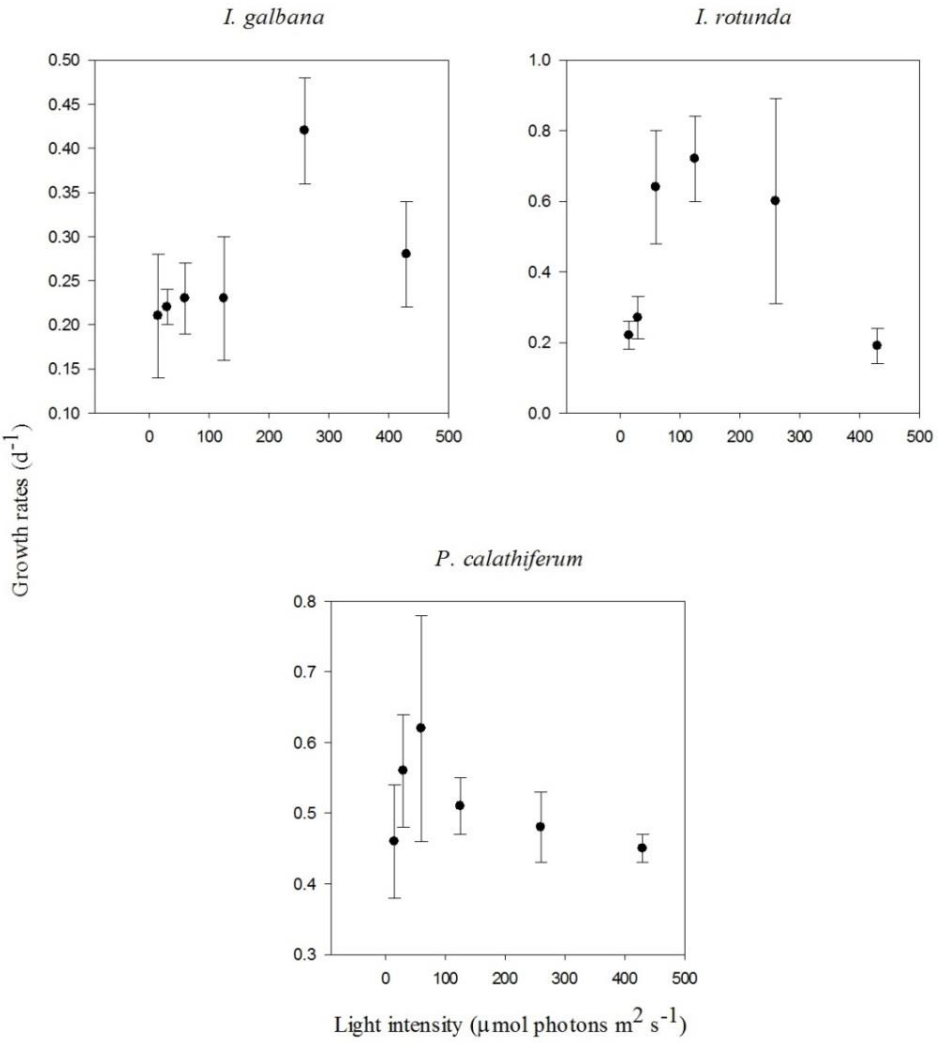

Figure 4.9 Light dependent growth rates for haptophytes. Plots shown with standard error bars.

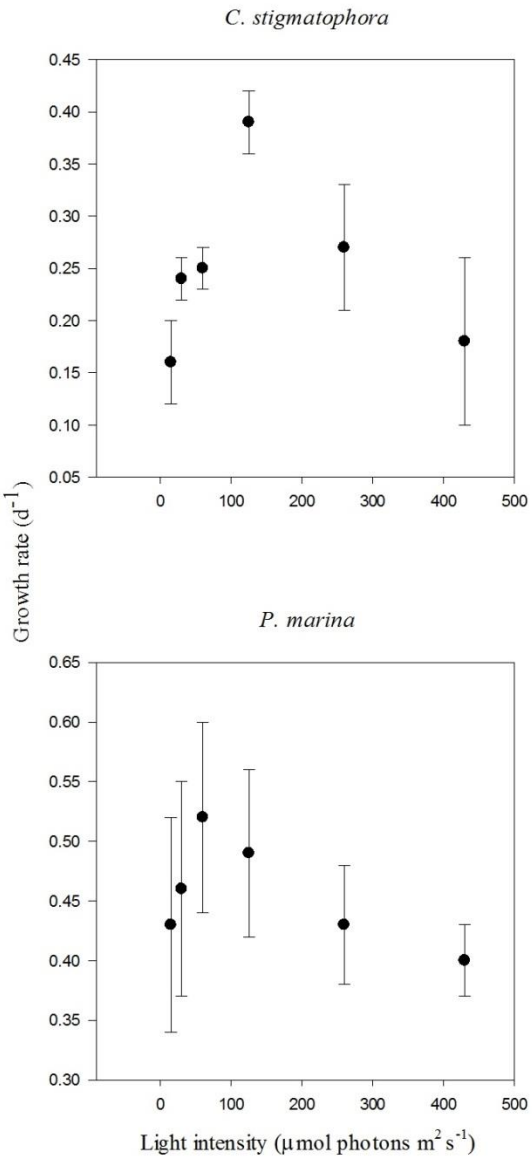

Figure 4.10 Light dependent growth rates for chlorophytes. Plots shown with standard error bars.

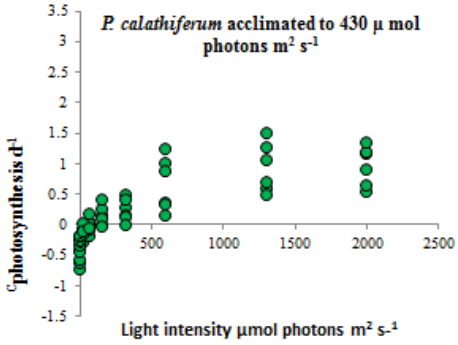
P. calathiferum acclimated to 430 µ mol photons m² s⁻¹
Cphotosynthesis d⁻¹
Light intensity µmol photons m² s⁻¹

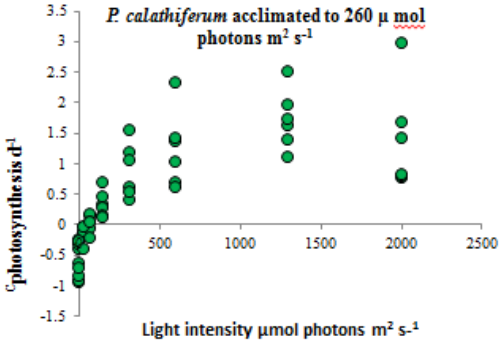
P. calathiferum acclimated to 260 µ mol photons m² s⁻¹
Cphotosynthesis d⁻¹
Light intensity µmol photons m² s⁻¹

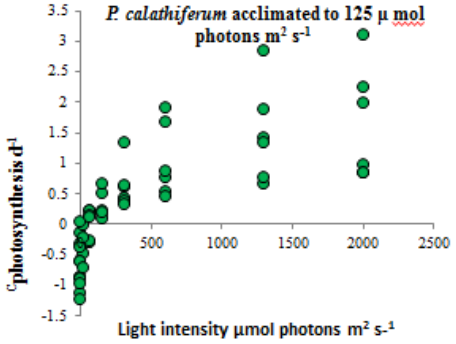
P. calathiferum acclimated to 125 µ mol photons m² s⁻¹
Cphotosynthesis d⁻¹
Light intensity µmol photons m² s-¹

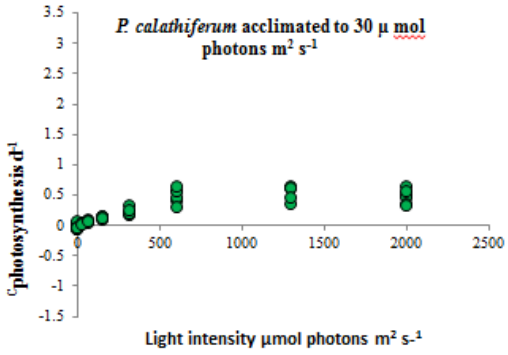
P. calathiferum acclimated to 30 µ mol photons m² s⁻¹
Cphotosynthesis d⁻¹
Light intensity µmol photons m² s⁻¹

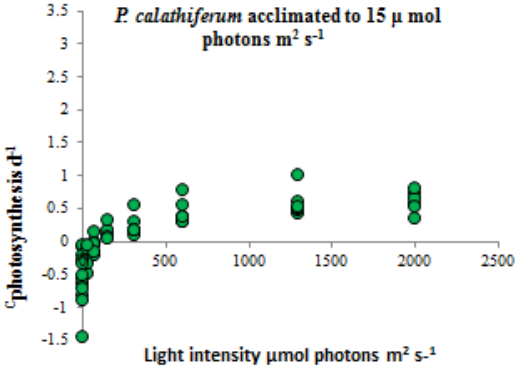
P. calathiferum acclimated to 15 µ mol photons m² s⁻¹
Cphotosynthesis d⁻¹
Light intensity µmol photons m² s⁻¹

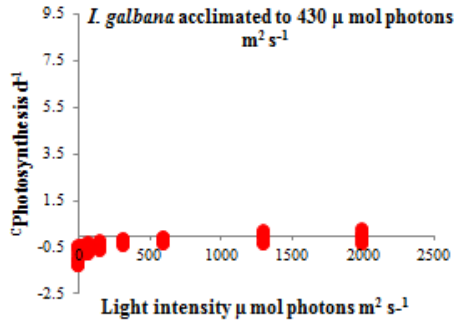
I. galbana acclimated to 430 µ mol photons m² s⁻¹
CPhotosynthesis d⁻¹
Light intensity µ mol photons m² s⁻¹

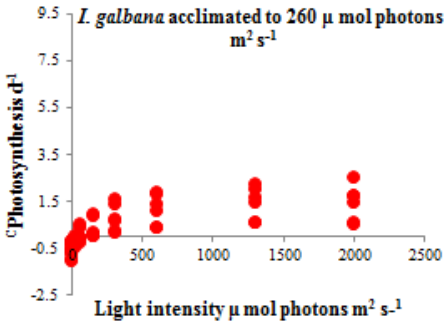
I. galbana acclimated to 260 µ mol photons m² s⁻¹
CPhotosynthesis d⁻¹
Light intensity µ mol photons m² s⁻¹

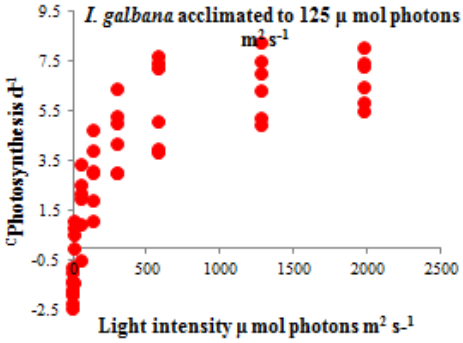
I. galbana acclimated to 125 µ mol photons m² s⁻¹
Photosynthesis d⁻¹
Light intensity µ mol photons m² s⁻¹

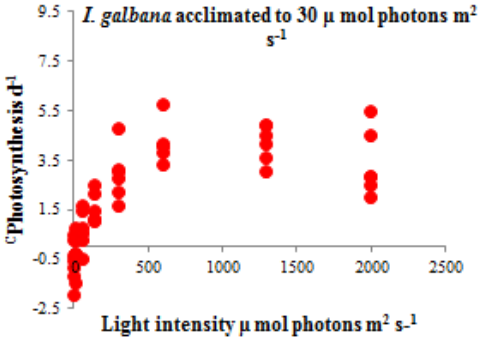
I. galbana acclimated to 30 µ mol photons m² s⁻¹
Photosynthesis d⁻¹
Light intensity µ mol photons m² s⁻¹

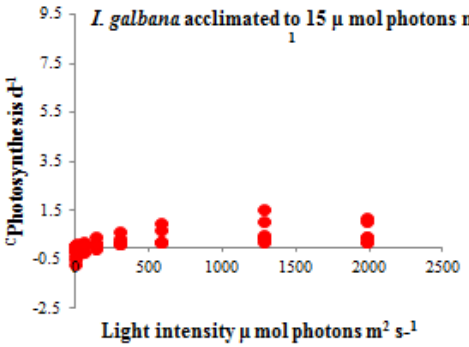
I. galbana acclimated to 15 µ mol photons m² s⁻¹
Photosynthesis d⁻¹
Light intensity µ mol photons m² s⁻¹

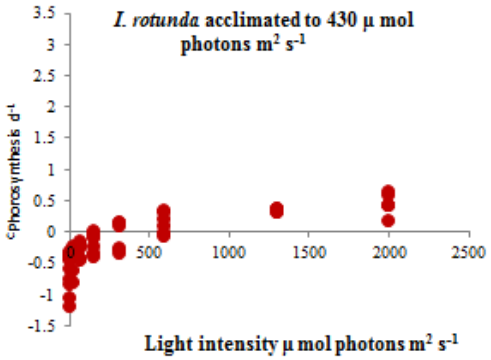
I. rotunda acclimated to 430 µ mol photons m² s⁻¹
Phorosynthesis d⁻¹
Light intensity µ mol photons m² s⁻¹

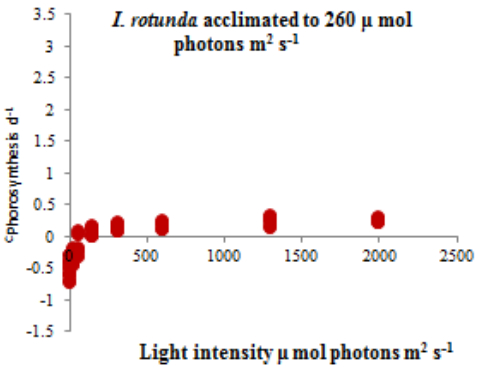
I. rotunda acclimated to 260 µ mol photons m² s⁻¹
Phorosynthesis d⁻¹
Light intensity µ mol photons m² s⁻¹

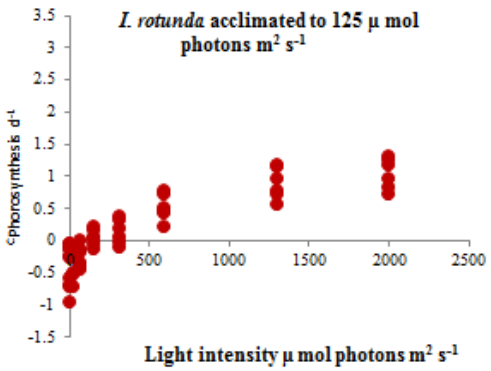
I. rotunda acclimated to 125 µ mol photons m² s⁻¹
Phorosynthesis d⁻¹
Light intensity µ mol photons m² s⁻¹

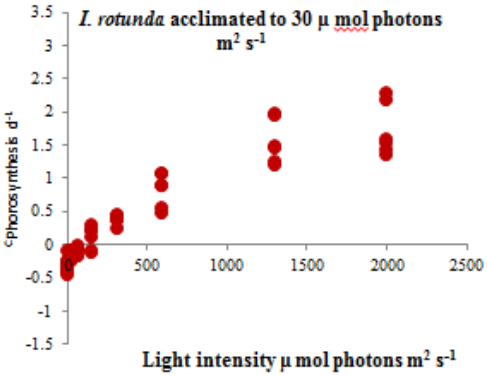
I. rotunda acclimated to 30 µ mol photons m² s⁻¹
Phorosynthesis d⁻¹
Light intensity µ mol photons m² s⁻¹

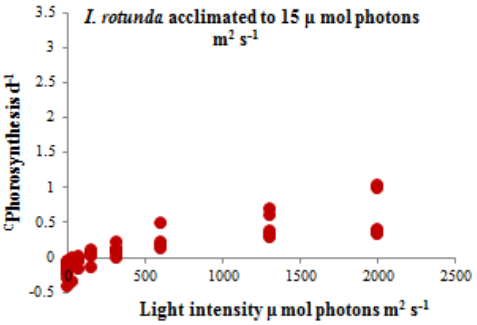
I. rotunda acclimated to 15 µ mol photons m² s⁻¹
CPhotosynthesis d⁻¹
Light intensity µ mol photons m² s⁻¹

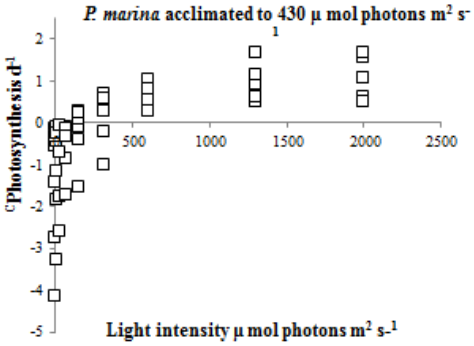
P. marina acclimated to 430 µ mol photons m² s⁻¹
CPhotosynthesis d⁻¹
Light intensity µ mol photons m² s⁻¹

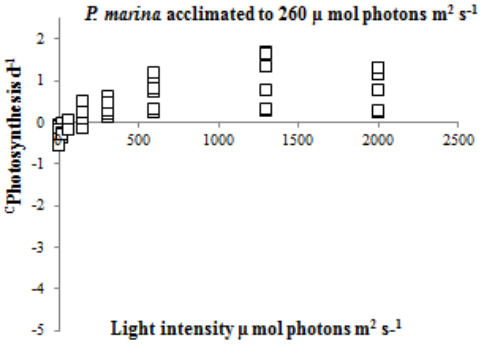
P. marina acclimated to 260 µ mol photons m² s⁻¹
CPhotosynthesis d⁻¹
Light intensity µ mol photons m² s⁻¹

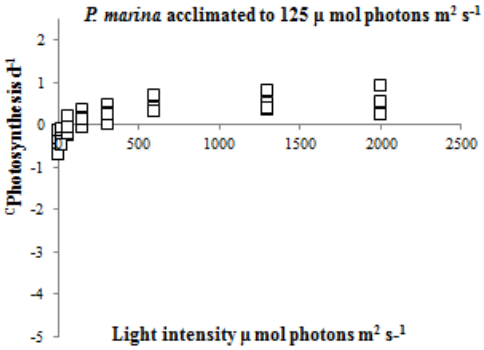
P. marina acclimated to 125 µ mol photons m² s⁻¹
CPhotosynthesis d⁻¹
Light intensity µ mol photons m² s⁻¹

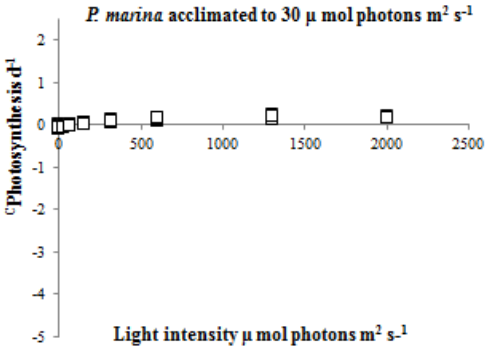
P. marina acclimated to 30 µ mol photons m² s⁻¹
CPhotosynthesis d⁻¹
Light intensity µ mol photons m² s⁻¹

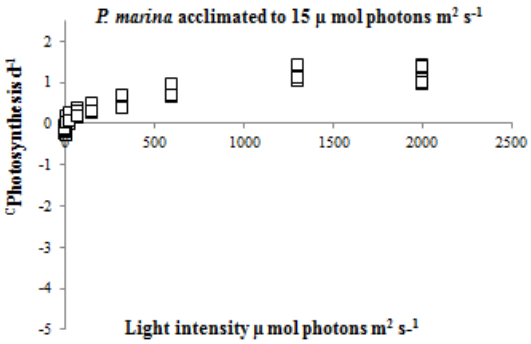
P. marina acclimated to 15 µ mol photons m² s⁻¹
CPhotosynthesis d⁻¹
Light intensity µ mol photons m² s⁻¹

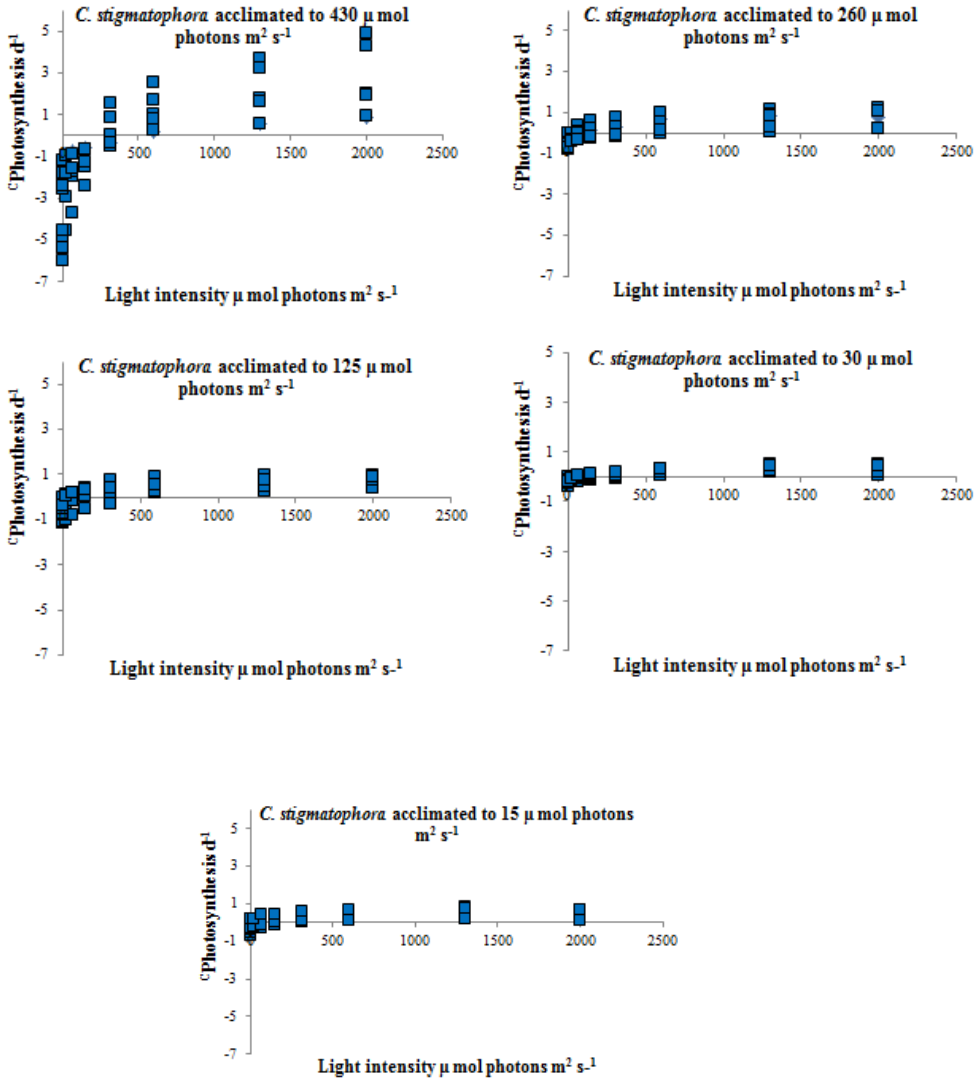

Figure 4.104.11 PE curves corrected for carbon and measured at light intensities between 0 – 2000 µ mol photons m^2 s^{-1}. For the haptophytes: *P. calathiferum* (green circles); *I. galbana* (red circles); *I. rotunda* (dark red circles).For the chlorophytes: *P. marina* (white squares) *C. stigmatophora* (blue squares). Individual plots are for the species acclimated to specific light intensities from 15 – 430 µ mol photons m^2 s^{-1}).

5 Chapter 5: Nanophytoplankers alter their elemental stoichiometry under nutrient saturation in response to changing environmental conditions

5.1 Abstract

The variability in nutrient stoichiometry under differing temperature conditions is presented for ten nanophytoplankton species, and under differing light conditions for 5 nanophytoplanker species. Mean C:N for the haptophytes is 8.5 ± 0.5 for the chlorophytes it is 8.2 ± 0.8, for the chrysophyte it is 10 ± 0.7 and for the dinoflagellate it is 8.9 ± 0.7. There is a statistically significant difference between C:N of the chrysophyte and the haptophytes, and between the chrysophyte and the dinoflagellate (P = 0.05) but not among any of the other groups. Mean N:P for the haptophytes is 21 ± 1.3, for the chlorophytes it is 18 ± 0.88, for the chrysophyte it is 15 ± 0.47 and for the dinoflagellate it is 18 ± 0.37. These data suggest that none of the nanophytoplankers were N-limited (N:P < 10:1). The mean C:P for the haptophytes is 171 ± 8.2, for the chlorophytes it is 147 ± 7.5, for the chrysophyte it is 153 ± 4.2 and for the dinoflagellate it is 155 ± 4.4. Under nutrient saturated conditions, nitrogen and phosphorus are taken up in excess resulting in a deviation from the Redfield ratio (C:N:P = 106:16:1). The C:N:P is 150:21:1 for haptophytes; 139:18:1 for chlorophytes; 153:15:1 for the chrysophyte and 155:18:1 for the dinoflagellate.

5.2 Introduction

If climate change causes changes in the nutrient stoichiometry then the utilization of carbon relative to the other limiting nutrients could mean that either more or less carbon will be exported. Physiological experimentation to see whether the nutrient uptake generally differs from the Redfield Ratio or if it remains the same with climate change parameters will allow insights into biological mechanisms and carbon export as well as the inferred degree of nutrient limitation of phytoplankton growth and cellular composition. In 1934, Redfield investigated the elemental composition of particulate organic matter of plankton and found a relationship in the nutrient stoichiometry; this ratio is

now known as the Redfield ratio and is defined as 106C:16N:1P (Redfield, 1958). Since this time, this ratio has been used to define how different biogeochemical cycles are coupled in the marine environment.

The results from the cellular composition analyses are used to determine the ratios of organic carbon, nitrogen phosphorus and chlorophyll so that they can be compared to the Redfield ratio and to assess the importance of temperature on the Chl *a*:C - that it increases linearly with increasing temperature (or decreases with decreasing temperature due to chlorosis, resource reallocation and/or slower metabolic rates (Geider, 1987; Raven *et al*., 1988).

Literature suggests that smaller-size classes have superior uptake efficiencies than do larger size classes (Smith *et al*., 1992; Raven, 1988). With climate change likely to lead to an extension of subtropical oligotrophic gyres, increased stratification and decreased nutrient availability smaller size classes may become more dominant in these areas.

As the anthropogenic CO_2 in the ocean increases, the carbon-to-nutrient ratios of the marine phytoplankton are expected to be higher due to the increases in carbon availability (Schoo *et al*., 2012; Bianucci *et al*., 2012). If this is the case it may have an ecosystem effect because the food quality available up the food web may alter (Schoo *et al*., 2012) possibly resulting in variations in carbon sinks and chemical compositions (Schoo *et al*., 2012; Bianucci *et al*., 2012). Two important nutrients for phytoplankton are N and P, however, Si:P is ~ 6:1 and in diatoms Si:N is ~ 1 (Collos *et al*., 2004. It is known that different phytoplankton assemblages (PFTs) alter their nutrient stoichiometry in response to changing environmental conditions, as well as taking up nutrients in excess of their minimum requirements when conditions allow. This latter phenomenon is generally reflected in lower N:P ratios and Redfield-like C:N ratios (Geider *et al*., 2002). Because these differences can be seen on large-scales across ocean regions it has become important to investigate the changes in elemental stoichiometry for a given PFT (Bertilsson *et al*., 2003). N:P ratios are important since they are used to describe nutrient limited regions (Geider *et al*., 2002; Tagliabue *et al*., 2011; Toseland *et al*., 2013).

5.2.1 Nitrogen

Nitrogen is one of the most important elements for biological organisms, nitrogen is present primarily as amino acids and it also occurs in nucleic acids (DNA and RNA) and it is essential for many biological processes including cell maintenance, acclimation to changes in environmental conditions (like light, temperature, nutrients and salinity) and cell defence against pathogens (Berges, 2003; Collos *et al*., 2004). Nitrogen is limiting because the ratio between supply and demand is lower than that for other elements found in the eutrophic zone (Berges, 2003; Collos *et al*., 2004). Phytoplankton is responsible for ~70% of global nitrogen assimilation and is therefore very important in transforming incoming radiation into biomass (Berges, 2003; Collos *et al*., 2004). Nitrogen is one of the most important life-giving elements and without this assimilation; very little nitrogen would be available to other marine organisms that live near the surface of the ocean.

In oligotrophic oceans, which are generally dominated by nano- and pico-sized plankton, the majority of primary production is thought to be driven by remineralized nitrogen; conversely, larger cells tend to dominate in areas with a relatively high supply of new nitrogen which supports a relatively large phytoplankton biomass (Dugdale *et al*., 1967; Eppley *et al.*, 1979; Malone, 1980a/b; Chisholm, 1995). This trend may suggest that larger cells primarily utilize NO_3^- as their nitrogen source, and smaller cells primarily utilize NH_4^+ (Malone, 1980a/b; Chisholm, 1995). So the relative biomass of pico/nano phytoplankton and larger phytoplankton may simply be a consequence of the total nitrogen concentration below the mixed layer and which form the nitrogen source is in (Chisholm, 1995). Intense mixing may favour larger cells and where there is a dominance of small plankton (and subsequent low f-ratios) it may be suggestive of low mixing regimes (Chisholm, 1995).

5.2.2 Phosphorus

Other research suggests that P is the limiting nutrient in oligotrophic oceans (as well as several coastal systems) (Cotner *et al*., 1997; Karl *et al*., 1997; Ivančić

et al., 2012). Phosphorus is the other major nutrient for life in biological organisms considered here because phosphate is a component of DNA and RNA, ATP (adenosine triphosphate) and phospholipids that form all cell membranes (Spector *et al*., 1985). Phosphorus normally occurs in nature as part of a phosphate ion $(PO_4)^{3-}$ of which the most abundant form is orthophosphate. The main source to the marine environment comes from terrestrial runoff or dust deposition (Libes, 2009). The availability of P is restricted greatly by the rate of release of this element from weathering processes and the only sink for P is via sedimentary deposition (Libes, 2009). P limitation is apparent in many oligotrophic gyres as well as other low nutrient, low chlorophyll (LNLC) areas. Marine organisms have evolved mechanisms for dealing with the changes in P concentration (Ivančić *et al*., 2012); for example cyanobacteria like *Synechococcus* and *Prochlorococcus* that dominate in low P environments have synthesized their cell membranes primarily from sulphur and sugar rather than the phospholipids of eukaryotic cells (Dyhrma *et al*., 2007; Van Mooy *et al*., 2009; Ivančić *et al*., 2012).

5.2.3 Stratification and nutrient availability

Rising temperatures with climate change are likely to lead to increased stratification and perhaps an extension of the subtropical oligotrophic gyres (Gerecht *et al*., 2014; Morán *et al*., 2010; Emerson *et al*., 2008; Kwon *et al*., 2008; Doney *et al*., 2012; Behrenfeld *et al*., 2006; Bopp *et al*., 2001). The increased intensity of stratification will decrease the mixing rate between the surface water and the deep water thus reducing nutrient input into the upper sunlit layers from the nutrient-rich deep ocean water (Gerecht *et al*., 2014). The result of this will likely be nutrient limitation and ultimate changes in abundance and composition of plankton communities affecting global biogeochemical cycling – and in particular – the carbon cycle (Gerecht *et al*., 2014). Increased stratification may mean that phytoplankton communities adapt to low nutrient concentrations all year round (Behrenfeld *et al*., 2009) or there will be a move towards smaller phytoplankton assemblages like pico- and nanophytoplankton (Bopp *et al*., 2005; Ivančić *et al*., 2012).

All marine phytoplankton affects the carbon cycle because it fixes CO_2 into particulate organic carbon (POC) via photosynthesis.

Phosphate and nitrate limited experiments are designed to specifically test the nutrient stoichiometry of the phytoplankton in order to determine physiological effects.

5.3 Materials & Methods

5.3.1 Culture media

For this thesis, an axenic experiment was carried out so that the bacteria could not interfere with the results.

5.3.2 Light and temperature

Light intensities were measured using a Radiometer Scalar PAR (QSL2101 Light Biospherical Instrument, San Diego, USA) and the temperatures were measured using a Grant ® Squirrel (Grant instruments 1000 series). For the continuous cultures, Sanyo MLR-351 incubators were kept at a constant temperature (22°C) and light (to ensure steady state in the culture without a diel cycle) of 125 µmol photon m^{-2} s^{-1}. Experimental batch cultures for the continuous culture experiment were grown at 22°C and maintained at a light intensity of 125 µmol m^{-2} s^{-1}, with a L:D cycle of 24 hours and were grown in nutrient replete ESAW medium (Harrison *et al*., 1980).

5.3.3 Growth rate measurements and cell composition sampling

Maximum growth rates were measured in batch cultures as described in 2.1.4. Sampling and analyses of cellular composition are described in 2.1.4 – 2.1.7. After acclimation the continuous cultures were sampled on consecutive days for the organic nutrients POC/PON (collectively), Chl *a* and POP; and for the inorganic nutrients PO_4 (phosphate), NH_3 (ammonia) and NO_3 (nitrate). PO_4 analyses were determined in a similar manner to POP (Section 2.1.7) except that the digestion step was omitted.

NO_3 and NH_4 were analysed using a San++ Automated Wet Chemistry Analyzer- Continuous Flow Analyzer (CFA, Skalar Analytical, 2014) according to Wood *et al*. (1967).

5.3.4 Statistical analysis

Normality and p values were tested with ANOVAs and conducted in Sigmaplot © version 12.5.

5.4 Results

5.4.1 Nutrient saturated quotas

Under nutrient saturated conditions carbon quotas increase with increasing temperature and decrease with increasing light (ANOVA $p = 0.07$ and 0.003 respectively); nitrogen quotas decrease with increasing light ($p = 0.007$); and phosphorus decreases with increasing light ($p = 0.009$) (Figure 5.1). There was no significant relationship between nitrogen or phosphorus quotas and temperature.

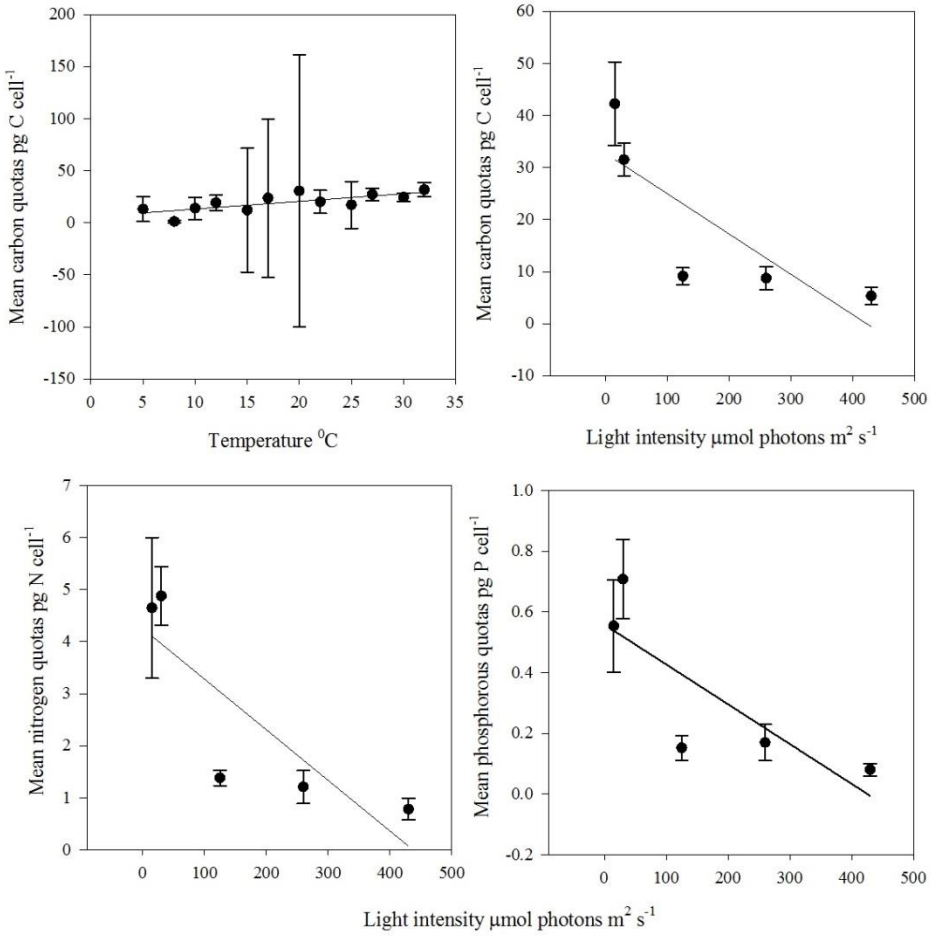

Figure 5.1 Mean carbon quotas (pg cell^{-1}) in nanophytoplankton species obtained from temperature – $r^2 = 0.60$ (top left plot) and light – $r^2 = 0.67$ (top right plot) experiments. Mean nitrogen quotas decreasing with increasing light – $r^2 = 0.71$ (bottom left plot) and mean phosphorous quotas decreasing with increasing light – $r^2 = 0.67$ (bottom right plot). The lines show linear regressions. Data is shown ± standard error.

The mean species specific ranges of elemental quotas were quite similar between the temperature and light experiments; however two of the haptophyte species (*I. galbana* and *P. calathiferum*) show statistically significant differences across all three elements and *I. rotunda* showed statistically significant differences between the carbon and nitrogen quotas (for light and temperature).

Table 5.1 shows a statistical comparison of the particulate organic matter for all species from the temperature and light experiment using a Pairwise Multiple Comparison (Dunn's

Method).Where P values are highlighted in red, this indicates a strong significant statistical difference between the tested pairs (P = < 0.01).

Species	RCC number	Carbon	Nitrogen	Phosphorus
I. galbana (haptophyte)	1348	0.008	0.005	0.003
P. calathiferum (haptophyte)	1448	0.002	0.005	0.004
I. rotunda (haptophyte)	905	0.003	0.001	0.112
P. marina (chlorophyte)	261	0.642	0.515	0.926
C. stigmatophora (chlorophyte)	661	0.513	0.385	0.513
Haptophytes		0.003	0.002	0.001
Chlorophytes		0.140	0.168	0.074
All		0.148	0.089	0.072

Within the temperature and light experiments there was strong interspecific statistically significant differences for cellular carbon content (ANOVA on Ranks) P = <0.001 for temperature, and for cellular nitrogen P = <0.001 for temperature and P = 0.045 for light and finally for cellular phosphorous P = <0.001 for temperature. For nanophytoplankers combined there was no significant difference between the elemental quotas (Figure 5.2).

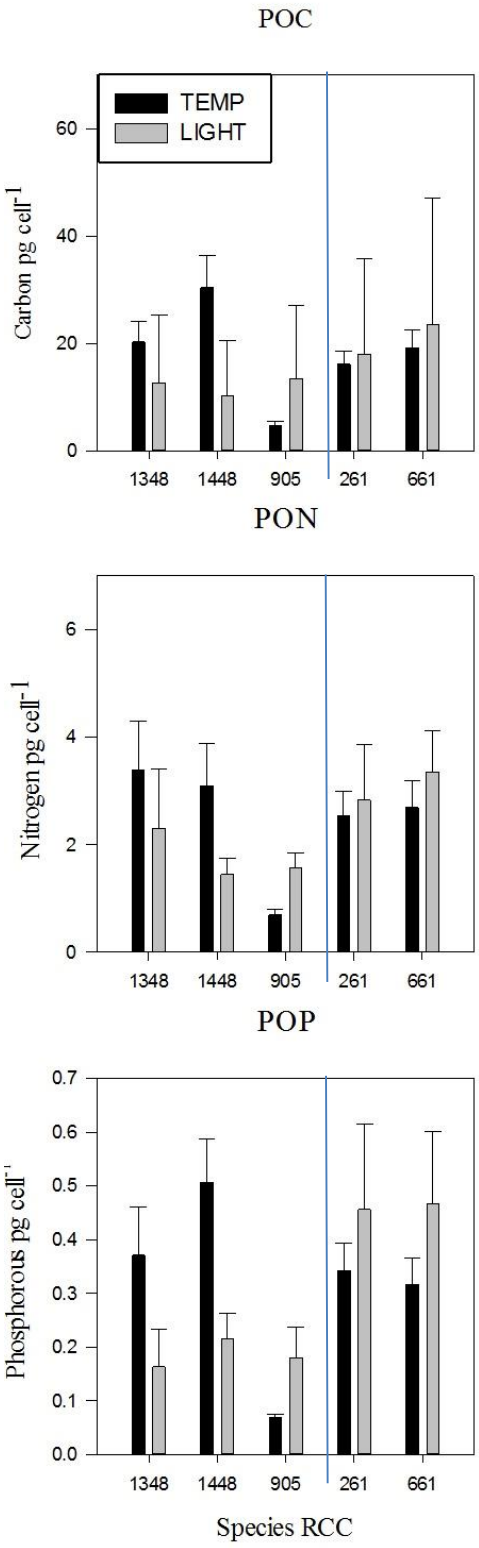

Figure 5.2 Mean carbon, nitrogen and phosphorus quotas (pg cell^{-1}) in nanophytoplanker species obtained from temperature (black bars) and light (grey bars) experiments. The whiskers show standard deviations. Left side of the plots are haptophytes, right are chlorophytes.

5.4.2 Nutrient saturated quotas and cell volume

Nanophytoplankton nutrient saturated quotas increase with cell volume (Mann-Whitney Rank Sum Test) P = <0.01 (Figure 5.2). Although there is a scaling with μ_{max} and cell volume, in the literature volume generally decreases as carbon quotas increase. Here, the inverse is true.

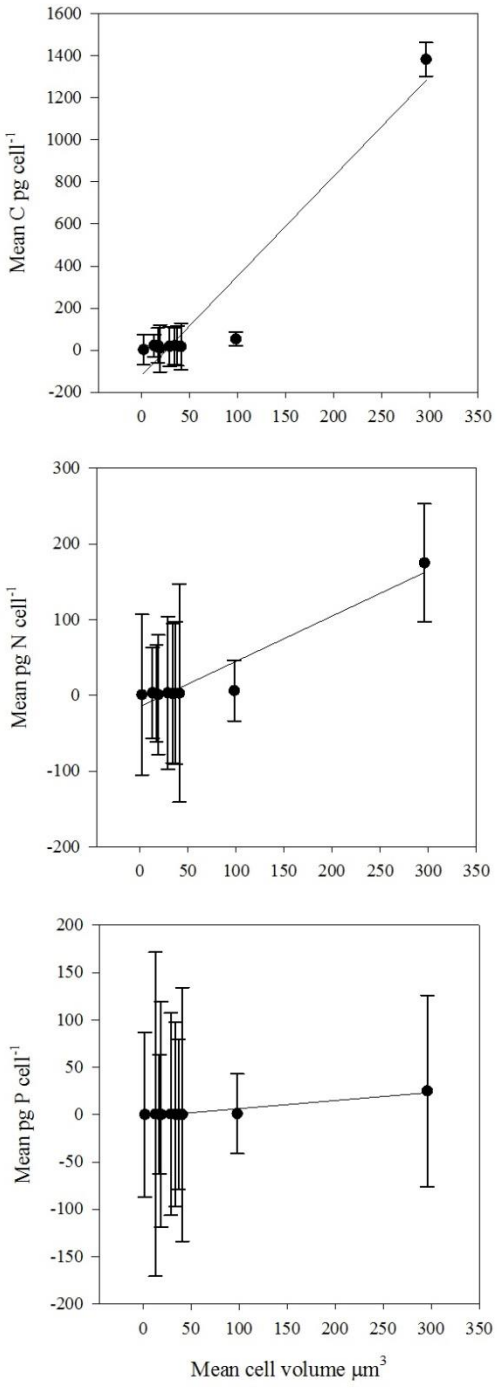

Figure 5.3 Mean carbon, nitrogen and phosphorus quotas (pg cell^{-1}) in nanophytoplankton. The lines through each plot are linear regressions. r^2 = 0.93 for carbon, 0.92 for nitrogen and 0.92 for phosphorus. Whiskers show the CV%.

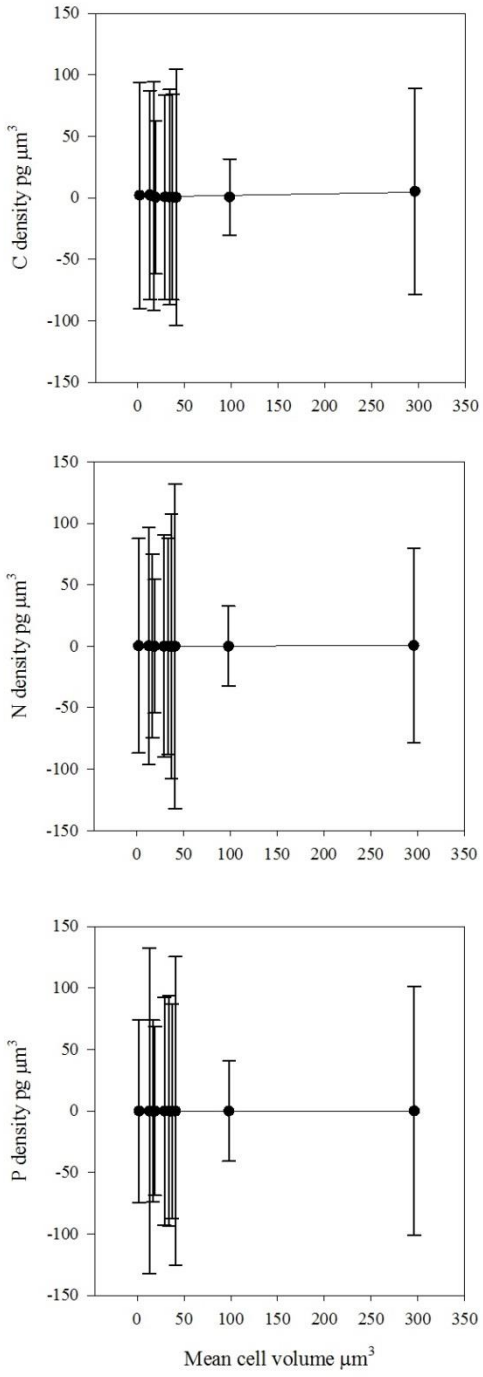

Figure 5.4 Mean carbon, nitrogen and phosphorus density (pg µm^3) in nanophytoplankton. The lines through each plot are linear regressions. r^2 = 0.60 for carbon, 0.59 for nitrogen and 0.59 for phosphorus. Whiskers show the CV%.

Figure 5.3 and Table 5.2 shows broad flexibility in nutrient uptake strategies under differing temperature and light conditions. To show this broad flexibility, data are shown from Figure 5.3 and Table 5.2 with the coefficient of variation. Table 5.2 also shows the cellular nutrient density per cellular volume for each species (as shown in Figure 5.4). Figure 5.4 shows that as the cell volume in nanophytoplankton increases, there is no statistical significance in the increase in nutrient density.

Table 5.2 Cell volume (μm^3), C and N quotas (pg $cell^{-1}$) and density (pg μm^3) of all the nanophytoplanker species measured under variable light and temperature conditions. Nutrient quota data are shown with the coefficient of variance.

RCC	Mean cell volume μm^3	CV %	Pg C $cell^{-1}$	CV %	C density Pg μm^3	Pg N $cell^{-1}$	CV %	N density Pg μm^3	Pg P $cell^{-1}$	CV %	P density μm^3
1348	41	29	18	111	0.45	3	144	0.1	0.29	134	0.007
1448	37	26	21	94	0.56	3.1	94	0.1	0.38	79	0.01
905	19	49	9	112	0.43	1.1	79	0.1	0.11	119	0.006
1406	13	63	23	53	2.37	3.4	60	0.3	0.58	171	0.05
647	2	34	4	72	1.99	0.9	106	0.4	0.12	87	0.05
661	34	19	21	88	0.61	2.8	92	0.1	0.4	97	0.01
261	29	37	19	94	0.73	3.2	101	0.1	0.5	107	0.02
916	17	27	24	83	1.47	2.7	64	0.2	0.27	63	0.02
21	98	31	54	33	0.58	6.4	40	0.1	0.92	42	0.01
91	296	35	1382	80	5.24	175	78	0.7	25	101	0.11

5.4.3 Nutrient stoichiometry

Nanophytoplankers show broad flexibility in nutrient stoichiometry under broad temperature and light conditions. There are strong statistical differences (Dunn's Method) in C:N ratios (P = <0.001), in N:P ratios (P = <0.001) and in C:P ratios (P = <0.001).

Nanophytoplankers uptake nutrients in excess of their requirements. This is reflected by lower, or similar N:P ratios to Redfield (Tables 5.4 and 5.7) and C:N ratios close to Redfield (Tables 5.5 and 5.8). There is no statistically significant difference between N:P ratios for nanophytoplanker and Redfield. All nanophytoplankers had N:P ratios in excess of 10:1 suggesting none were N-limited. None of the N:P ratios were in excess of 30:1 suggestions that there were not P-limited either. The two larger species (*O. distigma* and *S. trochoidea*) had higher C:N ratios than Redfield, which is expected since generally larger cells have higher ratios of respiration to photosynthesis (Marañón *et al*., 2013).

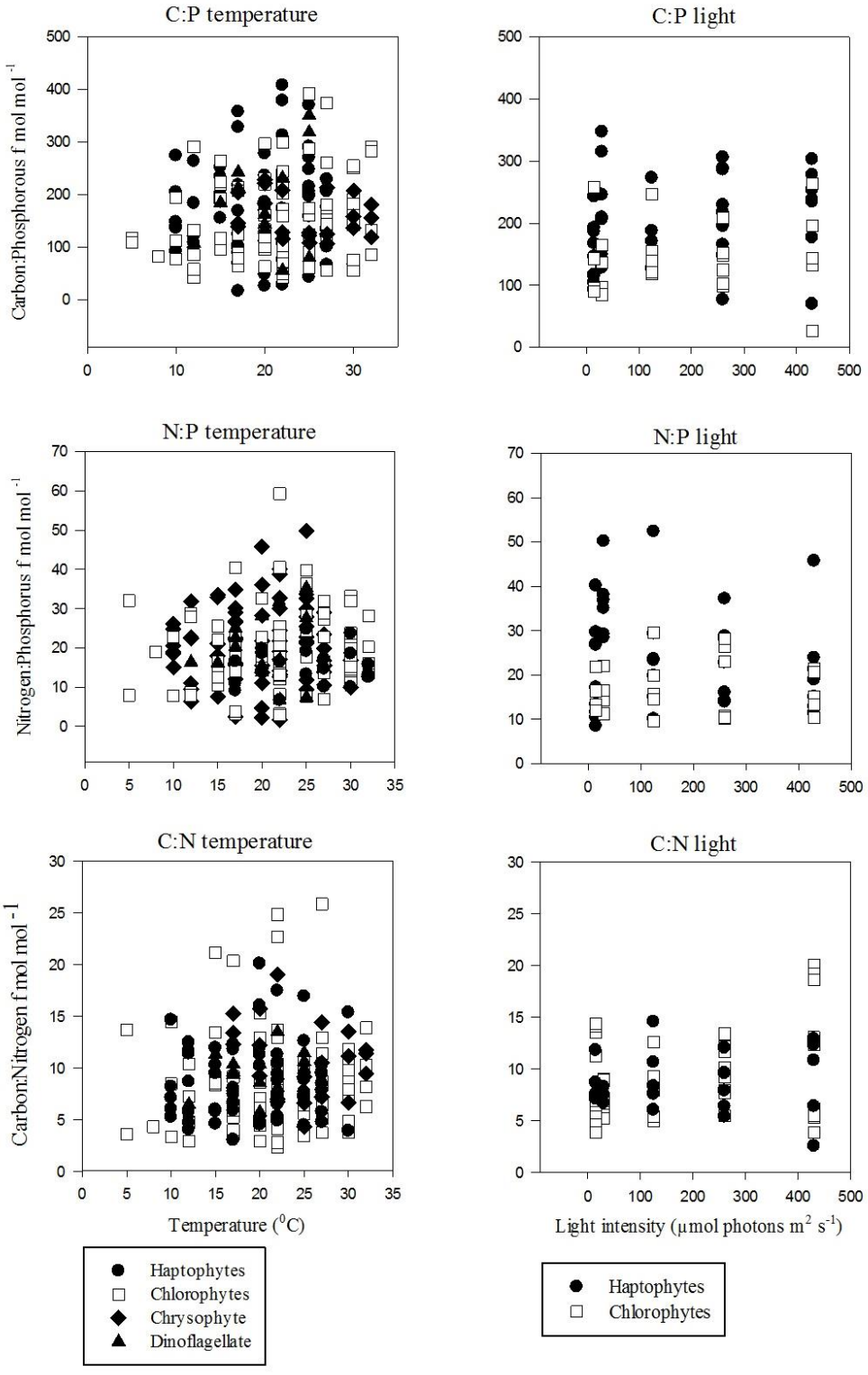

Figure 5.5 C:P, N:P and C:N ratios (in mol:mol) for different classes of nanophytoplankton.

Table 5.3 Mean species specific C:P ratios in the temperature experiment. The first four are haptophytes; the second four are chlorophytes, then the chrysophyte and the

dinoflagellate. For completeness, the minimum and maximum values are shown and all data are shown with their standard deviation.

Species	RCC number	n =	Mean C:P	SD	Min	Max
I. galbana	1348	8	249	(7)	96	157
P. calathiferum	1448	6	179	(19)	79	372
P. gayraliae	1406	8	208	(11)	69	261
I. rotunda	905	7	180	(5)	79	373
P. marina	261	6	123	(3)	99	147
C. stigmatophora	661	12	146	(5)	82	254
P. coloniale	916	6	221	(4)	189	251
M. pusilla	647	8	109	(5)	61	168
O. distigma	21	7	153	(4)	120	208
S. trochoidea	91	6	155	(4)	106	184
	Haptophytes	28	171	(7)	69	373
	Chlorophytes	33	147	(10)	62	254
	All	90	157	(6)	89	255

The mean C:P ratios from Figure 5.3 and from Table 5.3 shows nanophytoplankters under differing temperatures with values far in excess of Redfield ($P = <0.001$). For haptophytes the mean C:P ratio was 62% higher than Redfield. For chlorophytes the mean C:P ratio was 38% higher. The mean C:P ratio for the chrysophyte was 44% higher than Redfield and for the dinoflagellate it was 47% higher.

Table 5.4 Mean N:P ratios in the temperature experiment.

Species	RCC number	n =	Mean N:P	SD	Min	Max
I. galbana	1348	8	20	(0.9)	13	30
P. calathiferum	1448	6	22	(1.4)	8	32
P. gayraliae	1406	8	25	(0.8)	9	40
I. rotunda	905	7	22	(1.7)	10	32
P. marina	261	6	17	(0.5)	19	24
C. stigmatophora	661	12	17	(0.5)	9	23
P. coloniale	916	6	22	(0.4)	19	24
M. pusilla	647	8	18	(0.7)	12	26

O. distigma	21	7	15	(0.5)	11	19
S. trochoidea	91	6	18	(0.4)	11	19
Haptophytes		28	21	(0.6)	9	40
Chlorophytes		33	18	(0.3)	9	26
All		90	18	(0.3)	11	26

Figure 5.3 and Table 5.4 shows the mean N:P ratios from nanophytoplankers under differing temperatures. For haptophytes the mean N:P ratio was 30% higher than Redfield. For chlorophytes the mean N:P ratio was 13% higher. The mean N:P ratio for the chrysophyte was 4% lower than Redfield and for the dinoflagellate it was 10% higher.

Table 5.5 Mean C:N ratios in the temperature experiment.

Species	**RCC number**	**n =**	**Mean C:N**	**SD**	**Min**	**Max**
I. galbana	1348	8	7.9	(0.6)	4	12
P. calathiferum	1448	6	8.6	(2)	3	15
P. gayraliae	1406	8	9.6	(1.8)	7	13
I. rotunda	905	7	8.6	(0.7)	3	15
P. marina	261	6	7.5	(0.5)	6	9
C. stigmatophora	661	12	8.8	(0.8)	4	18
P. coloniale	916	6	8.8	(0.3)	8	11
M. pusilla	647	8	6.1	(0.6)	3	9
O. distigma	21	7	10	(0.7)	6	14
S. trochoidea	91	6	8.9	(0.7)	7	11
Haptophytes		28	8.6	(1)	3	15
Chlorophytes		33	8.2	(0.5)	3	18
All		90	8.9	(0.3)	5	14

The mean C:N ratios from Figure 5.3 and from Table 5.5 shows nanophytoplankers under differing temperatures with values far in excess of Redfield ($P = < 0.001$). For haptophytes the mean C:N ratio was 30% higher than Redfield. For chlorophytes the mean C:N ratio was 24% higher. The mean C:N ratio for the chrysophyte was 54% higher than Redfield and for the dinoflagellate it was 34% higher.

Table 5.6 Mean C:P ratios in the light experiment. The first three are haptophytes; the next two are chlorophytes. For completeness, the minimum and maximum values are shown. All data is shown with their standard deviation.

Species	RCC number	n =	Mean C:P	SD	Min	Max
I. galbana	1348	8	130	(14)	99	186
P. calathiferum	1448	6	135	(3)	101	172
I. rotunda	905	7	118	(9)	94	134
P. marina	261	6	118	(2.6)	95	175
C. stigmatophora	661	12	143	(10)	114	166
	Haptophytes	15	128	(8)	94	186
	Chlorophytes	10	130	(12)	95	175
	All	25	129	(3)	95	180

The mean C:P ratios from Figure 5.3 and from Table 5.6 shows nanophytoplankers under differing light intensities with values far in excess of Redfield (P = <0.001). For haptophytes the mean C:P ratio was 20% higher than Redfield. For chlorophytes the mean C:P ratio was 23% higher.

Table 5.7 N:P ratios in the light experiment.

Species	RCC number	n =	Mean N:P	SD	Min	Max
I. galbana	1348	8	17	(5)	10	24
P. calathiferum	1448	6	15	(1)	14	16
I. rotunda	905	7	16	(6)	7	25
P. marina	261	6	15	(2)	10	18
C. stigmatophora	661	12	18	(4)	15	27
	Haptophytes	21	16	(1)	7	25
	Chlorophytes	18	17	(1)	11	24
	All	39	17	(2)	9	25

Figure 5.3 and Table 5.7 shows the mean N:P ratios from nanophytoplankers under differing light intensities. For haptophytes the mean N:P ratio was the same as Redfield. For chlorophytes the mean N:P ratio was 2% higher than Redfield.

Table 5.8 C:N ratios in the light experiment.

Species	RCC number	n =	Mean C:N	SD	Min	Max
I. galbana	1348	8	7.9	(1)	6	12
P. calathiferum	1448	6	9.1	(0.6)	7	12
I. rotunda	905	7	8.6	(1)	7	12
P. marina	261	6	8.2	(4)	7	10
C. stigmatophora	661	12	8.1	(0.4)	6	11
	Haptophytes	21	8.3	(0.7)	6	12
	Chlorophytes	18	8.2	(2)	6	11
	All	39	8.3	(0.8)	6	12

The mean C:N ratios from Figure 5.3 and from Table 5.8 shows nanophytoplankers under differing light intensities with values far in excess of Redfield (P = <0.001). For haptophytes the mean C:N ratio was 29% higher than Redfield. For chlorophytes the mean C:N ratio was 24% higher.

5.4.4 Chlorophyll a to carbon ratios

The measurement of Chl *a*:C (θ) has been used frequently to assess the physiological state of phytoplankton relative to a specific environmental condition, usually either light (Geider, *et al*., 1985, 1986, 1987, 1996 and 1997), temperature (Eppley *et al*., 1976; Geider *et al*., 1987; Raven *et al*., 1988) or nutrients (Geider *et al*., 1997; Geider *et al*., 1998). The ratio is an indication of an organism's photosynthetic capacity. From the literature we see that the general response is an exponential decrease in the Chl *a*:C with increased temperature at a given light intensity and a linear decrease with increased light at constant temperature; similarly for nutrient deplete conditions with constant light and temperature (Geider, 2006). The Chl *a*:C ratios of nanophytoplankton follows those assumptions in the literature.

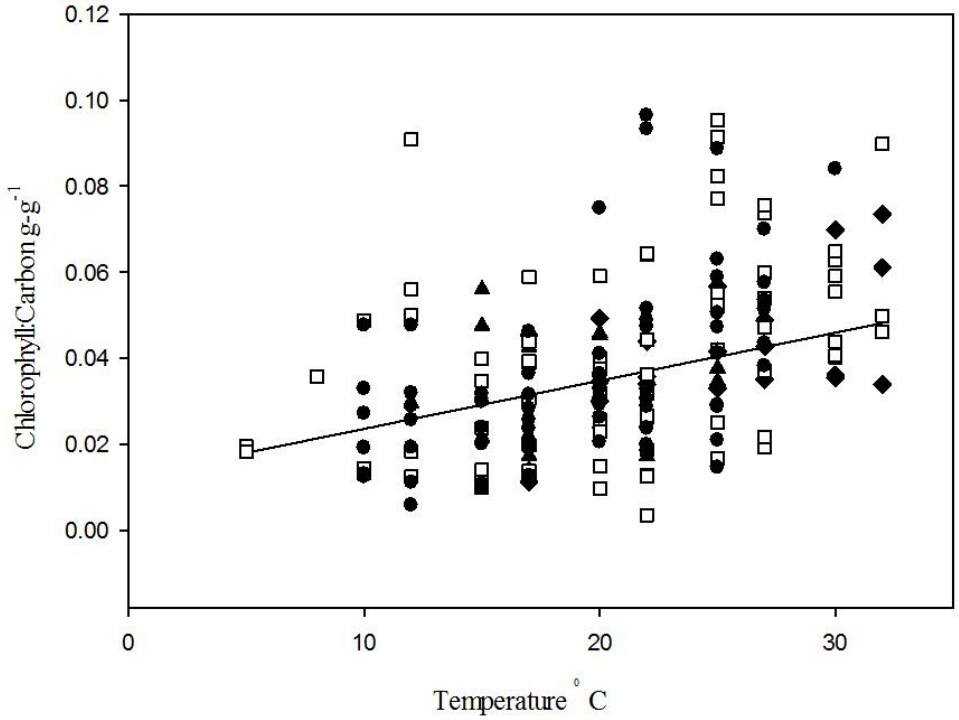

Figure 5.6 Chl *a*:C ratio as a linear function of temperature. Haptophytes filled circles; chlorophytes white squares; chyrsophyte filled diamond; dinoflagellate filled triangles. P = <0.05.

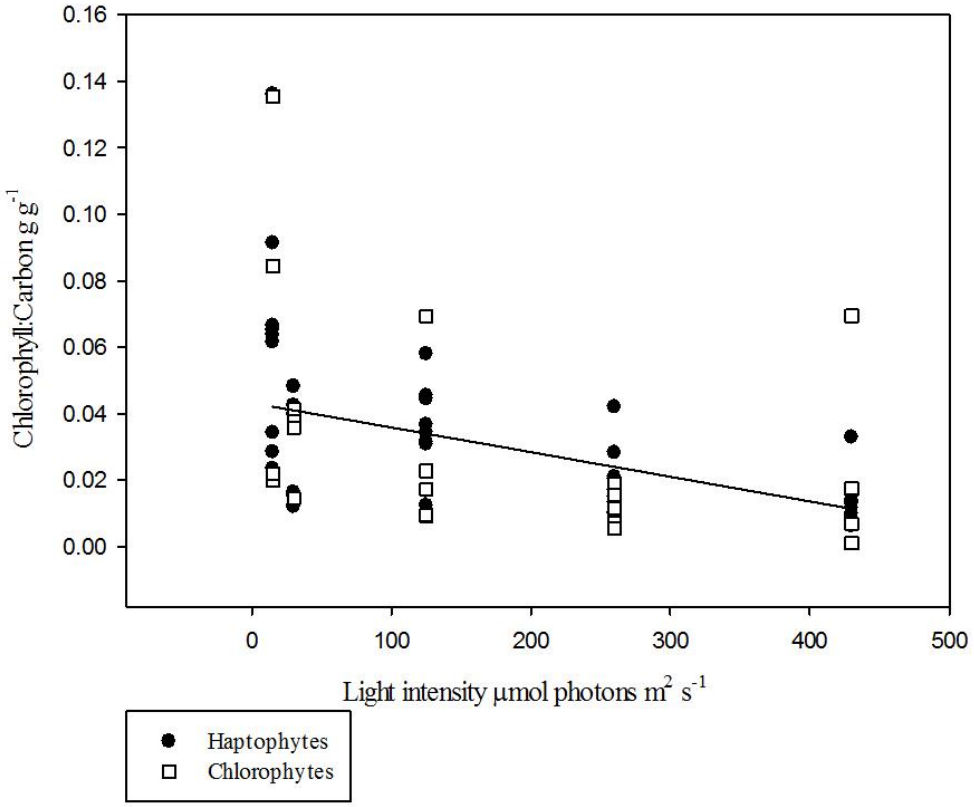

Figure 5.7 shows the Chl *a*:C ratio with light. Haptophytes filled circles; chlorophytes white squares. P = <0.05.

For haptophytes, the mean Chl *a*:C (g Chl *a* g^{-1} C) ratio for temperature and light respectively was 0.04 (for both) for *I. galbana*; 0.05 and 0.04 for *P. calathiferum*; 0.04 and 0.02 for *I. rotunda* and 0.04 (temperature only) for *P. gayraliae*. For the chlorophytes it was 0.06 (temperature only) for *M. pusilla*; 0.04 and 0.03 for *C. Stigmatophora*; 0.05 and 0.03 for *P. marina*; and 0.04 (temperature only) for *P. colonial.* For the chrysophyte the mean Chl *a*:C ratio for temperature was 0.03 and for the dinoflagellate it was 0.05.

Reduced chlorophyll at low temperatures and at high light intensities can be interpreted as an adaptive response in allocation of resources (Raven *et al*., 1988; Geider, 1987). Chl *a*:C reduced with increasing light intensity due to an increase in light acquisition and ranges between 0.001 and 0.14 g Chl *a* g^{-1} C but falls within the range of the

measured Chl *a*:C ratios at 260 μmol photons m^{-2} s^{-1}, which is approximately the light intensity at which the temperature experiments were conducted. Chl *a*:C decreases with decreasing temperature due to low temperature chlorosis and an increase in lipid production to maintain membrane fluidity (Geider, 1987; Raven *et al*., 1988). Chl *a*:C ratios range from 0.004 and 0.24 g Chl *a* g^{-1} C.

5.4.5 Comparison to Redfield

Nanophytoplankton does not statisically differ from Redfield. Acclimation to differing environmetal conditions like temperature and light causes variations in elemental ratios as well as the chlorophyll *a*:C ratio. Deviations from Redfield have been used to infer the growth limiting nutrient. Phytoplankton deprived of P typically have N:P in excess of 30:1, those deprived of N typically have ratios less than 10:1 (Levings, 1980; Geider *et al*., 2002). C:N and C:P are also dependent on growth conditions, but it is generally accepted that those growing near to Redfield are growing at their maximum rates (Levings, 1980; Goldman, 1986; Morel, 1987). Nanophytoplankton was neither N or P limited.

The following plots (Figures 5.6 – 5.11) show the nutrient stochiometry results compared to the Redfield ratios. Modeling efforts assume constant Redfield ratios and therefore the nutrient saturated stochiometry of nanophytoplankton could be used to inform physioloigcal responses under nutrient replete conditions.

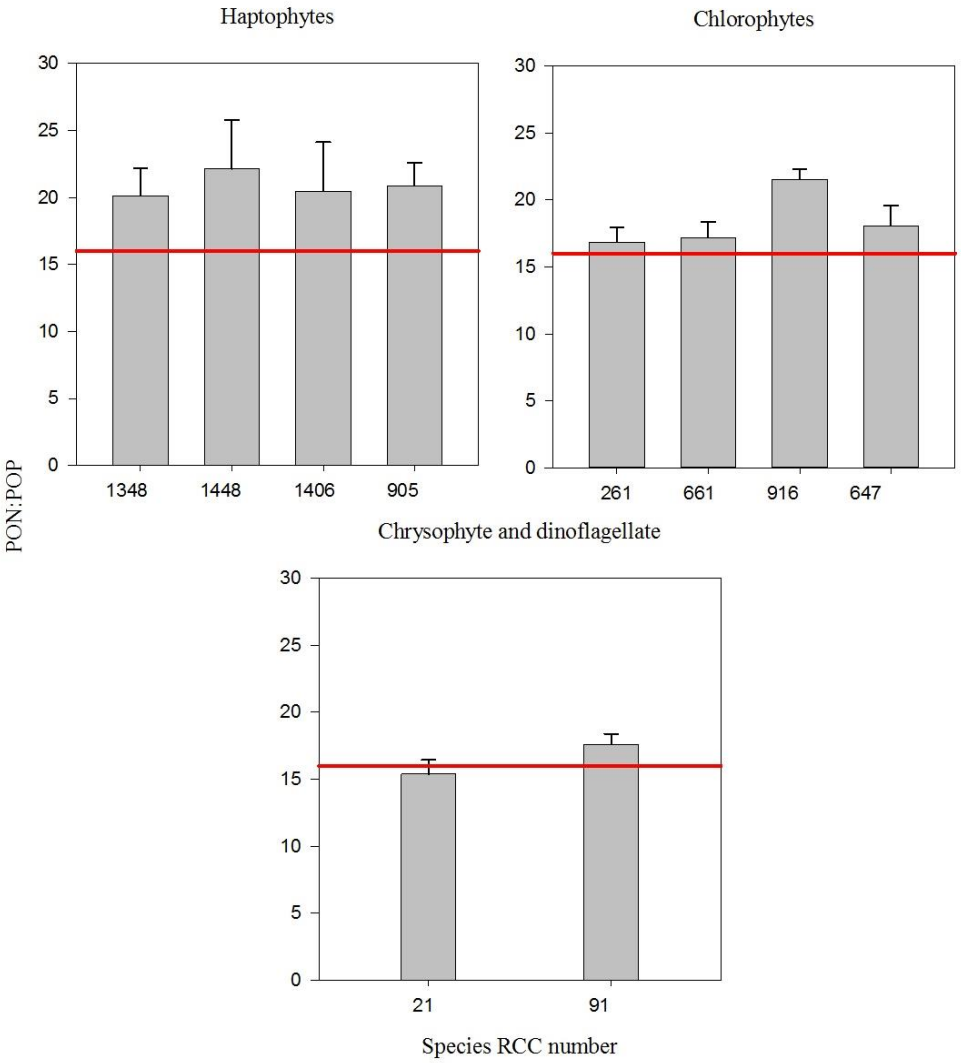

Figure 5.8 N:P ratios from the temperature experiment. The red line through each plot is the Redfield ratio. Data is shown ± SE.

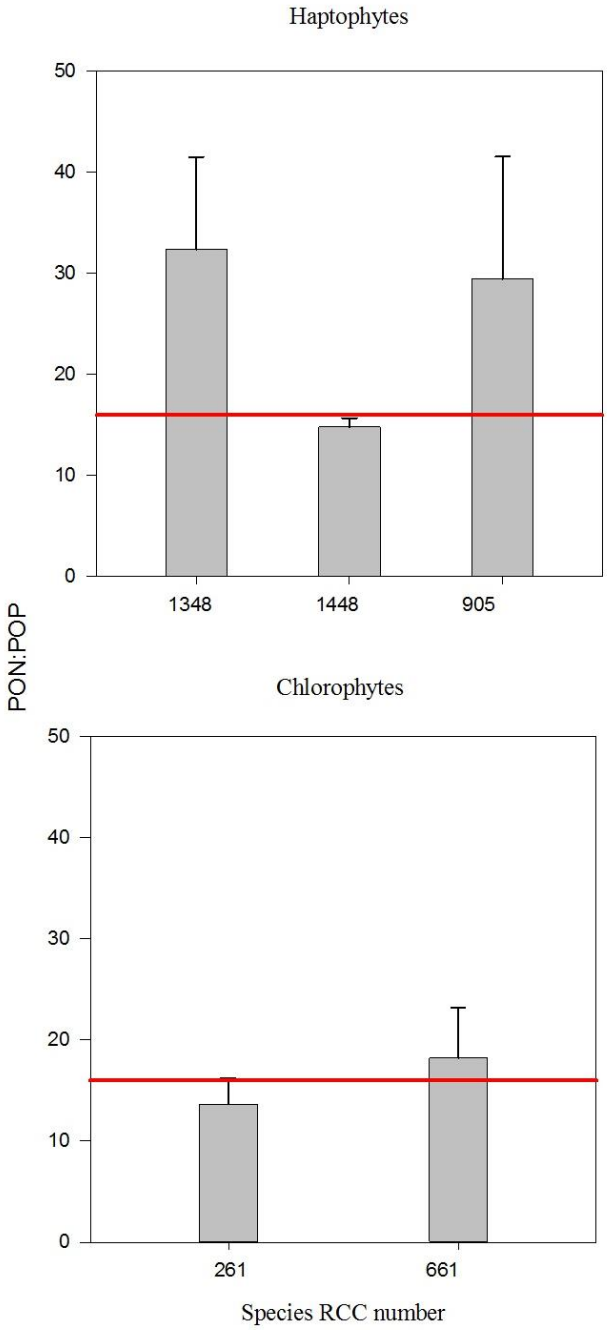

Figure 5.9 N:P ratios from the light experiment. The red line through each plot is the Redfield ratio. Data is shown ± SE.

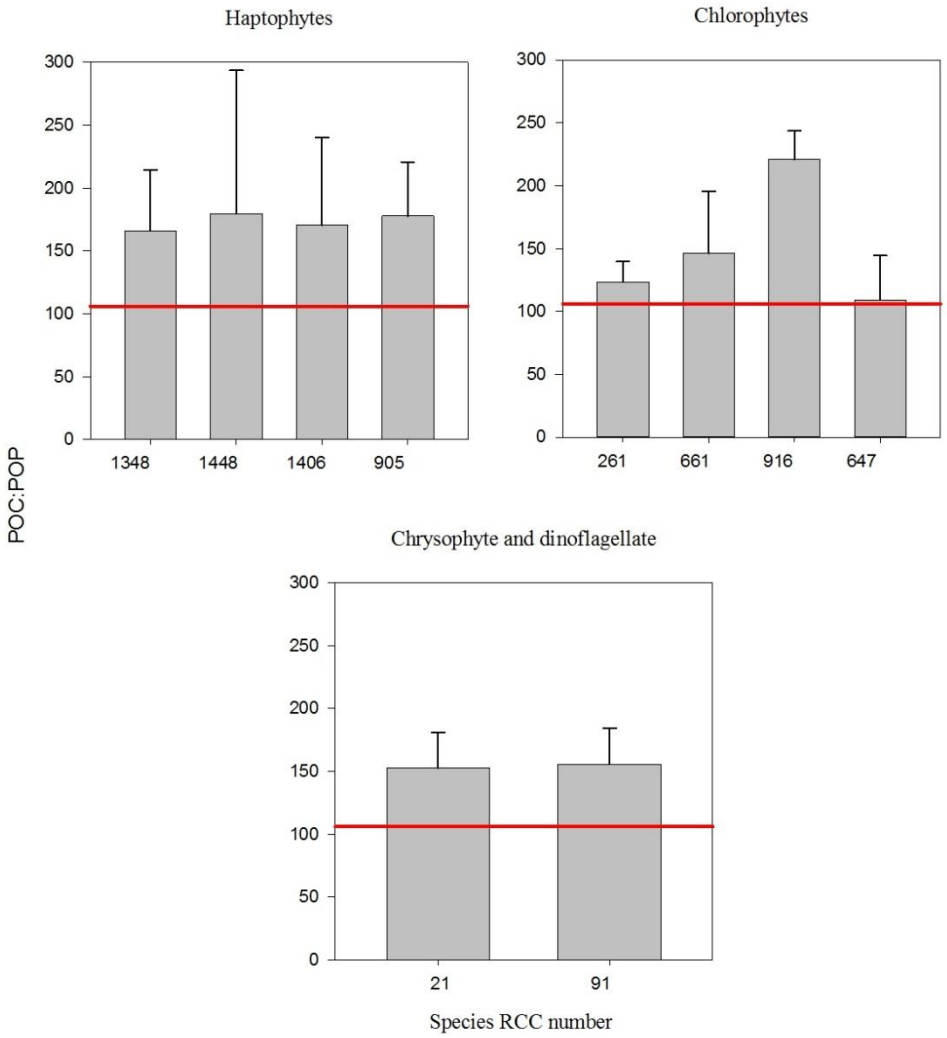

Figure 5.10 C:P ratios from the temperature experiment. The red line through each plot is the Redfield ratio. Data is shown ± SE.

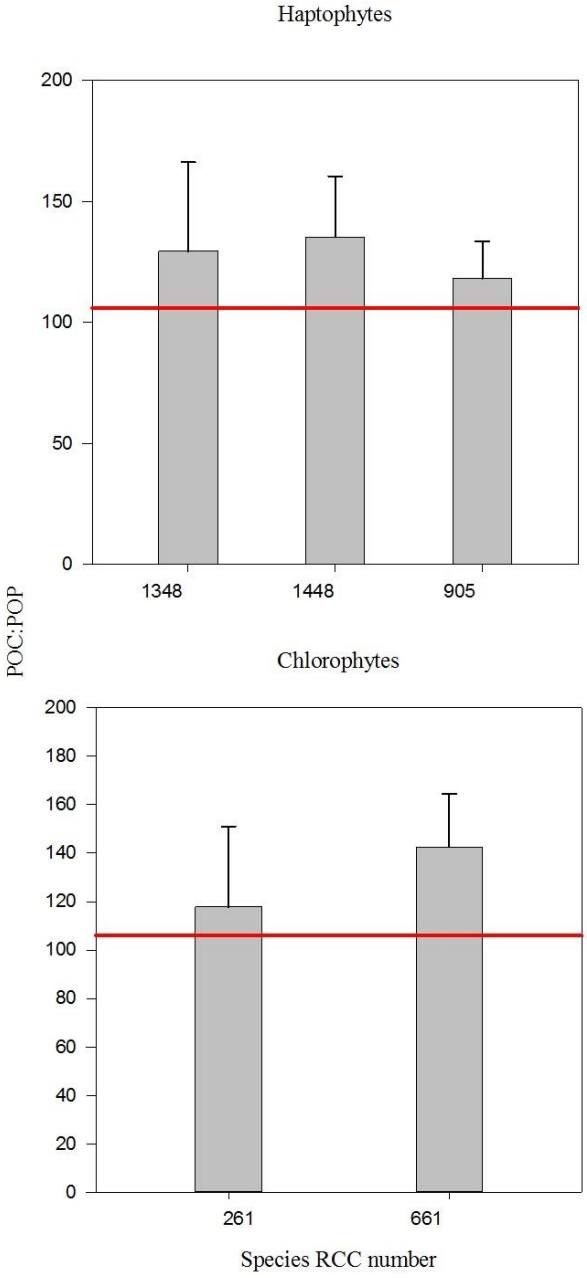

Figure 5.11 Mean C:P ratios from the light experiment. The red line through each plot is the Redfield ratio. Data is shown ± SE.

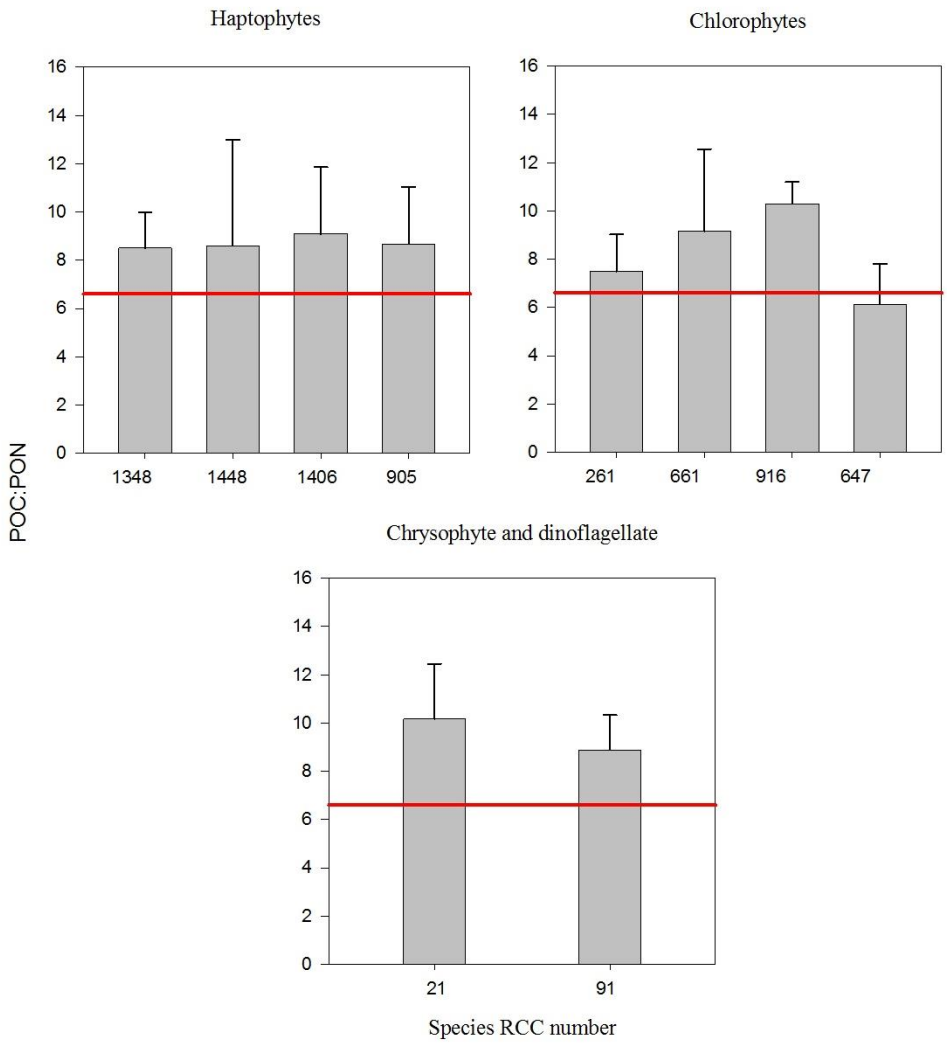

Figure 5.12 Mean C:N ratios from the temperature experiment. The red line through each plot is the Redfield ratio. Data is shown ± SE.

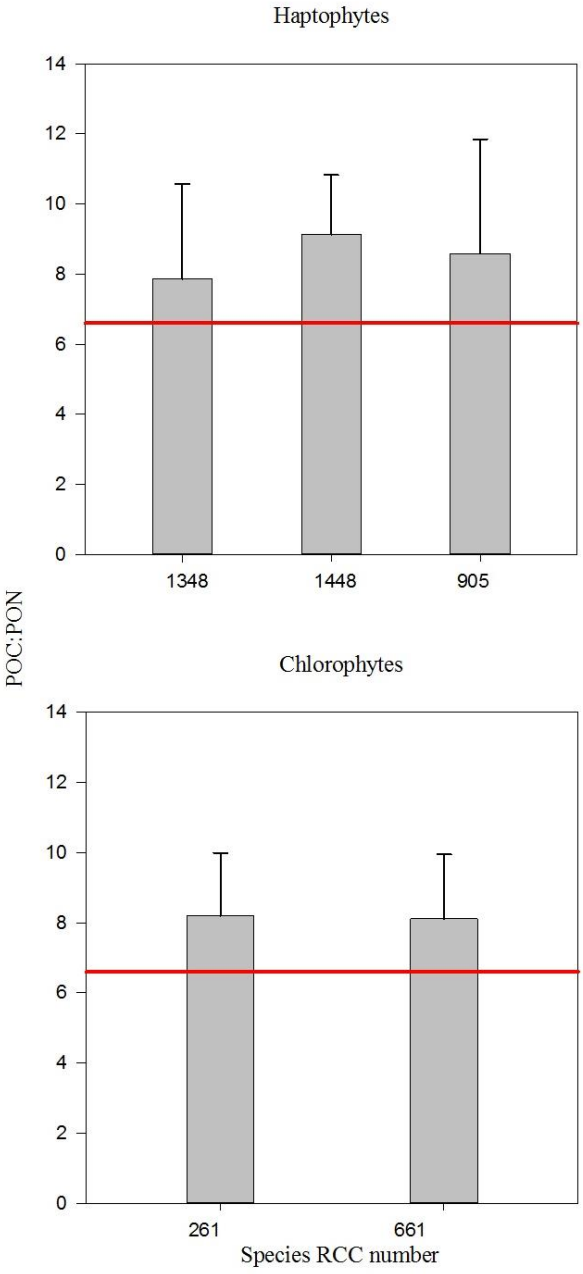

Figure 5.13 Mean C:N ratios from the light experiment. The red line through each plot is the Redfield ratio. Data is shown ± SE.

5.5 Discussion

5.5.1 Nutrient quotas

Global phytoplankton carbon is difficult to estimate because of the co-occurrence of other particulate organic matter in the ocean. Estimates

of carbon biomass have previously been determined using empirically derived carbon quota to cell volume relationships (Ishiwata *et al*., 2013). Carbon quotas are known to alter during the diel cycle – cells divide faster with increasing irradiance reflected in a decrease in the average cell size and carbon quotas and under differing environmental conditions – when cells are N-limited, cell volumes decrease and carbon quotas generally increase (Ishiwata *et al*., 2013). Carbon quotas increase with increasing cell size (Figure 5.3) and range between 4 pg C $cell^{-1}$ for the smallest species (2 μm) to 1263 pg C $cell^{-1}$ for the largest species (20 μm). From the literature for example; *I. galbana* (RCC 1348) has a carbon quota of 6.97 pg C $cell^{-1}$ at 16°C under 20–60 μmol m^2 sec^{-1} on a 14/10 h light/dark cycle with batch culture, with a growth rate of 0.32 d^{-1} (Montagnes *et al*., 1994) and 23.8 pg C $cell^{-1}$ at 25°C under 45 μmol m^2 sec^{-1} on a 12/12 h light/dark cycle with continuous culture, with a growth rate of 0.12 d^{-1} (Ishiwata *et al*., 2013). The mean carbon quota for this species under variable environmental conditions is 20.3 ± 3.6 pg C $cell^{-1}$. In this thesis, overall carbon quotas for haptophytes ranged from 1.1 – 79 pg C $cell^{-1}$ (mean = 20 pg C $cell^{-1}$, n = 4) which is in line with the literature. Combined mean carbon quotas ranged from 4 - 1263 pg C $cell^{-1}$ which demonstrates the diversity of the nanophytoplanker sizes and therefore contributes to greater variability. Nanophytoplankton nitrogen quotas in the literature range from 0.68 – 15.11 pg N $cell^{-1}$ (Bienfang *et al*., 1984; Montagnes *et al.,* 1994) which is in agreement with the nitrogen quotas in this thesis except for the dinoflagellate which is 10 times larger than many of the other species tested.

5.5.2 Cell volume

Cell volume is an adaptive trait, larger cell volumes are favoured when growth rate is limited by the rate at which cellular inorganic nutrients can be converted into biomass, and where maximum nutrient quotas increase with cell volume faster than minimum nutrient quotas (Verdy *et al*., 2009). In diatoms, their larger size and storage capacity

allows for increased ability to take up nitrogen relative to requirements, therefore, despite their larger nutrient requirements, increased internal quotas accelerate rates of biomass production in larger cells (Verdy *et al*., 2009). Smaller cell volumes are thought to possess similar nutrient-uptake abilities to larger cells, but consequently have higher nitrogen requirements, i.e. some larger cells that have a larger storage capacity possess a greater ability to uptake N relative to requirement but growth is limited by conversion of nutrients into biomass (Verdy *et al*., 2009).

Larger species have smaller surface to volume ratios and therefore are thought to be out competed in oligotrophic regions (mostly by nano and picophytoplankton); diatoms uniquely are claimed to be better nutrient competitors in varying conditions due to their vacuole spaces and ability to store nutrients. However, contrary to scaling expectations, Marañón *et al*., show that intermediately sized species may actually be better nutrient competitors (Marañón *et al*., 2013). Picophytoplankton in oligotrophic waters, are obviously very small (< 2 μm), but are better adapted to low nutrient availability (Taniguchi *et al*., 2014).

Figure 5.3 shows the considerable interspecific variability in nutrient to volume quotas for carbon, nitrogen and phosphorus and demonstrates that nutrient quotas increase with cell volume. Average volumes ranged from 2.3 – 296 μm^3 with a coefficient of variation of between 19 and 63%; literature ranges from 422 –1.2 $*10^7$ μm^3 with a coefficient of variation of between 22 – 56% (Verity *et al*., 1992; Menden-Deuer *et al.,* 2000). C, N and P showed considerable variation: C (pg C $cell^{-1}$) ranges from 4 – 1383 pg C $cell^{-1}$ with a coefficient of variation of between 33 – 112%. The literature ranges from 47.8 – 35,340 pg C $cell^{-1}$ with a coefficient of variation of between 1 – 68% (Menden-Deuer *et al*., 2000). Carbon density ranges from 0.45 – 5.24 pg C μm^3; literature ranges from 0.03 – 0.297 pg C μm^3 (Menden-Deuer *et al.,* 2000). Cell volume can influence carbon

density, but other factors may influence the interspecific variation which will become increasingly important to understand when modelling PFT biogeochemistry and climate change. For example, when cells are N-limited, cell volume can decrease as carbon quotas increase (Ishiwata *et al*., 2013). N (pg N $cell^{-1}$) ranges from 0.9 – 175 pg N $cell^{-1}$ with a coefficient of variation of between 40 – 144%; literature ranges from 10.62 – 2,656 pg N $cell^{-1}$ with a coefficient of variation of between 2 – 14% μm^3 (Menden-Deuer *et al.,* 2000). Nitrogen density ranges from 0.1 – 0.7 pg N μm^3 and in the literature it ranges between 0.02 – 0.1 pg N μm^3 (Menden-Deuer *et al.,* 2000). P (pg P $cell^{-1}$) ranges from 0.1 – 25 pg P $cell^{-1\ 1}$ with a coefficient of variation of between 42 – 171%. P density ranges from 0.006 – 0.1 Pg P μm^3. CVs are not a good indicator of variations in measurements because the number of replicates varies between samples; however, it is acceptable to describe variation between nanophytoplanker PFTs and data from the literature, further demonstrating that nanophytoplanker cell volumes can be very variable and dependent on nutrient concentration (Riegman *et al*., 2000).

5.5.3 Nutrient stoichiometry

Further to the interspecific variations found among these four classes of nanophytoplankton, in the literature, there are significant differences in the C:P and C:N ratios between phyla and superfamilies (Quigg *et al*., 2003). In the Quigg study, the C:P ratio for the chlorophytes was approximately 200 mol C:mol P which is higher than the C:P ratio here (mean was 149 mol C:mol P). The Quigg study was conducted under the same environmental conditions. Nutrient stoichiometry for nanophytoplankers in this thesis was conducted under variable light and temperature conditions and therefore the calculated values differ from the literature; however, it is an indication of how flexible members of the nanophytoplankton can be in their nutrient strategies under variable environmental conditions. The dinoflagellates were approximately 135 mol C:mol P which is lower

than *S. trochoidea* (mean was 155 mol C:mol P). The haptophytes were approximately 55 mol C:mol P which is considerably lower than the haptophytes here (mean 150 mol C:mol P). The N:P ratios in the literature review were higher, presumably they were P-limited for chlorophytes because N:P is approximately 31 mol N:mol P for chlorophytes. In this thesis the mean N:P for chlorophytes was 18 mol N:mol P. N:P was approximately 13 mol N:mol P for dinoflagellates which is not too indifferent from *S. trochoidea* (mean was 18 mol N:mol P). N:P was approximately 9 mol N:mol P for haptophytes, which is lower than the haptophytes here which had a mean of 19 mol N:mol P. C:N ratios were approximately 7 mol C:mol N for the chlorophytes, which is in line with the chlorophytes here which also had a mean of 8.2 mol C:mol N. The dinoflagellates were approximately 10.5 mol C:mol N, and here, *S. trochoidea* was slightly lower (mean was 8.9 mol C:mol N). Finally for the haptophytes it was approximately 7.5 mol C:mol N, which is in good agreement with the haptophytes here, which had a mean of 8.5 mol C:mol N. The nanophytoplankers presented here show no statistical relationship between C:N, C:P or N:P ratios and increasing temperature and light. C:N:P ratios are 150:21:1 for haptophytes (red superfamily; prymnesium phyla); 139:18:1 for chlorophytes (green superfamily); 153:15:1 for the chrysophyte (red superfamily) and 155:18:1 for the dinoflagellate (red superfamily).

Further examples from the literature under nutrient saturated conditions show C:N varies from between 3 – 17 mol C:mol N^{-1} (Verity *et al*., 1992; Geider *et al*., 2002). Here, values for C:N (mol C:mol N) range from 3 – 18 for the temperature experiment and from 6 – 12 for the light experiment. The mean C:N is 8.6 for haptophytes, 8.2 for chlorophytes and 8.6 for all nanophytoplankton. There is no clear increase in C:N with temperature. C:N increased with increasing light for the haptophytes, higher N relative to C at low light is likely either indicative of an accumulation of N-rich light harvesting

components or C-rich energy stores being used up under low light (Geider *et al*., 1988). There was no trend found for the chlorophytes.

N:P ratios less than 10:1 (mol N:mol P) are generally assumed to be nitrogen limited. All nutrient saturated measurements had mean N:P ratios higher than 10:1. High temperature is known to significantly affect phytoplankton metabolism, in particular protein synthesis increases, but the number of phosphate-rich ribosomes and associated rRNAs decrease producing higher N:P ratios and consequently an increased N-demand and therefore a shift to PFTs that are better adapted to N-limitation (Toseland *et al*., 2013). N:P can also increase with light likely as a physiological consequence of N-rich light and nutrient acquisition components altering within their cells (Toseland *et al*., 2013). In the literature values for N:P range from 5 – 19 mol N:mol P (Verity *et al*., 1992; Geider *et al*., 2002). Here, they range from 8 – 40 for varying temperature conditions and 7 – 27 (mol N: mol P) for varying light conditions.

In the literature, values of C:P (mol C:mol P) range from 27 to 135 (Verity *et al*., 1992; Geider *et al*., 2002). Here, they range from 61 – 372 for varying temperature conditions and 94 – 186 for varying light conditions (mol C: mol P). For temperature the mean C:P for haptophytes was 171 ± 7, for chlorophytes it was 147 ± 10 and for all nanophytoplankton it was 157 ± 6. (mol C:mol P). For the light experiment the C:P for haptophytes is 128 ± 8, for chlorophytes it is 130 ± 12 and for all nanophytoplankon it was 129 ± 3 (mol C:mol P). C:P was higher than Redfield for both experiments (Figures 5.8 and 5.9) so they were never P-limited. This would be expected to change in continuous cultures rather than in batch cultures. Lower C:P ratios under nutrient replete conditions indicate that species use more phosphorous relative to carbon, so when phosphorous is limited in nature, nanophytoplankton may be outcompeted by cells that generally have a lower C:P ratio.

5.5.4 Chlorophyll a:C

In order to compete in changing environmental conditions, members of the phytoplankton are able to change their cellular composition (on a timescale from hours to days) in a process known as acclimation. One measure of this physiological change is the chlorophyll *a* to carbon ratio which is a good indicator for measuring biomass and primary production.

It is known that with increases in temperature chlorophyll *a* increases linearly in relation to carbon. The Chl *a*:C results for the nanophytoplankton PFT confirm that there is a linear increase in Chl *a*:C with increasing temperature. Additionally, chlorophyll *a*: C ratios increased linearly with decreasing light intensity. At low light, more nitrogen is required for chlorophyll *a* synthesis and at low temperatures there is a decline in the chlorophyll *a* quota due to chlorosis (Geider *et al*., 1998).

The chlorophyll *a* quotas for the haptophytes ranged from 0.04 – 3 pg Chl *a* $cell^{-1}$ (mean = 0.77 pg Chl *a* $cell^{-1}$, n = 4). For the chlorophytes, chlorophyll *a* quotas ranged from 0.05 – 2.6 pg Chl *a* $cell^{-1}$ (mean = 0.53 pg Chl *a* $cell^{-1}$, n = 4). For the chrysophyte the chlorophyll *a* quota ranges from 1.5 – 4.3 pg Chl *a* $cell^{-1}$ (mean = 2.4 pg Chl *a* $cell^{-1}$, n = 1). For the dinoflagellate, the chlorophyll *a* quota ranged from 22 – 166 pg Chl *a* $cell^{-1}$ (mean = 66 pg Chl *a* $cell^{-1}$, n = 1).

5.6 Conclusions

Nanophytoplankton alters its elemental stoichiometry and assimilates nutrients in excess of its requirements under nutrient saturation in response to changing environmental conditions, there is no statistically significant difference between nanophytoplankton and the Redfield ratios (Paired T-test P = 0.36).

The defining use of the Redfield ratio in plankton physiology cannot necessarily be taken as the only explanation for biogeochemical cycling of carbon and nutrients. It may not be an entirely accurate tool to describe limiting nutrients. It is well known that phytoplankton cells can acclimate to environmental conditions by changing the proportional of their elemental components towards a homeostatic protein-rRNA ratio e.g. C and N-rich proteins or pigments, or P-rich RNA in order to compete and maximize growth, or reduce the impacts of damage such as photoinhibition. It is also known that phytoplankton up take nutrients in excess of their requirements under replete conditions (lower N:P ratios and C:N similar to those described by Redfield). Although Redfield remains a useful comparative tool, the deviations from Redfield are important enough that they can be seen on a global scale (geographical and seasonal differences). This further indicates the importance for plankton physiological data, as well as perhaps rethinking the use of traditional methods such as constraining phytoplankton into biogeochemical functional groups.

The elemental stoichiometry in this thesis do not statistically deviate from Redfield under nutrient replete conditions, perhaps this is because the plankters are striving towards homeostasis, and this is what Redfield saw in his original experiments. For example, where plankton strategies differ, one group may outcompete another until a homeostatic balance is achieved. Perhaps Redfield is simply only able to predict a global balance where the status quo exists.

These findings can contribute to the understanding of variability in C:N:P ratios in nanophytoplankton and their subsequent luxury nutrient quotas. Species-specific variability needs to be taken into account when defining PFTs and the wide variety of cell volumes as an adaptive response within nanophytoplankton can further confuse the defining nutrient parameters for nanophytoplankton. These results reflect the need for continuing empirical data on PFTs for elemental

composition and species specific differences for nutrient saturated and especially nutrient limited conditions.

5.7 Appendix

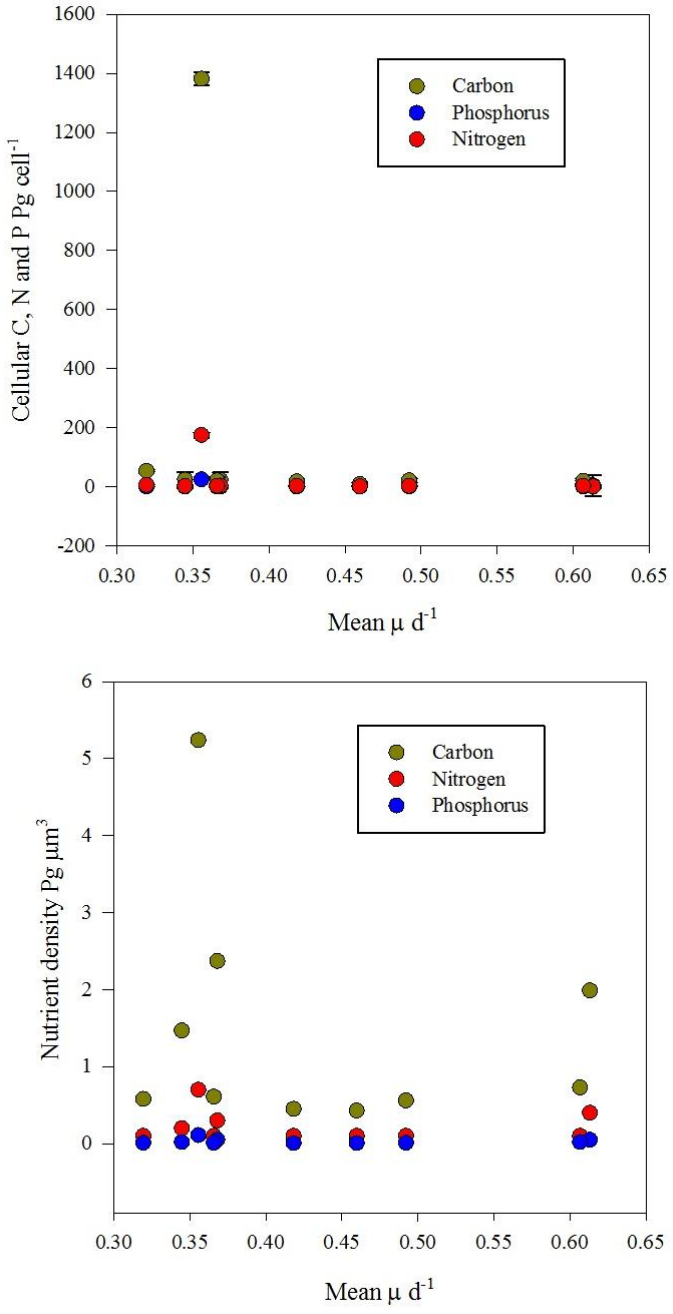

Figure 5.12 The top plot shows mean growth rate versus mean cellular C,N and P quotas and the bottom plot shows mean growth rate versus mean nutrient density for all nanophytoplankers.

6 Chapter 6: Discussion

6.1 Temperature effects on physiology

This research was conducted with the intent of characterizing the physiological parameters of nanophytoplankton in order to inform on modelling in PlankTOM10. The results from this thesis show that nanophytoplanker cannot be characterized as a PFT. Nanophytoplankton doed not follow all of the distinct characteristics governing the conceptual groupings of other PFTs. More data are required to parameterize the model.

For example, from Chapter 3 (temperature limitation) experiments were conducted on ten nanophytoplanker species from four classes and over a broad range of temperatures (0 – 32°C). Three fits (linear, exponential and optimum function) were calculated to the empirical data and there was significant support for two hypotheses: the temperature dependent maximum growth rates of single nanophytoplanker species fit best to an optimum function and the temperature dependent maximum growth rates of a nanophytoplanker PFT fit best to an optimum function. Therefore for nanophytoplankon optimum growth rates, optimum temperature and temperature tolerance ranges are the best parameters to identify nanophytoplankton temperature dependent physiological responses.

The use of Q_{10} and μ_{max0} in biogeochemical models for temperature dependent physiological responses therefore may be inappropriate for nanophytoplankton. Two of the species showed statistical significance for a linear relationship (non-linear curve-fitting regression) between growth rate and temperature – *M. pusilla* ($P = < 0.001$; $r^2 = 0.84$; mean slope = 0.03 ± 0.009) and *S. trochoidea* ($P = < 0.001$; $r^2 = 0.60$; mean slope = 0.02 ± 0.008). If growth rate responds linearly, this may suggest that the use of the Q_{10} could be inappropriate.

Data were also fitted to a 99% exponential quantile, but this gave a poor fit, and overall the results contradict that of Eppley (1972) and Bissinger *et al.* (2008). The Q_{10} value was also much lower than Bissinger (2008). Furthermore, the data from the other PFTs do not follow the Eppley curve, collectively; these PFTs differ from Eppley by 63% and differ from Bissinger by 73%.

It was hypothesized, that due to their smaller sizer, nanophytoplankers would have high growth rates. Additionally, since the majority of the nanophytoplankers were isolates from subtropical and tropical latitudes, it was hypothesized that they would be well adapted to warmer temperatures since algae tend to grow below their T_{opt} (to allow for interspecific competition). Although there was no significant relationship between T_{opt} and µopt, data from Figure 3.6 contradicts this hypothesis because it shows nanophytoplankers are not well adapted to higher temperatures. With increasing climate change and warming of SST, nanophytoplankton may be outcompeted by faster growing PFTs or those with much higher Q_{10} values. Since nanophytoplankers do not follow an exponential curve at warmer temperatures, the increase in global SST with increasing climate change may have a negative effect, especially for those geographically distributed close to their T_{opt}. With global warming, existing temperature niches will likely move north and newly created niches in the tropics might not be suitable for nanophytoplankton.

Generally, there is an expected intraspecific inverse relationship between cell volume with increasing temperature (and growth rates) (Brown e*t al*., 2004), and an interspecific expectation that there is a decrease in growth rate with increasing cell volume, nanophytoplankers show either a positive relationship, or a very smaller dependence of cell volume on growth rate. However, Figure 3.10 shows that for nanophytoplankers the optimum growth rate decreased as a function of the cell volume. The fit to Equation 3.5 shows a relatively small dependence on cell volume with an exponent of -0.095 (*vs.* -0.13 Sarthou *et al*., 2005 and -0.32 Buitenhuis *et al*., 2008). This result is a further indication that nanophytoplankton does not conform to expectations from the literature.

6.2 Light effects on physiology

Furthermore, in Chapter 4 light limited experiments were conducted on five nanophytoplanker species from two classes over a range of light intensities from 15 – 430 μmol photons m^2 s^{-1}. Growth rates were measured in species acclimated to specific light intensities. Instantaneous response rates of photosynthesis were also measured at different light intensities. From these measurements, five photophysiological parameters were derived including the maximum photosynthesis rate (P^C_{max}), respiration rate (resp), the initial slope of the PI curve (a^{chl}), light inhibition (β^{chl}) and the maximum chlorophyll to carbon ratio (θ_{max}) by fitting the measurements to a dynamic photosynthesis model. The first four parameters were also defined directly from curve fits to the photosynthesis *vs*. light (PE) curves.

To define nanophytoplankton as a PFT, it was expected that the photophysiological parameters would best fit to a dynamic model (Geider *et al*., 1996, 1998). This hypothesis was tested and rejected based on the results of the AIC. The AIC indicated that in fact the acclimated model is a better fit than the dynamic model (-3.75 *vs*. -0.95). If the difference is greater than 2 it is said to be statistically different.

Within nanophytoplankton there was a statistically significant species-specific difference between the growth rates within the haptophytes and between the two chlorophytes. However, there was no significant difference when taken collectively.

Size is an important indicator of phytoplankton physiology. The geometry of cells determines the photosynthetic capacity of cells via absorption and diffusion. Size determines the loss by sedimentation which is important for climate change modeling and carbon export. It is also important for surface-to-volume ratios relevant for determining nutrient uptake strategies. μ_{max} is also an important indicator of phytoplankton physiology because species with too low a μ_{max} will be naturally selected against. Evolutionarily speaking, it makes sense to adopt a higher μ_{max} under sufficient resources to combat the environmental experiences of resource fluctuations and mortality. Therefore

scaling μ_{max} with cell volume is used to help characterize phytoplankton physiology. Previous studies have used either a Euclidean 2/3 volume scaling exponent, or a metabolic theory ¾ volume scaling exponent. However, literature reviews have seen strong deviations in phytoplankton responses from both of these scaling exponents. Perhaps this is due to different methods (e.g. biovolume *vs*. carbon weight). Both photosynthesis and growth differ by losses in respiration, which also scale with size. The common variable among all phytoplankton is metabolism, but other factor that need to be take account of include taxonomic differences, physiological state as well as cell shape. Results from this thesis indicate that the light dependent maximum growth rates increases with increasing cell volume for nanophytoplankton (i.e. μmax scales with cell volume). However, a non-uniform scale has also been proposed (Wirtz, 2011), particularly to predict the response of smaller cells. For example, the ¾ scale exponent generally predicts very high μ_{max}; something in the order of 5 d^{-1} therefore may only be relevant to macro phytoplankton.

Between the chlorophytes and the haptophytes, there was a statistically significant difference in photoinhibition. These results further indicate the diversity of physiological responses, and therefore the difficulties in PFT classification.

6.3 Nutrient effects on physiology

In Chapter 5, the physiological variability in nutrient stoichiometry under differing temperature conditions is presented for ten species of nanophytoplankton from four classes and under differing light conditions for five nanophytoplanker species from two classes. The hypothesis tested was that members of the nanophytoplankton assimilate nutrients in excess of their requirements by altering their elemental composition under nutrient saturated conditions resulting in N:P (18 *vs.*16); C:P (143 *vs.*106) and C:N (8.6 *vs*. 6.6) ratios that are higher than Redfield. The results from the tested temperature and light conditions confirm the hypothesis that members of the nanophytoplankton assimilate nutrients in excess of their requirements.

Nanophytoplankers do not have nutrient quotas statistically different from Redfield under nutrient saturated conditions. These results are actually positive for PFT modeling since constant Redfield models are assumed. Despite this, literature reviews have seen significant deviations from Redfield. For modelling purposes deviations from Redfield are used to infer the limiting nutrient, and although nanophytoplankers do deviate from Redfield (not significantly), N:P ratios were never in excess of 30:1 (not P-limited) and were never less than 10:1 (not N-limited). These ratios would be expected to change under nutrient deplete experiments.

Nutrients, light and temperature can affect C:N. In particular C:N can increase significantly when cells are subject to nutrient stress. Since these experiments were conducted under nutrient saturated conditions, this further demonstrates the need for nutrient limited data on the nanophytoplankton.

These findings can contribute to the understanding of variability in C:N:P ratios in the nanophytoplankton and subsequent luxury nutrient quotas. Species-specific variability needs to be taken into account when defining PFTs. There is a statistically significant difference between C, N and P content and cell volume for nanophytoplankers ($P = < 0.01$). Quigg *et al.*, 2003 suggest that further interpretation of PFT variation can be achieved by analysing the micro nutrient ratios as well as those of the macronutrients.

6.4 General conclusions and future work

Overall, this study provides good evidence that nanophytoplankton is not well adapted to high temperatures and therefore will likely be negatively affected by climate change (Figure 3.6). Evidence shows increasing SST over the past century has caused a decline of ~1% of global phytoplankton biomass per year (Boyce *et al.*, 2010), but the majority of this loss seems to be from larger eukaryotic PFTs like diatoms (which contribute to ~25% of the global carbon fixation (Field *et al.*, 1998; Toseland *et al.*, 2013). Increasingly there is evidence of shifts towards smaller size classes like nanophytoplankton and picophytoplankton. However, the current physiological responses of nanophytoplankton to climate change suggest that they would be negatively

affected, unless the complex environmental factors influencing their distribution also alter (e.g. possible reduction of competition from grazing pressures).

Nanophytoplankton demonstrates significant differences in its physiological responses to climate change indicators, reflected by its geographical distribution and temperature optima for growth. The increasing interspecific importance of cell size with climate change and stratification and the decrease in cell volume with growth rates that vary between species further demonstrate the diversity of nanophytoplankers.

Because nanophytoplankton may be affected negatively by climate change, it is important to investigate and include the physiological responses of this diverse group to understand fully the ecological niche of this PFT and biogeochemical cycles within the ocean and consequently, the impact on the biological pump and the global carbon cycle. In particular, it is important to study N-limitation and N:P ratios with increasing temperature.

Phytoplankton cultures are extremely important for investigating the physiological effects of climate change empirically. However, the strain of alga is often bought from culture collections or has been isolated from its natural environment for up to 17 years (as in this present study), which may have caused it to differ genetically from its natural counterparts. Generally, those physiological adaptations gleaned from experimental data can be representative of evolutionary adaptations in natural environments. However, increasingly, it is suggested that it is entirely plausible that the measured physiological responses under controlled laboratory conditions can be indicative of evolutionary adaptations to and/or non-adaptive changes to those controlled laboratory conditions rather than those imposed by their natural environment (Lakeman, 2009).

To address this, one aspect of future work should include the isolation of the same species from the same location as the original culture collection. Experiments should be repeated to see if there is any change from laboratory conditions. In addition, another caveat of using laboratory controlled

experiments is that it not always possible to account for all parameters in the laboratory that are present in nature.

Nevertheless, while trying to address these caveats, more empirical physiological responses are required for a wider variety of nanophytoplanker species, particularly for nutrient limitation and nutrient saturation to parameterize biogeochemical models. Applying Redfield ratios to PFT physiological responses can help define what is actually occurring within a PFT because nutrient stoichiometry does not differ significantly between nanophytoplankton classes under different and changeable environmental conditions. For example, in the literature it is generally expected that cell volume can decrease as carbon quotas increase, which can lead to N-limitation. However, the results from this thesis suggest that nutrient quotas increase with increasing cell volume (Figure 5.3).

Nanophytoplankton is an important competitor in the Southern Ocean and therefore species isolated from this geographical location would be beneficial for future investigation. For nutrient limitation experiments, nutrients other than carbon, nitrogen and phosphorus should be considered. For example, as alluded to, nanophytoplankton is important in the Southern Ocean where it has been suggested that iron is the limiting nutrient for growth. These investigations would improve the current understanding of nanophytoplankton physiological responses in high nutrient low chlorophyll (HNLC) geographical regions.

In temperate water, nanophytoplankton contribution to carbon fixation is 30 – 50% and higher than the total chlorophyll *a* concentrations – 10 – 20% (Poulton *et al*., 2006). Changes in light intensity cause variations in photosynthesis and respiration rates and are controlled in geographical regions where light and temperature fluctuate seasonally. Temperature changes indirectly control algal community succession in these areas via the development of a thermocline. However, nanophytoplankton is also predominant throughout the water column irrespective of stratification or well mixed waters (Uitz *et al*., 2006). Nanophytoplankton also does well in

oligotrophic waters like the Southern Ocean (in number, not biovolume) (Jickells *et al*., 2007) and in HNLC regions (Detmer *et al*., 1997; Palevsky *et al*., 2013). In oligotrophic waters they are suggested to contribute 45% of the biomass *cf*. 21% in eutrophic water (Uitz *et al*., 2006) but with tripled chlorophyll *a* content in eutrophic water *vs*. oligotrophic water (Uitz *et al*., 2006).

Future work should include polar isolates as well as genetic analyses of HNLC species to establish if nanophytoplankton is not well adapted to higher temperatures. Additionally, adaptation vs. acclimation could be studied – especially where the use of culture collections vs. natural isolates are concerned. Modelling is an incredibly important aspect of climate change responses in the marine environment and therefore they must incorporate more physiological data simply because of the high diversity of physiological responses across plankton species and PFTs. Finally, nutrient limitation needs to be studied to inform on physiological responses to resource limitation.

7 Chapter 7: Bibliography

Adams, G.L., Picher, D.E., Cox, E.J., O'Gorman, E.J., Seeney, A., Woodward, G., Reuman, D.C. 2013. Diatoms can be an important exception to temperature-size rules at species and community levels of organization. *Global Change Biology*. Vol. **19**. pp. 3540-3552

Alvain, S., Moulin, C., Dandonneau, Y., Breon, F.M. 2005. Remote sensing of phytoplankton groups in case 1 waters from global SeaWiFS imagery. *Deep Sea Research Part 1 Oceanographic Research Papers*. Vol. **52**. No. 11. pp. 1-34

Aminot, A., Rey, F. 1999. Standard procedure for the determination of chlorophyll *a* by spectroscopic methods. *International Council for the Exploration of the Sea*. pp. 1-17

Anderson, A., Haecky, P., Hagström, Å. 1994. Effect of temperature and light on the growth of micro, nano and picoplankton: impact on algal succession. *Marine Biology*. Vol. **120**. pp. 511-520

Anderson, R.A. 2005a. *Algal Culturing Techniques*. Elsevier Inc. London. UK

Anderson, T.R. 2005b. Plankton functional type modelling: running before we can walk? *Journal of Plankton Research*. Vol. **27**. No. 11. pp. 1073-1081

Anderson, T.R., Hessen, D., Elser, J., Urabe, J. 2005. Metabolic stoichiometry and the rate of excess carbon and nutrients in consumers. *The American Naturalist*. Vol. **165**. No. 1. pp. 1-15

Apline, A.E., Cloern, J.E. 1988. Phytoplankton growth rates in a light-limited environment, San Francisco Bay. *Marine Ecology Progress Series*. Vol. **44**. pp. 167-173

Armstrong, R.A. 2006. Optimally-based modelling of nitrogen allocation and photoacclimation in photosynthesis. *Deep Sea Research*. Vol. **53**. No. 2. pp. 513-531

Armstrong, R.A., Lee, C., Hedges, J.I., Honjo. S., Wakeham, S.G. 2002. A new, mechanistic model for organic carbon fluxes in the ocean: based on the quantitative association of POC with ballast minerals. *Deep Sea Research*. Part 2. Vol. **49**. pp. 212-236

Arrigo, K.R. 2005. Marine microorganisms and global nutrient cycles. *Nature*. Vol. **437**. No. 7

Arrigo, K.R. 2007. Marine manipulations : Carbon Cycle. *Nature*. Vol. **450**. No. 22. pp. 491-492

Aumount, O., Maier-Reimer, E., Blain, S., Monfray, P. 2003. An ecosystem mode of the global ocean including Fe, Si, P colimitation. *Global Biogeochemical Cycles*. Vol. **17**. No. 2. pp.1-15

Bannister, T. T. 1979. Quantitative description of steady state, nutrient-saturated algal growth, including adaptation *Limnology and Oceanography*.Vol.24 pp. 76-96.

Barnosky, A.D., Hadly, E.A., Bascompte, J., Berlow, E.L., Brown, J.B., Fortelius, M., Getz, W.M., Hart, J., Hastings, A., Marquett, P.A., Martinez, N.D., Moores, A., Roopnarine, P., Vermeiji, G., Williams, J.W., Gillespie, R., Kitzes, J., Marshall, C., Matzke, N., Mindell, D.P., Revilla, E., Smith, A.B. 2012. Approaching a state shift in the Earth's biosphere. *Nature*. Vol. **486**. pp. 52-58

Bathmann, U., Priddle, J., Tréguer, P., Lucas, M., Hall, J., Parslow, J. 2000. *Plankton ecology and biogeochemistry in the Southern Ocean; A review of the Southern Ocean JGOFS*. pp. 300-331. In: Hanson, R.B., Ducklow, H.W., Filed, J.G. 2000. *The Changing Ocean Carbon Cycle: A midterm synthesis of the Joint Global Ocean Flux Study*. Cambridge University Press. Cambridge. UK.

Beardall, J., Ihnken, S., Quigg, A. 2009. Gross and net primary production: closing the gap between concepts and measurements. *Aquatic Microbial Ecology*. Vol. **53**. pp. 113-122

Beaugrand, G. 2004. The North Sea regime shift: evidence, causes, mechanisms and consequences. *Progress in Oceanography*. Vol. **60**. pp. 245-262

Beaugrand, G., Mc-Quatters-Gollop, A., Edwards, M., Goberville, E., 2013. Long-term responses of North Atlantic calcifying plankton to climate change. *Nature Climate Change*. Vol. **3**. pp. 263-267

Beckman Coulter, I. 2014. Multisizer 3 Coulter Counter: Coulter Counter Analyzers. Available at: www.beckmancoulter.com. Cited: 20/03/14

Behrenfeld, M. 2010. Abandoning Sverdrup's Critical Depth Hypothesis on phytoplankton blooms. *Ecology*. Vol. **91**. No. 4. pp. 977-989

Behrenfeld, M. J., Marañón, E., Siegel, D.A., Hooker, S.B. 2002. A photoacclimation and nutrient based model of light-saturated photosynthesis for quantifying oceanic primary production, Marine Ecology Progress Series. Vol. **228**. pp. 103-117

Behrenfeld, M., O'Malley, R.T., Siegel, D.A., McClain, C.R., Sarmiento, J.L., Feldman, G.C., Milligan, A.J., Falkowski, P.G., Letelier, R.M., Boss, E.S. 2006. Climate-driven trends in contemporary ocean productivity. *Letters to Nature*. Vol. **444**. pp.752-755

Behrenfeld, M.J., Boss, E., Siegel, D.A., Shea, D.M. 2005. Carbon-based ocean productivity and phytoplankton physiology from space. *Global Biogeochemical Cycles*. Vol. **19**. No. 1. pp. 1-14

Behrenfeld, M.J., Siegel, D. A., O'Malley, R. T., Maritorena, S. 2009. Global ocean phytoplankton. In Peterson, T.C., Baringer, M.O. (Eds.) State of the Climate in 2008. *Bulletin of the American Meteorological Society*. Vol. **90**. No.8. pp. 68-73

Benson B.B., Krause D. Jr. 1984. The concentration and isotopic fractionation of oxygen dissolved in freshwater and seawater in equilibrium with the atmosphere. *Limnology and Oceanography*. Vol. **29**. pp. 620–632

Berges, J.A., Falkowski, P.G. 1998. Physiological stress and cell death in marine phytoplankton: Induction of proteases in response to nitrogen or light limitation. *Limnology and Oceanography*. Vol. **43**. pp. 129-135

Berges, J.A., Franklin, D. ,Harrison, P.J. 2001. Evolution of an artificial seawater medium: Improvements in enriched seawater, artificial water over the last two decades. *Journal of Phycology*. Vol. **37**. pp.1138–1145.

Berges, J.A., Varela, D.E., Harrison, P.J. 2002. Effects of temperature on growth rate, cell composition and nitrogen metabolism in the marine diatom *Thalassioria pseudonana* (Bacillariophyceae). *Marine Ecology Progress Series*. Vol. **225**. pp. 139-146

Bertilsson, S., Berglund, O., Karl, D.M., Chisholm, S.W. 2003. Elemental composition of marine *Prochlorococcus* and *Synechococcus*: Implications for the ecological stoichiometry of the sea. *Limnology and Oceanography*. Vol. **48**. No. 5. pp.1721–1731

Bianucci, L., Denam, K.L. 2012. Carbon and oxygen cycles: Sensitivity to changes in environmental forcing in a coastal upwelling system. *Journal of Geophysical Research*. Vol. **117**. pp.1-13

Bidwell, R. G. S. 1977. Photosynthesis and light and dark respiration in freshwater algae. *Canadian Journal of Botany*. Vol. **5**. pp 809-818

Bienfang, P.K., Harrison, P.J. 1984. Co-variation of sinking rate and cell quota among nutrient replete marine phytoplankton. *Marine Ecology – Progress Series*. Vol. **14**. pp. 297-300

Bissinger, J. E., Montagnes, D.J.S., Sharples, J., Atkinson, D. 2008. Predicting marine phytoplankton maximum growth rates from temperature: Improving on the Eppley curve using quantile regression. *Limnology and Oceanography*. Vol. **53**. Vol. 2. pp. 487-493

Bittar, T.B., Lin, Y., Sassano, L.R., Wheeler, B.J. 2013. Carbon allocation under light and nitrogen resource gradients in two marine model phytoplankton. *Journal of Phycology*. Vol. **49**. No. 3. pp. 523-535

Booth, B.C. 1987. The use of autofluorescence for analysing oceanic phytoplankton communities. *Botanica Marina.* Vol. **30**. pp. 101-8

Booth, B.C. 1988. Size classes and major taxonomic groups of phytoplankton at two locations in the subarctic Pacific Ocean in May and August, 1984. *Marine Biology*. Vol. **97**. pp. 257-86

Booth, B.C., Lewin, J., Norris, R.E. 1982. Nanophytoplankton species dominant in the subarctic pacific in May and June, 1978. *Deep-Sea Research*. Vol. **29**. pp. 185-200

Bopp, L., Monfray, P., Aumont, O., Dufresne, J-L., Le Treut, H., Madec, G., Terray, L., Orr, J.C. 2001. Potential impact of climate change on marine export production. *Global Biogeochemical Cycles.* Vol. **15**. No. 1. pp. 81-99

Bopp. L., Aumont, O., Cadule, P., Alvain, S., Gehlen, M. 2005. Response of diatoms distribution to global warming and potential implications: A global model study. *Geophysical Research Letters*. Vol. **32**. No. 19. pp. 1-4

Boyce, D.G., Lewis, R.M. Worm, B. 2010. Global phytoplankton decline over the past century. *Nature*. Vol. **466**. pp. 591-596

Brand, L.E., Guillard, R.R.L. 1981. The effects of continuous light and light intensity on the reproduction rates of twenty-two species of marine phytoplankton. *Journal of Experimental Marine Biology and Ecology*. Vol. **50.** pp 119-132

Brand, L.E., Guillard, R.R.L., Murphy, L.S. 1981 (b). A method for the rapid and precise determination of acclimated phytoplankton reproduction rates. *Journal of Plankton Research* Vol. **3**. pp. 193-201

Brock, T.D., Brock, M.L. 1966. Temperature optima for algal development in Yellowstone and Iceland hotsprings. *Nature.* Vol. **209**. pp. 733-734

Brown. J.H., Gillooly, J.F., Allen, A.P., Savage, V.M., West, G.B. 2004. Towards a metabolic theory of ecology. *Ecology.* Vol. **85**. No. 7. pp. 1771-1789

Buitenhuis, E. 2011. A temperature gradient bar for measuring phytoplankton physiology. In prep.

Buitenhuis, E. 2012. *Description of the PlankTOM10 equations*. Available at: http://lgmacweb.env.uea.ac.uk/green_ocean/model/PlankTOM10_equations_Feb2012.pdf. Cited: 25/10/13

Buitenhuis, E., Geider, R. 2010. A model of phytoplankton acclimation to iron-light colimitation. *Limnology and Oceanography*. Vol. **55.** No. 2. pp. 714-724

Buitenhuis, E., Hashioka, T., Le Quèrè, C. 2013a. Combined restraints on global ocean primary production using observations and models. *Global Biogeochemical Cycles*. Vol. **27**. No. 3. pp. 847-858

Buitenhuis, E., Le Quéré, C., Aumont, O., Beaugrand, G., Bunker, A., Hirst, A., Tsutom, I., O'Brien, T., Piontkovski, S., Straile, D. 2006. Biogeochemical fluxes through mesozooplankton. *Global Biogeochemical Cycles*. Vol. **20**. No. 2. pp. 1-33

Buitenhuis, E., Pangerc, T., Franklin, D., Le Quéré, C., Malin, G. 2006. Growth rates of six coccolithophorid strains as a function of temperature. *Limnology and Oceanography*. Vol. **53**. No. 3. pp. 1181-1185

Buitenhuis, E., Vogt, M. 2008. *The practical user guide to DGOM-PlankTOM or: How to survive the fight against the dragon*. Available at: http://lgmacweb.env.uea.ac.uk/green_ocean/model/internal/keinepanikuea.pdf. Cited: 25/10 2013

Buitenhuis, E.T., van der Wal., P., de Baar, H.J.W. 2001. Blooms of *Emiliania huxleyi* are sinks of atmospheric carbon dioxide: A field and mesocosm study derived simulation. *Global Biogeochemical Cycles*. Vol. **15**. No. 3. pp. 577-587

Buitenhuis, E.T., Vogt, M., Moriarty, R., Bednaršek, N., Doney, S.C., Leblanc, K., Le Quéré, C., Luo, Y-W., O'Brien, C.O., Brien, T.O., Peloquin, J., Schiebel, R., Swan, C. 2013b. MAREDAT : towards a world atlas of MARine Ecosystem DATa. *Earth Systems Science Data*. Vol. **5**. pp. 227-239

Burnham, K.P., Anderson, D.R. 2004. Multimodel Inference: Understanding AIC and BIC in model selection. *Sociological Methods and Research*. Vol. **33**. pp. 261-304

Buskey, E.J. 1995. Growth and bioluminescence of *Noctiluca scintillans* on varying algal diets. *Journal of Plankton Research*. Vol. **17**. No. 1. pp. 29-40

Buxton, L., Takahashi, S., Hill, R., Ralph, P.J. 2011. Variability in the primary site of photosynthetic damage in *Symbiodinium sp*. (Dinophyceae) exposed to thermal stress. *Journal of Phycology*. Vol. **47**. pp. 1-10

Calbet, A., Landry, M.R. 2004. Phytoplankton growth, microzooplankton grazing and carbon cycling in marine systems. *Limnology and Oceanography*. Vol. *49*. No. 1. pp. 51-57

Calderia, K., Wickett, M.E. 2005. Ocean model predictions of chemistry changes from carbon dioxide emissions to the atmosphere and ocean. *Journal of Geophysical Research*. Vol. **110**. pp. 1-12

Canadell, J.G., Le Quèrè, C., Raupach, M.R., Field, C.B., Buitenhuis, E.T., Ciais, P., Conway, T.J., Gillett, N.P., Houghton, R.A., Marlan, G. 2007. Contributions to accelerating atmospheric CO_2 growth from economic activity, carbon intensity and the efficiency of natural sinks. *Proceedings of the National Academy of Science*. Vol. **104**. No. 47. pp. 18866-18870

Chalup, M.S., Laws, E.A. 1990. A test of the assumptions and predictions of recent microalgal growth models with the marine phytoplanker *Pavlova lutheri. Limnology and Oceanography.* Vol. **35**. No. 3. pp. 583-596

Chavez, F.P., Toggweiler, J.R. 1995. Physical estimates of global new production: The upwelling contribution. In: Summerhayes, C.P., Emeis, K.C., Angel, M.V., Smith, R.L., Zeitschel, B. (eds) *Upwelling in the Ocean: Modern Processes and Ancient Records*. Vol **7**. John Wiley&Sons, Chichester, UK. pp. 383-404

Chisholm, S.W. 1992. Phytoplankton Size. *Primary Productivity and Biogeochemical Cycles in the Sea*. Edited by Falkowski, P.G., Woodhead, A.D. Plennum Press. New York. pp. 231-237

Chollet, S. 2013. *The role of diatoms in the Antarctic carbon cycle*. Doctoral thesis. University of East Anglia. Available at: lgmacweb.env.uea.ac.uk. Cited: 22/06/15

Claquin, P., Probert, I., Lefebvre, S., Veron, B. 2008. Effects of temperature on photosynthetic parameters and TEP production in eight species of marine microalgae. *Aquatic Microbial Ecology*. Vol. **51.** pp. 1-11

Collier, J.L., Lovinder, R., Xi, Y., Radway, J.C., Armstrong, R.A. 2011. Differences in growth and physiology of marine *Synechococcus* (Cyanobacteria) on nitrate versus ammonium are not determined solely by nitrogen source redox state. *Journal of Phycology*. Vol. **47**. pp. 1-11

Collos, Y. 2002. Determination of particulate carbon and nitrogen in coastal waters. In: Subba Rao DV (ed) *Pelagic Ecology Methodology*, Balke ma. Netherlands. pp. 333-341

Collos, Y., Berges, B.A. 2004. *Nitrogen metabolism in phytoplankton*. Marine Ecology. In. Encyclopaedia of Life Support Systems (EOLSS).UNESCO. EOLSS Publishers. Oxford. UK

Collos, Y., Hadjadji, I., Plisson, B., Cecchi, P., Laabir, M. 2011. Phased oscillations in cell numbers and nitrate in batch cultures of *Alexandrium tamarense* (Dinophyceae). *Journal of Phycology*. Vol. **47**. pp. 1-6

Cotner, J.B., Ammerman, J.W., Peele, E.R., Bentzen, E. 1997. Phosphorus-limited bacterioplankton growth in the Sargasso Sea. *Aquatic Microbial Ecology*. Vol. **13**. pp. 1881-1893

Cullen, J.J., Davis, R.F., Huot, Y. 2012. Spectral model of depth-integrated water column photosynthesis and its inhibition by ultraviolet radiation. *Global Biogeochemical Cycles*. Vol. **26**. pp. 1-19

da Silva, A.F., Lourenco, S.O., Chaloub, R.M. 2009. Effects of nitrogen starvation n teh photosynthetic physiology of tropical marine microalga *Rhodomonas sp.* (Cryptophyceae). *Aquatic Botany*. Vol. **91**. pp. 291-297

Davison, I. R. 1991. Environmental effects on algal photosynthesis: Temperature. *Journal of Phycology*. Vol. **27.** pp. 2-8

Denman, K.L., Peña, M.A. 2000. *Beyond JGOFS*. pp.469-486. In: Hanson, R.B., Ducklow, H.W., Filed, J.G. 2000. *The Changing Ocean Carbon Cycle: A midterm synthesis of the Joint Global Ocean Flux Study*. Cambridge University Press. Cambridge. UK.

Descamps-Julien, B., Gonzalez, A. 2005. Stable coexistence in a fluctuating environment: An experimental demonstration. *Ecology.* Vol. **86**. pp. 2815-2824

Detmer, A.E., Bathmann, U.V. 1997. Distribution patterns of autotrophic pico- and nanoplankton and their relative contributions to algal biomass during spring in the Atlantic sector of the Southern Ocean. *Deep-Sea Research*. Vol. **44**. No. 1-2. pp. 299-320

Diaz, R.J., Rosenberg, R. 2008. Spreading dead zones and consequences for marine ecosystems. *Science*. Vol. **321**. pp.926-929

Dietze, H., Loeptein, U. 2013. Revisiting "nutrient trapping" in global coupled biogeochemical ocean circulation models. *Global Biogeochemical Cycles*. Vol. **27**. pp. 1-19

Dimier, C., Brunet, C., Geider, R.J., Raven, R.A. 2009. Growth and photoregulation dynamics of the picoeukaryote *Pelagomonas calceolate* in fluctuating light. *Limnology and Oceanography*. Vol. **54**. No. 3. pp. 823-836

Doney, S.C., Fabry, V.J., Feely, R.A., Kleypas, J.A. 2009. Ocean acidification: The other CO_2 problem. *Annual Review of Marine Science*. Vol. **1**. pp. 162-192

Doney, S.C., Lindsay, K., Moore, J.K. 2003. Global Ocean Carbon Cycle Modeling, In: Ocean Biogeochemistry: The Role of the Ocean Carbon Cycle in Global Change. Ed. M. Fasham. Springer-Verlag. Berlin. pp. 217-238

Doney, S.C., Ruckelshaus, M., Duffy, J.E., Barry, J.P., Chan, F., English, C.A., Galindo, H.M., Grebmeier, J.M., Hollowed, A.B., Knowlton, N., Polovina, J., Rabalais, N.N., Sydeman, W.J., Talley, L.D. 2012. Climate change impacts on marine ecosystems. *Annual Review of Marine Science*. Vol. **4**. pp. 4.1-4.27

Doney, S.C., Wallace, W.R., Ducklow, H.W. 2000. The North Atlantic carbon cycle: new perspectives from JGOFS and WOCE. pp. 375-388. In: Hanson, R.B., Ducklow, H.W., Filed, J.G. 2000. *The Changing Ocean Carbon Cycle: A midterm synthesis of the Joint Global Ocean Flux Study*. Cambridge University Press. Cambridge. UK.

Droop, M. R. 1974. The nutrient status of algal cells in continuous culture. *Journal of Marine Biological Association. UK.* Vol. **54**. pp. 825-855

Droop, M.R. 1973. Some thoughts on nutrient Limitation in algae. *Journal of Phycology*. Vol. **9**. pp. 264-272

Druzhkova, E. I., Makarevich, P. R. 2008. Annual cycle of nanophytoplankton in coastal waters of the Barents Sea. *Biology Bulletin*. Vol. **4**. pp. 428-435

Dufresne, J.-L., Friedlingstein, P., Berthelot, M., Bopp, L., Ciais, P., Fairhead, L., LeTreut H., and Monfray. 2002. On the magnitude of positive feedback between future climate change and the carbon cycle. *Geophysical Research Letters*. Vol. **29**. No. 10. pp. 43_1-43_4

Dugdale, R.C., Goering, J.J. 1967. Uptake of new and regenerated forms of nitrogen in primary productivity. *Limnology and Oceanography*. Vol. **12**. No. 2. pp. 196-206

Dyhrma, S.T., Ammerman, J.W., Van Mooy, B.A.S. 2007. Microbes and the marine environment. *Oceanography*. Vol. **20**. No. 2. pp. 110-116

Eby, M., Zickfeld, K., Montenegro, A., Archer, D., Meissner, K.J., Weaver, A.J. 2009. Lifetime of anthropogenic climate change: Millennial time scales of

potential CO_2 and surface temperature perturbations. Journal of Climate. Vol. 22. pp. 2501-2511

Edeline, E., Lacroix, G., Delire, C., Pulet, N., Legendre, S. 2013. Ecological emergence of thermal clines in body size. *Global Change Biology*. Vol. **19**. No. 10. pp. 3062-3068

Emerson, S., Sabine, C., Cronin, M.F., Feely, R., Cullison Gray, S.E., DeGrandpre, M. 2011. Quantifying the flux of $CaCo_3$ and organic carbon from the surface ocean using *in situ* measurements of O_2, N_2, pCO_2, and pH. *Global Biogeochemical Cycles*. Vol. **25**. pp. 1-12

Emerson, S.R., Hedges, J.I. 2008. *Chemical oceanography and the marine carbon cycle*. Cambridge University Press. Cambridge. UK.

Enright, C., Buitenhuis, E.T., Vogt, M., Le Quèrè. 2009. *10 user manual version 1.02*. Available at: http://lgmacweb.env.uea.ac.uk/mbc/. Cited: 18/06/2013

Eppley, R.W. 1968. An incubation method for estimating the carbon content of phytoplankton in natural samples. *Limnology and Oceanography*. Vol. **13**. No. 741-751

Eppley, R.W. 1972. Temperature and phytoplankton growth in the sea. *Fishery Bulletin*. Vol. **70**. No. 4. pp. 1063-1085

Eppley, R.W., Peterson, B.J. 1979. Particulate organic matter flux and planktonic new production in the deep ocean. *Nature*. Vol. **282**. No. 13. pp. 677-680

Etheridge, D.M., Stelle, L.P., Langenfelds, R.L., Francey, R.J., Barnola, J-M., Morgan, V.I. 1996. Natural and anthropogenic changes in atmospheric CO_2 over the last 1000 years from air in Antarctic ice and firn. *Journal of Geophysical Research*. Vol. **101**. No. 2. pp. 4115-4128

Europe and North Atlantic Map. *European Map*. Available at commons.wikimedia.org. Cited: 14/07/14

Exeter Analyser Incorporated (EAI). 2009. Exeter Analyser Manual. Available at: (Exeter CHN manual available at: http://www.eai1.com/ce440.htm). Cited: 25/10/13

Fabregas, J. 1985 Growth, chlorophyll *a* and protein of the marine microalga *Isochrysis galbana* in batch cultures with different salinities and high nutrient concentrations. *Aquaculture*. Vol. **50**. No 1-2. pp. 1-11

Fabregas, J., Herrero, C., Buenaventura, C., Abalde, J. 1987. Growth and biochemical variability of the marine microalga *Chlorella stigmatophora* in batch cultures with different salinities and nutrient gradient concentrations. *European Journal of Phycology*. Vol. **22**. pp. 269-276

Falkowski, P. G. 1981. Light shade adaptation and assimilation numbers. *Journal of Plankton Research*. Vol. **3**. No. 2. pp 203-216

Falkowski, P. G. 1981. Light shade adaptation and assimilation numbers. *Journal of Plankton Research*. Vol. **3**. No. 2. pp 203-216

Falkowski, P. G. Dubinsky, Z. Wyman, D. 1985. Growth-irradiance relationships in phytoplankton. *Limnology and Oceanography*.Vol. **30**. pp. 311-321

Falkowski, P.G., Barber, R.T., Smetacek, V. 1998. Biogeochemical controls and feedbacks on ocean primary production. *Science*. Vol. 281. pp. 200-206

Falkowski, P.G., Greene, R.M., Geider, R.J. 1992. Physiological limitations on phytoplankton productivity in the oceans. *Oceanography*. Vol. 5. No. 2. pp. 84-91

Fasham, M..J.R. 2003. *Ocean Biogeochemistry: The role of the ocean carbon cycle in the global change*. Chapter 4. Falkowski, P.G., Laws, E.A., Barber, R.T., Murray, J.W *Phytoplankton and their role in primary, new and export production*. Springer-Verlag Berlin Heidelberg. New York

Field, C.B., Behrenfeld, M.J., Randerson, J.T., Falkowski, P.G. 1998. Primary production of the biosphere: Integrating terrestrial and oceanic components. *Science*. Vol. **281**. pp. 237-240

Finkel, Z. V. 2001. Light absorption and size-scaling of light limited metabolism in marine diatoms. *Limnology and Oceanography*. Vol. **46**. pp. 86–94

Finkel, Z.V., Beardall, J., Flynn, K.J., Quigg, A., Alwyn, T., Rees, V., Raven J.A. 2010. Phytoplankton in a changing world: cell size and elemental stoichiometry. *Journal of Plankton Research*. Vol. **32**. No. 1. pp. 119-137

Finkel, Z.V., Irwin, A.J. 2000. Modeling size-dependent photosynthesis: Light absorption and the allometric rule. *Journal of Theoretical Biology*. Vol. **204**. pp. 361-369

Flynn, K.J., Marshall, H., Geider, R.J. 2001. A comparison of two N-irradiance interaction models of phytoplankton growth. *Limnology and Oceanography*. Vol. **46**. No. 7. pp. 1794-1802

Follows M. J., Dutkiewicz, S., Grant, S., Chisholm, S.W. 2007. Emergent biogeography of microbial communities in a model ocean. *Science*. Vol. **315**. pp. 1843-1846

Foy, R.H., Gibson, C.E., Smith, R.V. 1976. The influence of day length, light intensity and temperature on the growth rates of planktonic blue-green algae. *British Phycological Journal*. Vol. **11.** No. 2. pp. 151-163

Francis, T.B., Scheuerell, M.D., Brodeur, R.D., Levin, P.S., Ruzicka, J.J., Tolimieri, N., Pterson, W.T. 2012. Climate shifts the interaction web of a marine plankton community. *Global Change Biology*. Vol. **18**. No. 8. pp. 2498-2508

Franklin, D.J., Choi, C.J., Hughes, C., Malin, G., Berges, J.A. 2009. Effect of dead phytoplankton cells on the apparent efficiency of photosystem II. *Marine Ecology Progress Series*. Vol. **382**. pp. 35-40

Friedlingstein, P., Bopp, L., Ciais, P. 2001. Positive feedback between future climate change and the carbon cycle. *Geophysical Research letters*. Vol. **28**. No. 8. pp. 1543-1546

Friedlingstein, P., Dufresne J.-L., Cox P.M., Rayner P. 2003. How positive is the feedback between climate change and the carbon cycle? *Tellus*. Vol. **55**B. pp. 692-700

Fuschino, J.R., Gushina, I.A., Dobson, G., Yan, N.D., Harwood, J.L., Arts, M.T. 2011. Rising temperatures alter lipid dynamics and reduce N-3 essential fatty acid concentrations in *Scenedesmus obliquus* (chlorophyta). *Journal of Phycology*. Vol. **47**. pp. 763-774

Gaines, G., Taylor, F.J.R. 1985. Form and function of the dinoflagellate transverse flagellum. *Journal of Protozoology*. Vol. **32**. pp. 290–296

Gardner, W.D., Mishonov, A.V., Richardson, M.J. 2006. Global POC concentrations from *in-situ* and satellite data. *Deep-Sea Research*. Vol. **11**. pp. 718-740

Gause, G.F. 1932. Experimental studies on the struggle for existence. *Journal of Experimental Biology*. Vol. **9**. pp. 389-402

Geider, R. J. 1993. Quantitative phytoplankton physiology - implications for primary production and phytoplankton growth. *Measurement of Primary Production from the Molecular to the Global Scale*. Vol. **197**. pp. 52-62

Geider, R. J., Osborne, B.A. 1989. Respiration and microbial growth: A review of the quantitative relationship between dark respiration and growth. *New Phytology*. Vol. **112**. pp. 327-341

Geider, R. J., Osborne, B.A., Raven, J.A. 1985. Light dependence of growth and photosynthesis in *Phaeodactylum tricornutum* (bacillariophyceae). *Journal of Phycology*. Vol. **21.** No. 4. pp. 609-619

Geider, R., MacIntyre, H.L., Kana. T.M. 1996. A dynamic model of photoadaptation in phytoplankton. *Limnology and Oceanography*. Vol. **41.** No. 1. pp. 1-15

Geider, R., MacIntyre, H.L., Kana. T.M. 1998. A dynamic regulatory model of phytoplanktonic acclimation to light, nutrients, and temperature. *Limnology and Oceanography*. Vol. **43**. No. 4. pp. 679-694

Geider, R.J. 1987. Light and Temperature Dependence of the Carbon to Chlorophyll *a* Ratio in Microalgae and Cyanobacteria: Implications for Physiology and Growth of Phytoplankton. *New Phytologist*. Vol. **106**. No. 1. pp. 1-34

Geider, R.J., La Roche, J. 2002. Redfield revisited: variability of C:N:P in marine microalgae and its biochemical basis. *European Journal of Phycology*. Vol. **37**. pp. 1–17

Geider, R.J., MacIntyre, H.L., Kana, T.M. 1997. Dynamic model of phytoplankton growth and acclimation: responses of the balanced growth rate and the chlorophyll *a*:carbon ratio to light, nutrient-limitation and temperature. *Marine Ecology Progress Series*, Vol. **148**, pp. 187-200

Geider, R.J., Osborne, B.A. 1986. Light absorption, photosynthesis and growth of *Nannochloris atomus. Marine Biology*. Vol. **93**. pp. 351-360

Gerecht, A.C., Supraha, L., Edvardsen, B., Probert, I., Henderiks, J. 2014. High temperture decreases the PIC/POC ratio and increases phosphorus requirements in *Coccollithus pelagicus* (Haptophyta). *Biogeosciences Discussions*. Vol. **1**. pp. 1021-1051

Gilbert, J.A. 2013. Biological oceanography: Some phytoplankton like it hot. *Nature Climate Change*. Vol. **3**. pp. 954-955

Global Carbon Budget, 2013. *Global Carbon Project*. Available at: www.globalcarbonproject.org. Cited: 31/01/14

Global Carbon budget. 2013b. Global Carbon Project. Available at: http://www.globalcarbonproject.org/carbonbudget/13/files/GCP_budget_2013.pdf. Cited: 31/01/14

Glover, H.E., Keller, M., Spinrad, R. 1987. The effects of light quality and intensity on photosynthesis and growth of marine eukaryotic and prokaryotic phytoplankton clones. *Journal of Experimental Marine Biology and Ecology*. Vol. **105**. No. 2-3. pp.137–159

Goldman, C.R. 1986. On phytoplankton growth rates and [articulate ratios at low light C:N:P. *Limnology and Oceanography* (Goldman, 1980). pp. 1358-1363

Goldman, J.C., Carpenter, E.J. 1974. A kinetic approach to the effect of temperature on algal growth. *Limnology and Oceanography*. Vol. **19.** No. 5. pp. 756-766

Goldman, J.C., Dennet, M.R. 1985. Susceptibility of some marine-phytoplankton species to cell breakage during filtration and post-filtration rinsing. *Journal of Experimental Marine Biology and Ecology*. Vol. **86**. pp. 47-58

Gómez, F. 2005. A list of free-living dinoflagellate species in the world's oceans. *Acta Botanica Croatia*. Vol. **64**. No. 1. pp. 129-212

Gorsky, G., Chrétiennot-Dinet, M.J., Blanchot, J., Palazzoli, I., 1999. Picoplankton and nanoplankton aggregation by appendicularians: Faecal pellet contents of *Megalocercus huxleyi* in the equatorial Pacific. *Journal of Geophysical Research*. Vol. **104**. No. C2. Pp. 3381-3390

Gregg, W.W., Casey, N.W. 2007. Sampling biases in MODIS and SeaWiFS ocean chlorophyll data. *Remote Sensing of Environment*. Vol. **111**. pp. 25-35

Gregg, W.W., Casey, N.W., Rousseaux, C.S. 2014. Sensitivity of simulated global ocean carbon flux estimates to by reanalysis products. *Ocean Modeling*. Vol. **80**. pp. 24-35

Gregg, W.W., Ginoux, N.W., Schopf, P.S., Casey, N.W. 2003. Phytoplankton and iron: validation of a global three dimensional ocean biogeochemical model. *Deep Sea Research Part II Topical Studies in Oceanography*. Vol. **54**. pp. 447-477

Gruber, N., Sarmiento, J.L. 1997. Global patterns of marine nitrogen fixation and denitrification. *Global Biogeochemical Cycles*. Vol. **11**. No. 2. pp. 1-33

Guillard, R.R.L. 1975. *Culture of phytoplankton for feeding marine invertebrates*. Culture of Marine Invertebrate Animals. (eds: Smith W.L. and Chanley M.H.) Plenum Press, New York, USA. pp. 26-60

Guillard, R.R.L., Ryther, J.H. 1962. Studies of marine planktonic diatoms. *I. Cyclotella nana Hustedt* and *Detonula confervacea* Cleve. *Canadian Journal of Microbiology*. Vol. **8**. pp. 229-239

Gustavs, L., Schumann, R., Eggert, A., Karsten, U. 2009. In vivo growth fluorometry: accuracy and limits of microalgal growth rate measurements in ecophysiological investigations. *Aquatic Microbial Ecology*. Vol. **55**. pp. 95-104

Halsey, K.H., Milligan, A.J., Behrenfeld, M. 2010. Physiological optimization underlies growth rate-independent chlorophyll-specific gross and net primary production. *Photosynthesis Research*. Vol. **103**. pp. 125-137

Hansatech, 2014. *Hansatech Instruments. Oxygraph Plus System*. Available at: http://hansatech-instruments.com/products/introduction-to-oxygen-measurements/complete-systems/2079-2/. Cited: 14/07/14

Hansell, D.A., Carlson, C.A., Schlitzer, R. 2012. Net removal of major marine dissolved organic carbon fractions in the subsurface ocean. *Global Biogeochemical Cycles*. Vol. **26**. pp. 1-9

Hansell., D.A., Carlson, C.A. 2013. Localized refractory dissolved organic carbon sinks in the deep ocean. *Global Biogeochemical Cycles*. Vol. **27**. No. 3. pp. 705-710

Hansen, P.J., Bjornsen, P.K., Hanse, B.W. 1997. Zooplankton grazing and growth: scaling within the 2-2000 μm body size range. *Limnology and Oceanology*. Vol. **42**. pp. 687-704

Harris, G.N., Scanlan, D.J., Geider, R.J. 2005. Acclimation of *Emiliana huxleyi* (Prymnesiophyceae) to photon flux density. *Journal of Phycology*. Vol. **41**. No. 4. pp. 851-862

Harrison, P.J., Waters, R.E., Taylor, F.J.R. 1980. A broad spectrum artificial medium for coastal and open ocean phytoplankton. *Journal of Phycology*. Vol. **16**. pp. 28-35

Hasselmann, K. 1991. Ocean circulation and climate change. *Tellus*. Vol. **43** AB. pp. 82-103

Hays, G.C., Richardson, A.J., Robinson, C. 2005. Climate change and marine plankton. *Trends in Ecology and Evolution*. Vol. **20**. No. 6. pp. 337- 344

Healey, F.P, 1993. Effect of temperature and light intensity on the growth rate of *Sunura sphagnicola*. *Journal of Plankton Research.* Vol. **5**. No. 5. pp. 767-774

Healey, R.E. 1973. Characteristics of phosphorus deficiency in *Anabaena*. *Journal of Phycology*. Vol. **9**. pp. 383-394

Heinle, M. 2013. *The effects of light, temperature and nutrients on coccolithophores and implications for biogeochemical models*. Doctoral thesis. University of East Anglia. Available at: www.ueapreints.uea.ac.uk. Cited: 22/06/15

Henson, S. A., Sanders, R., Madsen, R., Morris, P.J., Le Moigne, F., Quartly, G.D., 2011. A reduced estimate of the strength of the ocean's biological pump. *Geophysical Research letters*. **Vol**. 38. pp. 1-5

Henson, S., Lampitt, R., Johns, D. 2012. Variability in phytoplankton community structure in repose to the North Atlantic Oscillation and implications for organic carbon flux. *Limnology and Oceanography*. Vol. **57**. No. 6. pp. 1591-1601

Hinder, S., Hays, G.C., Edwards, M., Roberts, E.C., Walne, A.W., Gravenor, M.B. 2012. Changes in marine dinoflagellate and diatom abundance under climate change. *Nature Climate Change*. Vol. **2**. pp. 271-275

Ho, T-Y., Quigg, A., Finkel, Z.V., Milligan, A.J., Wyman, K., Falkowski, P., Morel, F.M.M. 2003. The elemental composition of some marine phytoplankton. *Journal of Phycology*. Vol. **39**. pp. 1145-1159

Hof, C., Levinsky, I., Araújo, M.B., Rahbek, C., 2011. Rethinking species' ability to cope with rapid climate change. *Global Change Biology*. Vol. **17**. pp. 2987-2990

Hoogstraten, A., Timmermans, K.R. 2012. Morphological and physiological effects in *Proboscia alata* (bacillariophyceae) grown under different light and CO_2 conditions of the modern Southern Ocean. *Journal of Phycology*. Vol. **48**. No. 3. pp. 559-568

Houdan, A., Probert, I., Van Lenning, K., Lefebvre, S. 2005. Comparison of photosynthetic responses in diploid and haploid life-cycle phases of *Emiliania huxleyi* (Prymnesiophyceae). *Marine Ecology Progress Series*. Vol. 292. pp. 139-146

Huertas, E., Rouco, M., López-Rodas, V., Costas, E. 2011. Warming will affect phytoplankton differently: evidence through a mechanistic approach. *Proceedings of the Royal Society*. Vol. **278**. No. 1724. pp. 3534-3543

Huisman, J., Sharples, J., Stroom, J.M., Visser, P.M., Edwin, W., Kardinaal, W.E.A., Verspage, J.M.H., Sommeijer, B. 2004. Changes in turbulent mixing shift competition for light between phytoplankton species. *Ecology*. Vol. **85**. No. 11. pp. 2960-2970

Hutchinson, G.E. 1961. The paradox of the plankton. *American Naturalist*. Vol. **95**. pp. 137-145

IPCC Fourth Assessment Report. 2007. Available at: www.ipcc.ch. Cited: 02/12/11

IPPC Fifth Assessment Report. 2013. Available at: www.ipp.ch. Cited: 07/10/14

Irwin, A.J., Finkel, Z.V., Schofield, O.M.E., Falkowski, P.G. 2006. Scaling-up from nutrient physiology to the size-structure of phytoplankton communities. *Journal of Plankton Research*. Vol. **28.** No. 5. pp. 459-471

Ishiwata, Y., Ohi, N., Obata, M., Taguchi, S. 2013. Carbon to volume relationship of Isochrysis galbana (Prymnesiophyceae) during cell divisions. *Plankton Benthos Research*. Vol. **8**. No. 4. pp. 178-185

Ivančić, I., Godrijan, J., Pfannkuchen, M., Marić, D., Gašparović, B., Djakovac, T., Nadjek, M. 2012. Survival mechanisms of phytoplankton in conditions of stratification-induced deprivation of orthophosphate: Northern Adriatic case study. *Limnology and Oceanography*. Vol. **57**. No. 6. pp. 1721-1731

Jassby, A. D. Platt, T. 1976. Mathematical formulation of relationship between photosynthesis and light for phytoplankton. *Limnology and Oceanography*. Vol. **21**. No. 4. pp. 540- 547

Jickells, T.D., An, Z.S., Anderson, K.K., Bker, A.R., Bergametti, G., Brooks, N., Cao, J.J., Boyd, P.W., Duce, R.A., Hunter, K.A., Kawahat, H., Kubilay, N., LaRoche, J., lis, P.S., Mahowald, N., Prospero, J.M., Ridgwell, A.J., Tegen, I., Torres, R. 2005. Global iron connections between desert dust, ocean biogeochemistry and climate. *Science*. Vol. **308**. pp. 67-71

Karl, D.M., Harrison, W.G., Dore, J. 1991. Major bio-elements. In: Hurd, D.C., Spencer, D.W. Eds *Marine particles: analysis and characterization*. pp. 33-42

Karl, D.M., Yanagi, K. 1997. Partial characterization of the dissolved organic phosphorus pool in the oligotrophic north Pacfic Ocean. *Limnology and Oceanography*. Vol. **42**. pp. 1398-1405

Károlyi, G., Péntek, Á., Scheuring, I., Tél, T., Toroczkai, Z. 2000. Chaotic flow: the physics of species coexistence. *Proceedings of the National Academy of Sciences*. Vol. **97**. pp. 13661-13665

Karsten, U., Klimant, I., Holst, G. 1996 A new In vivo fluorimetric technique to measure growth of adhering phototrophic microorganisms. *Applied and Environmental Microbiology.* Vol. **62**. pp. 237-243

Keeling, R.F., Körtzinger, Gruber, N. 2010. Ocean deoxygenation in a warming world. *Annual Review of Marine Science*. Vol. **2**. pp. 199-229

Keller, K., Morel, F.M.M. 1999. A model of carbon isotopic fractionation and active carbon uptake in phytoplankton. *Marine Ecology Progress Series*. Vol. **182**. pp/ 295-298

Key, R.M., Kozyr, A., Sabine, C.L., Lee, K., Wanninkhof, R., Bullister, J.L., Feely, R.A., Millero, F.J., Mordy, C., Peng, T-H. 2004. A global ocean carbon climatology: results from global data analysis project (GLODAP). *Global Biogeochemical Cycles*. Vol. **18**. pp. 1-23

Kiefer, D. A. 1973. Chlorophyll *a* fluorescence in marine centric diatoms: Responses of chloroplasts to light and nutrient stress. *Marine Biology*. Vol. 23. pp. 39-46. – And Mitchell, B. G. 1983. A simple, steady description of phytoplankton growth based on absorption cross section and quantum efficiency. Limnology and Oceanography. Vol. 28. pp 770-776.

Kiefer, D. A., Mitchell, B.G. 1983. A simple, steady state description of phytoplankton growth based on absorption cross section and quantum efficiency. *Limnology and Oceanography*. Vol. **28**. No. 4. pp. 770-776

Kim, J-M., Lee, K., Shin, K., Yang, E.J., Engel, A., Karl, D.M., Kim, H-C. 2011. Shifts in biogenic carbon flow from particulate to dissolved forms under high carbon dioxide and warm ocean conditions. *Geophysical Research Letters*. Vol. **38**. pp. 1-5

Klaas, C., Archer, D.E. 2002. Association of sinking organic matter with various types of mineral ballast in the deep sea: Implications for the rain ratio. Global *Biogeochemical Cycles*. Vol. **16**. No. 4. pp. 1-14

Knapp, A.N., Sigman, D,M., Lipschultz, F., Kustka, A.B., Capone, D.G. 2011. Interbasin isotopic correspondence between upper-ocean bulk DON and subsurface nitrogen and its implications for marine nitrogen cycling. *Global Biogeochemical Cycles*. Vol. **25**. pp. 1-14

Koffi, E.N., Rayner, P.J., Scholze, M., Beer, C., 2012. Atmospheric constraints on gross primary productivity and net ecosystem productivity: Results from a carbon-cycle data assimilation system. *Global Biogeochemical Cycles*. Vol. **26**. pp. 1-15

Kwon, E.Y., Primeau, F., Sarmiento, J.L. 2009. The impact of remineralization depth on the air-sea carbon balance. *Nature Geoscience*. Vol. **2**. pp. 630-635

Lakeman, M.B., Dassow, P. v., Cattolico, R.A. 2009. The strain concept in phytoplankton ecology. *Harmful Algae*. Vol. **8**. pp. 746-758

Land and Sea Earth texture map. *World map*. Available at: www.planetaryvisions.com. Cited: 14/07/07

Laufkötter, C., Vogt, M., Gruber, N. 2013. Long-term trends in ocean plankton production and particle export between 1960-2006. *Biogeosciences Discussion*. Vol. **10**. pp. 7373-7393

Laws, E. A., Bannister, T.T. 1980. Nutrient-limited and light-limited growth of *Thalassiosira fluviatilis* in continuous culture, with implications for phytoplankton growth in the ocean. *Limnology and Oceanography*. Vol. **25.** No**.** 3. pp. 457-473

Laws, E.A. 1975. Importance of respiration losses in controlling size distribution of marine phytoplankton. *Ecology*. Vol. **56**. pp. 419–426

Laws, E.A. 1991. Photosynthetic quotients, new production and net community production in the open ocean. *Deep Sea Research Part A. Oceanographic Research Papers*. Vol. **38**. No. 1. pp. 143-167

Laws, E.A., Falkowski, P.G., Smith, W.O., Ducklow, H., McCarthy, J.J. 2000. Temperature effects on export production in the open ocean. *Global Biogeochemical Cycles*. Vol. **14**. No. 4. pp. 1231-1246

Le Quéré, C., Harrison, S. P., Prentice, I., Buitenhuis, E. T., Aumont, O., Bopp, L., Claustre, H., Cotrim Da Cunha, L., Geider, R., Giraud, X., Klaas, C., Kohfeld, K. E., Legendre, L., Manizza, M., Platt, T., Rivkin, R. B., Sathyendranath, S., Uitz, J., Watson, A. J., Wolf-Gladrow, D. 2005. Ecosystem dynamics based on plankton functional types for global ocean biogeochemistry models. *Global Change Biology*. Vol. **11.** pp. 2016-2040

Le Quéré, C., Pesant, S. 2009. Plankton functional types in a new generation of biogeochemical models: Integration of plankton abundance data for the

evaluation of marine biogeochemical models. *EOS. Transactions American Geophysical Union*. Vol. **90**. No. 4. pp. 30-31

Le Quéré, C., Takahashi, T., Buitenhuis, E.T., Rödenbeck, C., Sutherland, S.C. 2010. Impact of climate change and variability on the global oceanic sink of CO2. *Global Biogeochemical Cycles.* Vol. **24**. pp. 1-10

Lee, R.E. 1999. *Phycology*. 3rd Ed. Cambridge University Press. Cambridge

Lefebvre, S., Probert, I., Lefrancois, C., Hussenot, J. 2004. Outdoor phytoplankton continuous culture in a marine fish-phytoplankton-bivalve integrated system: Combined effects of dilution rate and ambient conditions on growth rate, biomass and nutrient cycling. *Aquaculture*. Vol. **240**. pp. 211-231

Lefebvre, S.C., Benner, I., Stillman, J.H., Parker, A.E., Drake, M.K., Pascale, E., Rossignol, P.E., Okimura, K.M., Komada, T., Carpenter, E.J. 2011. Nitrogen source and pCO_2 synergistically affect carbon allocation, growth and morphology of the coccolithophore *Emiliania huxleyi*: potential implications of ocean acidification for the carbon cycle. *Global Change Biology*. Vol. **18**. No. 2. pp. 495-503

Lefèvre, N., Taylor, A.H., Geider, R.J. 2001. Phytoplankton physiology can affect ocean surface temperatures. *Geophysical Research letters*. Vol. **28**. No. 7. pp. 1251-1254

Letscher, R.T., Hansell, D.A., Carlson, C.A., Lumpkin, R., Knapp, A.N. 2013. Dissolved organic nitrogen in the global surface ocean: Distribution and fate. *Global Biogeochemical Cycles*. Vol. **27**. pp. 1-13

Levings, C.D. 1980. C:N:P ratios of benthic marine plants. *Limnology and Oceanography*. Vol. **38**. No. 3. pp. 568-574

Libes, S.M. 2009. *Introduction to marine biogeochemistry*. 2nd Edition. Academic Press. USA

Lin, J.C., Pejam, M.R., Chan, E., Wofsy, S.C., Gottlieb, E.W., Margolis, H.A., McCaughey, J.H., 2011. Attributing uncertainties in simulated biospheric

carbon fluxes to different error sources. *Global Biogeochemical Cycles*. Vol. **25**. pp. 1-17

Lohbeck, K.T., Riebesll, U., Reusch, T.B.H. 2012. Adaptive evolution of a key phytoplankton species to ocean acidification. *Nature Geoscience*. Vol. **5**. pp. 346-351

Lorenzen C. J.1967. Determination of chlorophyll and phaeopigments: spectrophotometric equations. *Limnology and Oceanography*. Vol **12**

Losh, J.L., Morel, F.M.M., Hopkinson, B.M. 2012. Modest increase in the C:N ratio of N-limited phytoplankton in the Californian Current in response to high CO_2. *Marine Ecology Progress Series*. Vol. **468**. pp. 31-42

MacIntyre, H.L., Kana, T.M., Anning, T., Geider, R.J. 2002 Photoacclimation of photosynthesis irradiance response curves and photosynthetic pigments in microalgae and cyanobacteria. *Journal of Phycology*. Vol. **38**. pp. 17-38

Madec, G. 2008. NEMO ocean engine. Note the pole modelling. Institute of Pierre-Simon Laplace (IPSL) France. Vol. 27. No. 1288-1619

Maier-Reimer, E., 1993. Geochemical cycles in an ocean general circulation model. Preindustrial tracer distributions. *Global Biogeochemical Cycles*. Vol. **7**. pp. 645-677

Malone, T.C. 1971. The relative importance of nanoplankton and netplankton as primary producers in the Californian current system. *Fisheries Bulletin*. Vol. **69**. pp. 799

Malone, T.C. 1975. Environmental control of phytoplankton cell size. *Limnology and Oceanography*. Vol. **20**. pp. 490

Malone, T.C. 1980a. Algal size. In: *The physiological ecology of phytoplankton*. Morris, I. Ed. University of California Press. Berkeley. Los Angeles

Malone, T.C. 1980b. Size-fractioned primary productivity of marine phytoplankton. In: *Primary productivity in the sea*. Falkowski, P.G. Ed. Brookhaven Symposium in Biology. Plenum. New York

Maraňón, E., Cermeňo, P., López-Sandoval, D.C., Rodriguez-Ramos, T., Sobrino, C., Huete-Ortega, M., Blanco, J.M., Rodriguez, J. 2013. Unimodal size scaling of phytoplankton growth and the size dependence of nutrient uptake and use. *Ecological Letters*. Vol. **16.** No. 3 pp. 371-9

Marinov, I., Doney, S.C., Lima, I.D., Lindsay, K., Moore, J.K., Mahowald, N. 2013. North-South asymmetry in the modelled phytoplankton response to climate change over the 21st century. *Global Biogeochemical Cycles*. Vol. **27**. No. 4. pp. 1274-1290

Martiny, A.C., Pham, C.T.A., Primeau, F.W., Vrugt, J.A., Moore, J.K., Levin, S.A., Lomas, M.W. 2013. Strong latitudinal patterns in the elemental ratios of marine plankton and organic matter. *Nature Geoscience*. Vol. **6**. pp. 279-283

Matsumoto, M., Tokos, K.S., Chikamoto, M., Ridgwell, A. 2010. Characterizing post-industrial changes in the carbon cycle in an Earth system model. *Tellus*. Vol. **62** (B). pp. 296-313

Mattox, K.R.,.Stewart, K.D. 1984. Classification of the green algae: A concept based on comparative cytology. pp.29-72 in: Systematics Association Special. Vol. **27**, *Systematics of the Green Algae*. Edited by Irvine, D.E.G.,.John, D.M. Academic Press. London. UK.

Mc Rose., D. 2008. Effects on growth dynamics of key picoeukaryotic species. Published thesis. Available at: www.mbari.org. Cited: 02/12/11

Menden-Deuer, S., Lessard, E.J. 2000. Carbon to volume relationships for dinoflagellates, diatoms and other protest plankton. *Limnology and Oceanology*. Vol. **45**. pp. 569-579

Miao, Z., Yang, D. 2009. Solar light, seawater temperature, and nutrients, which one is more important in affecting phytoplankton growth? *Chinese Journal of Oceanography and Limnology*. Vol. **27.** No. 4. pp. 825-831

Michaels, A.F., Karl, D.M., Knpa, A.H. 2000. *Temporal studies of biogeochemical dynamics in oligotrophic oceans*. pp. 392-412. In: Hanson, R.B., Ducklow, H.W., Filed, J.G. 2000. *The Changing Ocean Carbon Cycle: A midterm synthesis of the Joint Global Ocean Flux Study*. Cambridge University Press. Cambridge. UK.

Miyazaki, T., Tainaka, K., Togashi, T., Suzuki, T., Yoshimura, J. 2006. Spatial coexistence of phytoplankton speices in ecological timescale. *Population Ecology*. Vol. **48**. No. 2. pp. 107-112

Moazami-Goudarzim M., Colman, B. 2012. Changes in carbon uptake mechanisms in two green marine algae by reduced seawater pH. *Journal of Experimental Marine Biology and Ecology*. **Vol**. 413. pp. 94-99.

Molina Grima, E., García Camacho, F., Sánchez Pérez, J.A., García Sánchez, J.L. 1994. Biochemical productivity and fatty acid profiles of *Isochrysis galbana* Parke and *Teraselmis sp*. as a function of incident light intensity. *Processes of Biochemistry*. Vol. **29**. pp. 119-126

Monod, J. 1949. The Growth of Bacterial Cultures. *Annual Review of Microbiology*. Vol. **3**. No. 24. pp. 371-394

Montagnes, D.J.S., Berges, J.A., Harrison, P.J., Taylor, F.J.R. 1994. Estimating carbon, nitrogen, protein, and chlorophyll *a* from volume in marine phytoplankton. *Limnology and Oceanography*.. Vol. **39**. pp. 1022-1060

Moore, M.C., Mills, M.M., Langlois, R., Milne, A., Achterberg, E.P., La Roche, J., Geider, R.J. 2008. Relative influence of nitrogen and phosphorus availability on phytoplankton physiology and productivity in the oligotrophic sub-tropical North Atlantic Ocean. *Limnology and Oceanography*. Vol. **53**. No. 1. pp. 291-305

Morán, X.A.G., López-Urrutia, A., Calvo-Dĭaz, A., Li, W.K.W. 2010. Increasing importance of small phytoplankton in a warmer ocean. *Global Change Biology*. Vol. 16. No. 3. pp.1137–1144

Morel F. M. M. 1987. Kinetics of nutrient uptake and growth in phytoplankton. *Journal of Phycology*. Vol. **23**. pp.137-150

Morel, F.M.M., Hudson, R.J., Price, N.M. 1991. *Trace metal limitation in the sea*. In: What controls phytoplankton production in nutrient rich areas of the open sea? Chisholm, S.W., Morel, F.M.M. Ed. Limnology and Oceanography. Special Issue in press.

Morris, I., Glover, H.E., Yentsch, C.S. 1974. Products of photosynthesis by marine phytoplankton: the effect of environmental factors on the relative rates of protein synthesis. *Marine Biology*. Vol. **27**. pp. 1-9

Mridul, T.K., Kremer, C.T., Klausmeier, C.A., Litchman, E. 2012. A global pattern of thermal adaption in marine phytoplankton. *Science*. Vol. **338**. No. 6110. pp. 1085-1088

Muggli, D.L., Lecourt, M., Harrison, P.J. 1996. Effects of iron and nitrogen source on the sinking rate, physiology and metal composition of an oceanic diatom from the subarctic Pacific. *Marine Ecology Progress Series.* Vol. **132.** pp. 215-227

Najjar, R.G., Sarmiento, J.L., Toggweiler, J.R., 1992. Downward transport and fate of organic matter in the ocean: Simulations with a general circulation model. *Global Biogeochemical Cycles*. Vol. **6**. pp. 45-76

National Centre for Marine Algae and Microbiota. Available at: https://ncma.bigelow.org/. Cited: 02/12/11

National Oceanic and Atmospheric Administration. (NOAA). National Centres for Environmental Information. 2009. World Ocean Atlas 2009. Available at: www.nodc.noaa.gov. Cited: 16/06/15

Nelson, N.B., Prézelin, B.B., Bidigare, R.R. 1993. Phytoplankton light absorption and the package effect in Californian coastal waters. *Marine Ecology Progress Series*. Vol. **94**. pp. 217-227

Netzel, H., Dürr., G. 1984. Dinoflagellate cell cortex. In Spector, D. L. *Dinoflagellates*. Chapt. 3. New York: Academic Press

Nollet, L.M.L. 2007. Handbook of water analysis, 2nd ED. CRC Press.

Nùńez-Milland, D.R., Baines, S.B., Vogt, S., Twining, B.S. 2010. Quantification of phosphorus in single cells using synchrotron X-ray fluorescence. *Journal of Synchroton Radiation*. Vol. **17**. pp. 560-566

Okin, G.S., Baker, A.R., Tegen, I., Mahowald, N.M., Dentener, F.J., Duce, R.A., Galloway, J.N., Hunter, K., Kanakidou, M., Kubilay, N., Prospero, J.M., Sarin, M., Surapopith, V., Uematsu, M., Zhu, T. 2011. Impacts of atmospheric nutrient deposition on marine productivity: Roles of nitrogen, phosphorus and iron. *Global Biogeochemical Cycles*. Vol. **25**. pp. 1-10

Orr, J.C., Fabry, V.J., Aumont, O., Bopp, L., Doney, S.C., Feely, R.A., Gnanadesikan, A., Gruber, N., Ishida, A., Joos, F., Key, R.M., Lindsay, K., Maier-Reimer, E., Matear, R., Monfray, P., Mouchet, A., Najjar, R.G., Plattner, G-K., Rodgers, K.B., Sabine, C.L., Sarmiento, J.L., Schlitzer, R.D., Totterdell, I.J., Weirig, M-F., Yamanaka, Y., Yool, a. 2005. Anthropogenic ocean acidification over the twenty-first century and its impact on calcifying organisms. *Nature*. Vol. **437**. pp. 681-686

Palevsky, H.I., Ribalet, F., Swalwell, J.E., Cosca, C.E., Cokelet, E.D., Feely, R.A., Armbrust, E.V., Quay, P.D. 2013. The influence of net community production and phytoplankton community structure on CO_2 uptake in the Gulf of Alaska. *Global Biogeochemical Cycles*. Vol**. 27**. pp. 664-676

Paquay, F.S., Zeebe, R.E. 2013. Assessing possible consequences of ocean liming in ocean atmospheric CO_2 concentration and associated costs. *International Journal of Greenhouse Gas Control*. Vol. **17**. pp. 183-188

Pearson, P.N., Palmer, M.R. 2000. Atmospheric carbon dioxide concentrations over the past 60 million years. *Nature*. Vol. **406**. No. 6797. pp. 695-699

Pedrotti, M.L., Fiorini, S., Kerros, M-E., Middelburg, J.J., Gattuso, J-P. 2012. Variable production of transparent exopolymeric particles by haploid and diploid life stages of coccolithophores grown under different CO_2 concentrations. *Journal of Plankton Research*. Vol. **34**. No. 5. pp. 1-11

Peterson, T. C., Baringer, M. O. 2009. State of the Climate in 2008. *Bulletin of the American Meteorological Societ.* Vol. **90**. No. 8. pp 1-196

Piepho, M., Arts, M.T., Wacker, A. 2011. Species-specific variation in fatty acid concentrations of four phytoplankton species: Does phosphorus supply influence the effect of light intensity or temperature? *Journal of Phycology*. Vol. **47**. pp. 1-10

Planetary Visions. 2014. Land and Sea Earth Texture maps. Available at: www.planetaryvision.com. Cited: 15/07/15

Poulton, A.J., Holligan, P.M., Hickman, A., Kim, Y-N., Adey, T.R., Stinchcombe, M.C., Holeton, C., Root, S., Wooodward, M.S. 2006. Phytoplankton carbon fixation, chlorophyll-biomass and diagnostic pigments in the Atlantic Ocean. *Deep-Sea Research*. Vol. **11**. No. 53. pp. 1593-1610

Quigg, A., Finkel, Z.V., Irwin, A.J., Rosenthal, Y., Tung-Yuan, H., Reinfelder, J.R., Schofield, O., Morel, F.M., Falkowski, P.G. 2003. The evolutionary inheritance of elemental stoichiometry in marine phytoplankton. *Nature*. Vol. **425**. pp. 291-294

Quigg, A., Irwin, A.J., Finkel, Z.V. 2011. Evolutionary inheritance of elemental stoichiometry in phytoplankton. *Proceeding of the Royal Academy of Science*. Vol. **278**. pp. 526-534

Regaudie-de-Gioux, A., Duarte, C.M. 2012. Temperature dependence of planktonic metabolism in the ocean. *Global Biogeochemical Cycles*. Vol. **26**. pp. 1-10

Richardson, T.L., Jackson, G.A. 2006. Small phytoplankton and carbon export from the surface ocean. *Science*. Vol. **315**. pp. 838-840

Ridgwell, A., Schmidt, D.N., Turley, C., Brownlee, C., Maldonado, M.T., Tortell, P., Young, J.R. 2009. From laboratory manipulations to Earth system models: predicting pelagic calcifaction and its consequences. *Biogeosciences Discuss*. Vol. **6**. pp. 3455-3480

Rigby, C.H., Craig, S.R., Budd, K. 1980. Phosphate uptake by *Synechococcus lepoliensis* (Cyanophyceae): Enhancement by calcium ion. *Journal of Phycology*. Vol. **16**. pp. 389-393

Riley, J.S., Sanders, R., Marsay, C., Le Moigne, F.A.C., Achterberg, E.P., Poulton, A.J. 2012. The relative contribution of fast and slow sinking particles to ocean carbon export. *Global Biogeochemical Cycles*. Vol. **26**. pp. 1-10

Roscoff Culture Collection. Available at: roscoff-culture-collection.org. Cited: 22/06/15

Ross, O.N., Geider, R.J. 2009. New cell-based model of photosynthesis and photo-acclimation: accumulation and mobilization of energy reserves n phytoplankton. *Marine Ecology Progress Series*. Vol. **383**. pp. 53-71

Rousseaux, C.S., Gregg, W.W. 2012. Climate variability and phytoplankton composition in the Pacific Ocean. *Journal of Geophysical Research*. Vol. **117**. pp. 1-10

Rousseaux, C.S., Gregg, W.W. 2014. Interannual variation in phytoplankton primary production at a global scale. *Remote Sensing*. Vol. **6**. pp. 1-19

Rousseaux, C.S., Hirata, T., Gregg, WW. 2013. Satellite views of global phytoplankton community distribtions using an empirical algorithm and a numerical model. *Biogeosciences Discussions*, Vol. **10**. pp. 1083-1109

Roy, T., *et al*. 2011. Regional impacts of climate change and atmospheric CO_2 on future ocean carbon uptake: A multimodel linear feedback analysis. *Journal of Climate*. Vol. **24**. pp. 2300-2318

Ryther, J. H. 1954. The ratio of photosynthesis to respiration in marine plankton algae and its effect upon the measurement of productivity. *Deep Sea Research*. Vol. **2**. No. 2. pp. 134-139

Sabine, C.L., Feely, R.A., Gruber, N., Key, R.M., Lee, K., Bullister, J.L., Wanninkhof, R., Wong, C.S., Wallace, D.W.R., Tilbrook, B., Millero, F.J., Peng, T-H.,M Kozyr, A., Ono, T., Rios, A.F. 2004. The oceanic sink for anthropogenic CO_2. *Science*. Vol. **305**. No. 5682. pp. 367-371

Sabine, C.L., Feely, R.A., Wanninkhof, R., Takahashi, T., Khatiwala, S., Park, G-H. 2011. The global ocean carbon cycle. *The Bulletin of the American Meteorological Society*. Vol. **92**. No. 6. pp. 100-105

Sakamoto, T., BYrant, D.A. 1999. Nitrate transport and not photo inhibition limits growth of the freshwater cyanobacteria *Synechococcus* species PCC 6301 at low temperature. *Plant Physiology* (Bethesda). Vol. **119**. pp. 785-794

Sakshaug, E., Andreden, K. 1989. A steady state description of growth and light absorption in the marine planktonic diatom *Skeletonema costatum. Limnology and Oceanography*. Vol. **34**. No. 1. pp. 198-205

Sakshaug, E., Johnsen, G., Andresen, K. Vernet, M. 1991. Modeling of light-dependent algal photosynthesis and growth - experiments with the Barents sea diatoms *Thalassiosira nordenskioeldii* and *Chaetoceros furcellatus*. *Deep Sea Research Part I: Oceanographic Research Papers*. Vol. **38**. No.4. pp. 415-430

Sanders, R.W. 1991. *Trophic strategies among heterotrophic flagellates*. Biology of Free-Living Heterotrophic Flagellates, ed. D.J. Patterson & J. Larson, pp. 21-38. Clarendon Press, Oxford

Sarmiento, J.L., Hughes, T.M.C., Stouffer, R.J., Manabe, S. 1998. Simulated response of the ocean carbon cycle to anthropogenic climate warming. **Nature**. Vol. **393**. pp. 245-249

Sarthou, G., Timmermans, K.R., Blain, S., Tréguer, P. (2005) Growth physiology and fate of diatoms in the ocean: a review. *Journal of Sea Research*. Vol. **53**. pp.25-42

Sathyendranath, S., Stuart, V., Nairm A., Oka, K., Nakane, T., Bouman, H., Forget, M-H., Maass, H., Platt, T. 2009. Carbon-to-chlorophyll ratio and growth rate of phytoplankton in the sea. *Marine Ecology Progress Series*. Vol. **383**. pp. 73-84

Scheffer, M., Rinaldi, S., Huisman, J. and Weissing, F.J. 2003. Why plankton communities have no equilibrium: solutions to the paradox. *Hydrobiologia*. Vol. **491** pp. 9-18.

Schlitzer, R. 2004. Export production in the equatorial and North Pacific derived from dissolved oxygen, nutrient and carbon data. *Journal of Oceanography*. Vol. **60**. pp 53-62

Schoemann ,V., Becquevort, S., Stefels, J., Rousseau, W., Lancelot, C. 2005. Phaeocystis blooms in the global ocean and their controlling mechanisms: a review. *Journal of Sea Research*. Vol. **53**. pp.43-66

Schoo, K.L., Malzahn, A.M., Krause, E., Boersma, M. 2012. Increased carbon dioxide availability alters phytoplankton stoichiometry and affects carbon cycling and growth of marine planktonic herbivore. *Marine Biology*. International Journal on Life in oceans and Coastal Waters. Vol. **160**. pp. 2145-2155

Sigman, D.M., Haug, G.H. 2003. The biological pump in the past. *Treatise on Geochemistry*. Vol. **6**. pp. 491-528

Skalar Analytical. 2014. San++ Automated Wet Chemistry Analyzer. Continuous Flow Analyzer (CFA). Available at: www.skalar.com. Cited: 14/07/14

Slovacek, R.E., Hannan, P.J. 1977. In vivo fluorescence determinations of phytoplankton chlorophyll *a*. *Limnology and Oceanography*. Vol. **22**. pp. 919-925

Smayda, T.J. 1970. The suspension and sinking of phytoplankton in the sea. *Oceanography and Marine Biology Annual Review*. Vol. **8**. pp. 353-414

Smith, R.E.H., Kalff, J. 1982. Size-dependent phosphorus uptake kinetics and cell quota in phytoplankton. *Journal of Phycology*. Vol. **18**. No. 2. pp. 275-284

Smith, V.H., Tilman, G.D., Nekola, J.C. 1999. Eutrophication: impacts of excess nutrients on freshwater, marine and terrestrial ecosystems. *Environmental Pollution*. Vol. **100.** pp. 179-196

Solomon, S., Qin, D., Manning, M., Chen, Z., Marquis, M. 2007. *Climate Change 2007*: The Physical Science Basis: Contribution of Working Group I to

the Fourth Assessment Report of the Intergovernmental Panel on Climate Change. Cambridge. Cambridge University Press

Solorzano, L., Sharp, J.H. 1980. Determination of total dissolved phosphorus and particulate phosphorus in natural waters. *Limnology and Oceanography*. Vol. **25**. No. 4. pp. 754-758

Sommer, U. 1998. From algal competition to animal production: Enhanced ecological efficiency of *Brachionus plicatilis* with a mixed diet. *Limnology and Oceanography*. Vol. **41**. pp. 1151-1160

Sommer, U., Lengfellner, K. 2008. Climate change and the timing, magnitude and composition of the phytoplankton spring bloom. *Global Change Biology*. Vol. **14**. pp. 1199-1208

Sophisticated Analytical Instrument Facility. IIT-Bombay. *CHNS (O) Analyzer*. Available at: www.rsic.ac.in. Cited: 14/07/14

South Australian Medical Heritage Society Inc. *Coulter Counter and Coulter Principle*. Available at: samhs.org.au. Cited: 14/07/14

Spector, A.A., Yorek, M.A., 1985. Membrane lipid composition and cellular function. *Journal of Lipid Research*. Vol. **26.** No. 9. pp.1015-1035

Stawiarski, B. 2014. *Picophytoplankton physiology and the microbial loop*. Doctoral thesis. University of East Anglia. Available at: lgmacweb.env.uea.ac.uk. Cited: 22/06/15

Steidinger, K.A., Tangen, K. 1996. Dinoflagellates. *In:* C.R. Tomas (ed.), *Identifying Marine Diatoms and Dinoflagellates*. Academic Press. New York. pp. 387-598

Steinberg, D.K., Van Mooy, B.A.S., Buesseler, K.O. 2008. Bacterial *vs*. zooplankton control of sinking particle flux in the ocean's twilight zone. *Limnology and Oceanography*. Vol. **54**. No. 4. pp.1327-1338

Strickland, J,D,H., Holm-Hansen, O., Eppley, R.W, Linn, R.J. 1969. The use of a deep tank in phytoplankton ecology. Studies of the growth and composition

of phytoplankton crops at low nutrient levels. *Limnology and Oceanography*. Vol. **14**. pp. 23-34

Strickland, J.D.H., Parsons, T.R. 1972. A practical handbook of seawater analysis. 2nd Edition. *Bulletin of Fisheries Research*. No. **167**. pp. 310

Stukel, M.R., Landry, M.R., Benitez-Nelson, C.R., Goericke, R. 2011. Trophic cycling and carbon export relationships in the California Current Ecosystem. *Limnology and Oceanography*. Vol. **56**. No. 5 pp. 1866-1878

Suggett, D.J., Le Floc'H, E., Harris, G.N., Leonardos, N., Geider, R.J. 2007. Different strategies of photoacclimation by two strains of *Emiliania huxleyi* (Haptyophyta). *Journal of Phycology*. Vol. **43**. No. 6. pp. 1209-1222

Suntharalingam. P., Buitenhuis, E.T., Le Quéré, C., Dentener, F., Nevison, C., Butler, J.H., Bange, H.W., Forster, G. 2012. Quantifying the impact of anthropogenic nitrogen deposition on oceanic nitrous oxide. *Geophysical Research Letters*. Vol. **39**. pp. 1-6

Suzuki, Y., Kudoh, S., Takahashi, M. 1995. Photosynthesis characteristics of ice algae with special emphasis on temperature and light conditions (extended abstract). Proceedings of NIPR Symposium. *Polar Biology*. Vol. **2**. pp. 223-224

Suzumura, M. 2008. Persulfate chemical wet oxidation method for the determination of particulate phosphorus in comparison with a high-temperature dry combustion method. *Limnology and Oceanography: Methods*. Vol. **6**. pp. 619-629

Sverdrup, H.U., 1953. On the conditions for the vernal blooming of phytoplankton. *ICES Journal of Marine Science*. Vol. **18**. No. 3. pp. 287-295

Tada, K., Yamaguchi, H., Montani, S. 2004. Comparison of chlorophyll *a* concentrations obtained with 90% acetone and *N,N*-dimethylformamide extraction in coastal seawater. *Journal of Oceanography*. Vol. **60**. pp. 259-261

Tagliabue, A., Bopp, L., Gehlen, M. 2011. The response of marine carbon and nutrient cycles to ocean acidification: Large uncertainties related to

phytoplankton physiological assumptions. *Global Biogeochemical Cycles*. Vol. **25**. No. 3. pp. 1-13

Taniguchi, D.A.A., Landry, M.R., Franks, P.J.S., Selph, K.E. 2014. Size-pecific growth and grazing rates for picophytoplankton in coastal and oceanic regions of the eastern Pacific. *Marine Ecology Progress Series.* Vol. **509**. pp. 87-101

Tarran, G. A., Heywood, J. L., Zubkov, M.V. 2006. Latitudinal changes in the standing stocks of nano- and picoeukaryotic phytoplankton in the Atlantic Ocean. *Deep-Sea Research Part II.* Vol. **53**. No.14-16. pp. 1516-1529

Taylor, F.J.R., Hoppenrath, M., Saldarriage, J.F. 2008. Dinoflagellate diversity and distribution. *Biodiversity and Conservation*. Vol. **17**. pp. 408-418

Terry, K. 1983. Temperature dependence of ammonium and phosphate uptake and their interaction in the marine diatom *Phaeodactylum tricornutm* Bohlin. *Marine Biology Letters*. Vol. **4**. pp. 309-320

Thomas, W.H. 1966. Effects of temperature and illuminance on cell division rates if three species of tropical oceanic phytoplankton. Journal of Phycology. Vol. **2**. pp. 17-22

Thompson, P.A., Guo, P.A., Harrison, P.J. 1992. Effects of variation in temperature. I. On the biochemical composition of eight species of marine phytoplankton. *Journal of Phycology*. Vol. **28**. pp. 481-488

Thomsen, H.A., Buck, K.R., Chavez, F.P. 1994. *Haptophytes as components of the marine phytoplankton. In: The Haptophyte Algae* (eds. Leadbeater, B.S.C., Greene, J.). University Press Oxford. pp. 187-208

Thronsdon, J. 1978. The dilution-culture method. *Phytoplankton Manual*, (ed. A Sournia) pp. 218-24. UNESCO, Paris

Tilman, D., Kilham, S.S., Kilham, P. 1982. Phytoplankton community ecology: The role of the limiting nutrients. *Annual Review of Ecology and Systematics*. Vol. **13**. pp. 349-372

Tilstone, G.H., Figueira, F.G., Fermin, E.G., Arbones, B. 1999. Significance of nanophytoplankton photosynthesis and primary production in a coastal upwelling system (Rĭa de Vigo, NW Spain). *Marine Ecology Progress Series*. Vol. **183**. pp. 13-27

Timmermans, K.R., *et al*. 2005. Physiological responses of three species of marine pico-phytoplankton to ammonium, phosphate, iron and light limitation. *Journal of Sea Research*. Vol. **53**. pp. 109-120

Toseland, A., Daines, S.J., Clark, J.R., Kirkham, A., Strauss, J., Uhlig, C., Lenton, T., Valentin, K., Pearson, G.A., Moulton, V., Mock, T. 2013. The impact of temperature on marine phytoplankton resource allocation and metabolism. *Nature Climate Change*. Vol. **3**. pp. 979-984

Truesdale G.A., Downing A.L., 1954. Solubility of oxygen in water. *Nature*. No. **173**. pp. 1236

Tuck, C., Romanuk, T.N. 2011. Robustness to thermal variability differs along a latitudinal gradient in zooplankton communities. *Global Change Biology*. Vol. **18**. No. 5. pp. 1597-1608

Tung, J.W.T., Tanner, P.A. 2003. Instrumental determination of organic carbon in marine sedimetns. *Marine Chemistry*. Vol. **80**. pp 161-170

Tunzi, M.G., Chu, M.Y., Bain, Jr R.C. 1974. In vivo fluorescence, extracted fluorescence, and chlorophyll concentrations in algal mass measurements. *Water Research*. Vol. **8**. pp. 623-635

Turner Designs, 1999. Model 10-AU-005-CE. *Fluorometer User's Manual*. Version 1.4. Available at: www.turnerdesigns.com. Cited: 14/07/14

Turner, S.M., Harvey, M.J., Law, C.S., Nightingale, P.D., Liss, P.S. 2004. Iron-induced changes in oceanic sulphur biogeochemistry. *Geophysical Research Letters*. Vol. **31**. No. 14

Tyrrell, T. 1999. The relative influence of nitrogen and phosphorus on oceanic primary production. *Nature*. Vol. **400**. No. 5. pp. 525-531

U.N.E.S.C.O. 1966. Determinations of photosynthetic pigments in seawater. Rep. SCOR/UNESCO WG 17. U.N.E.S.C.O. *Monography Oceanography Methodology*. Vol **1**. Paris

Uitz, J., Claustre, H., Gentili, B., Stramski, D. 2010. Phytoplankton class-specific primary production in the world's oceans: Seasonal and interannual variability from satellite observations. *Global Biogeochemical Cycles*. Vol. **24**. pp. 1-19

Uitz, J., Claustre, H., Morel, A., Hooker, H.B. 2006. Vertical distribution of phytoplankton communities in open ocean: an assessment based on surface chlorophyll. *Journal of Geophysical Research*. Vol. **111.** No. C8. pp. 1-23

Van Bleijswijk, J.D.L., Kempers, R., Veldhuis, M.J., Westbroek, P. 1994. Cell and growth characteristics of types A and B of *Erniliania huxleyi* (Prymnesiophyceae) as determined by flow cytometry and chemical analysis. *Journal of Phycology*. Vol. **30**. pp. 230-241

Van Den Hoek, C., Mann, D.G., Jahns, H.M. 1995. *Algae: An introduction to phycology*. Cambridge University Press. UK

Van Mooy, B.A.S., Fredricks, H.F., Pedler, B.E., Dyhrman, S.T., Karl, D.M., Koblížek, M., Lomas, M.W., Mincer, T.J., Moore, L.R., Moutin, T., Rappe, M.S., Webb, E.A. 2009. Phytoplankton in the ocean use non-phosphorus lipids in response to phosphorus scarcity. *Nature*. Vol. **458**. pp. 69-72

Verdy, A., Follows, M., Flierl, G. 2009. Optimal phytoplankton cell size in an allometric model. *Marine Ecology Progress Series*. Vol. **379**. pp. 1-12.

Verity, P.G., Robertson, C.Y., Tronzo, C.R., Andrews, M.G., Nelson, J.R., Sieracki, M.E. 1992. Relationships between cell volume and the carbon and nitrogen content of marine photosynthetic nanoplankton. *Limnology and Oceanography*. Vol. **37**. No. 7. pp. 1434-1446

Versteegh, G.J.M., Riegman, R., de Leeuw, J.W., Jansen, J.H.F. 2000. $U_{37}^{K'}$ values for *Isochrysis galbana* as a function of culture temperature, light

intensity and nutrient concentrations. *Organic Geochemistry.* Vol. **32.** No. 6. pp. 785-794

Vichi, M., Allen, J.I., Masina, S., Hardman-Mountford, N.J. 2011. The emergence of ocean biogeochemical provinces: A quantitative assessment and a diagnostic for model evaluation. *Global Biogeochemical Modelling*. Vol. **25**. No. 2. pp. 1-17

Vogel, S. 1981. *Life in Moving Fluids: the Physical Biology of Flow*. Willard Grant Press, Boston, Massachusetts. USA

Vogt, M., Vallina, S.M., Buitenhuis, E.T., Bopp, L., Le Quéré, C. 2010. Simulating dimethylsulfide seasonality with the Dynamic Green Ocean Model PlankTOM5. *Journal of Geophysical Letters*. Vol. **115**. pp. 1-21

Waggoner, B. 1995. Introduction to the Chrysophytes. University of California Museum of Palaeontology (UCMP). Available at: 222.ucmp.berkeley.edu. Cited: 15/11/13

Walker, J.C.G. 1980. *The oxygen cycle in the natural environment and the biogeochemical cycles*. Springer. Berlin. Germany

Wang, X.J., Behrenfeld, M., Le Borgne, R., Murtugudde, R., Boss, E. 2008. Regulation of phytoplankton carbon to chlorophyll ratio by light, nutrients and temperature in the equatorial Pacific Ocean: a basin-scale model. *Biogeosciences Discussion*. Vol. **5**. pp. 3369-3903

Weber, T.S., Deutsch, C. 2010. Ocean nutrient ratios governed by plankton biogeography. *Nature*. Vol. **550**. pp. 1-5

Wernberg, T., Smale, D.A., Thomsen, M.S. 2011. A decade of climate change experiments on marine organisms: procedures, patterns and problems. *Global Change Biology*. Vol. **18**. No. 5. pp. 1491-1498

Whalen, S.C., Alexander, V. 1984. Influence of temperature and light on rates of inorganic nitrogen transport by algae in an Arctic lake. *Canadian Journal of Fish Aquatic Science*. Vol. **41**. pp. 1310-1318

Williams, P.J. le B. 2000. *Net production, gross production and respiration: what are the Interconnections and what controls what?* pp. 37-57. In: Hanson, R.B., Ducklow, H.W., Filed, J.G. 2000. *The Changing Ocean Carbon Cycle: A midterm synthesis of the Joint Global Ocean Flux Study*. Cambridge University Press. Cambridge. UK.

Winokar, M. 1948. Photosynthesis relationships of *Chlorella* species. *American Journal of Botany*. Vol. **35**. No. 4. pp. 207-214

Wirtz, K.W. 2001. Non-uniform scaling in phytoplankton growth rate due to intracellular light and CO_2 decline. Journal of Plankton Research. Vol 33. No. 9. pp. 1325-1341

Wohlers, J., Engel, A., Zöllner, E., Breithaupt, P., Jürgens, K., Hoppe, H-G., Sommer, U., Riebesell, U. 2009. Changes in biogenic carbon flow in response to sea surface warming. *Proceedings of the National Academy of Science*. Vol. **106**. No. 17. pp. 7067-7072

Wood, E.D., Armstrong, F.A., Richards, F.A. 1967. Determination of nitrate in sea water by cadmium-copper reduction to nitrite. *Journal of Marine Biological Association*. UK. Vol. **47**. pp. 23-31

Xiao, Y., Friedrichs, A.M. 2014. Using biogeochemical data assimilation to assess the relative skill of multiple ecosystem models: effects of increasing the complexity of the planktonic food web. *Biogeosciences Discussion*. Vol. **11**. pp. 481-520

Yamamoto, T. 1995. Contribution of micro- and nanoplankton cell carbon to particulate organic carbon in the East China Sea during May 1980. *Journal of the Faculty of Applied Biology Science*. Vol. **35**. pp. 147-160

Yoder, J. 1979. Effect of temperature on light limited growth and chemical composition of *Skeletonema costatum* (Bacillariophyceae). *Journal of Phycology*. Vol. **15**. pp. 362-370

Yool, A., Martin, A.P., Fernandez, C., Clark, D.R. 2007. The significance of nitrification for oceanic new production. *Nature*. Vol. **447**. No. 7147. pp. 999-1002

Yool, A., Popova, E.E., Anderson, T.R. 2013. MEDUSA-2.0: An intermediate complexity biogeochemical model of the marine carbon cycle for climate change and ocean acidification studies. *Geoscientific Model Development Discussions.* Vol. **6**. pp. 1259-1365

Zhenqing, M., Dongfang, Y. 2009. Solar light, temperature and nutrients, which one is more important in affecting phytoplankton growth? *Chinese Journal of Oceanography and Limnology*. Vol. **27**. No. 4. pp. 825-831

Zhu, C.J., Lee, Y.K., Chao, T.M. 1997. Effects of temperature and growth phase on liquid and biochemical composition of *Isochrysis galbana* TK1. *Journal of Applied Phycology*. Vol. **9**. No. 5. pp. 451-457

Zondervan, I., Rost, B., Riebesll, U. 2002. Effect of CO_2 concentration on the PIC/PON ratio in the coccolithophore *Emiliania huxleyi* grown under light-limiting conditions and different daylengths. *Journal of Experimental Biological Ecology*. Vol. **272**. pp. 55-70

The end